

HETEROLOGOUS AND HOMOLOGOUS EXPRESSION AND CHARACTERIZATION OF
A [NIFE]-HYDROGENASE FROM THE HYPERTHERMOPHILIC ARCHAEON
PYROCOCCUS FURIOSUS

by

ROBERT CHRISTOPHER HOPKINS

(Under the Direction of MICHAEL W. W. ADAMS)

ABSTRACT

The reality that fossil fuels exist in finite amounts has shifted a major focus of research to renewable energy generation. Energy sources of the future must be abundant and carbon neutral with minimal impact on the environment. Hydrogen has the potential to satisfy these requirements as it is clean burning and has high energy content per mass unit, but current methods of production rely on non-renewable resources. The biological production from sunlight or biomass is an attractive alternative to current production methods. Hydrogenase, the biological catalyst responsible for activating gaseous hydrogen, has been the subject of research for more than 80 years. The long tenure this enzyme has enjoyed in the sciences is not a badge of honor; rather it is a testament to the extreme difficulty associated with researching this complex metalloenzyme. While previous efforts have elegantly elucidated the structure, catalytic mechanism, and factors involved in assembling this enzyme, it has not been possible to readily manipulate these proteins or generate large quantities for research purposes. The model chosen

for these studies was *Pyrococcus furiosus* (*Pf*) a strictly anaerobic archaeon that grows in shallow marine volcanic vents at temperatures near 100°C. These enzymes and pathways involved in hydrogen metabolism in *Pf* are being investigated by a combination of biochemical, bioinformatical, and molecular approaches. This research developed a novel method to heterologously express a soluble hydrogenase from *Pf* in *E. coli* yielding preparative amounts of thermostable, active enzyme. Following genetic advances in *Pf* a heterodimeric module of the normally heterotetrameric soluble hydrogenase was homologously overexpressed and produced a stable, active enzyme with altered coenzyme specificity.

INDEX WORDS: Hyperthermophile, *Pyrococcus furiosus*, Hydrogenase, Bioenergy, Rhodopsin, 1,3-Propanediol

HETEROLOGOUS AND HOMOLOGOUS EXPRESSION AND CHARACTERIZATION OF
A [NIFE]-HYDROGENASE FROM THE HYPERTHERMOPHILIC ARCHAEON,
PYROCOCCUS FURIOSUS

ROBERT CHRISTOPHER HOPKINS

B.S. University of Georgia, 2004

A Dissertation Submitted to the Graduate Faculty of The University of Georgia in Partial
Fulfillment of the Requirements for the Degree

DOCTOR OF PHILOSOPHY

ATHENS, GEORGIA

2012

© 2012

Robert Christopher Hopkins

All Rights Reserved

HETEROLOGOUS AND HOMOLOGOUS EXPRESSION AND CHARACTERIZATION OF
A [NIFE]-HYDROGENASE FROM THE HYPERTHERMOPHILIC ARCHAEON,
PYROCOCCUS FURIOSUS

By

ROBERT CHRISTOPHER HOPKINS

Major Professor:
Michael W. W. Adams

Committee Members:
Michael K. Johnson
Robert Maier
Mark Eiteman

Electronic Version Approved:
Maureen Grasso
Dean of the Graduate School
The University of Georgia
May 2012

DEDICATION

This dissertation is dedicated to the two most important people in my life, Mom and Dad. A person could not ask for more loving and encouraging parents. Always there for me, emotionally... and financially; without their support I would not have accomplished anything close to what I have. I will never forget the opportunities they have opened for me and the motivation they instilled to always strive to be a better person. I hope one day to pass on their knowledge, passion for life, and love to children of my own.

ACKNOWLEDGEMENTS

First and foremost I would like to thank Dr. Michael W.W. Adams for his guidance and support throughout my graduate school career. I would like to thank my committee members (Dr. Michael K. Johnson, Dr. Robert Maier, and Dr. Mark Eiteman), for their support throughout my time at UGA. I would also like to thank Dr. Frank Jenney for his expertise and training that provided the basis for all of my accomplishments. Without the help of the entire Adams' lab my Ph.D. would have been a very long and difficult endeavor, and I thank everyone that helped me be where I am today.

TABLE OF CONTENTS

	Page
ACKNOWLEDGEMENTS	v
LIST OF TABLES	viii
LIST OF FIGURES	ix
CHAPTER	
1 INTRODUCTION AND LITERATURE REVIEW	1
IRON SULFUR CLUSTER FREE HYDROGENASES.....	6
IRON-IRON HYDROGENASES	9
NICKEL-IRON HYDROGENASES.....	18
THERMOPHILIC ANAEROBIC METABOLISM.....	37
PYROCOCCUS FURIOSUS METABOLISM AND HYDROGENASES ...	42
2 HETEROLOGOUS EXPRESSION AND MATURATION OF AN NADP- DEPENDENT [NIFE]-HYDROGENASE: A KEY ENZYME IN BIOFUEL PRODUCTION	53
ABSTRACT.....	54
INTRODUCTION	56
RESULTS	60
DISCUSSION.....	64
METHODS	67
REFERENCES	76

3	HOMOLOGOUS EXPRESSION OF A SUBCOMPLEX OF <i>PYROCOCCUS FURIOSUS</i> HYDROGENASE THAT INTERACTS WITH PYRUVATE FERREDOXIN OXIDOREDUCTASE	98
	ABSTRACT	99
	INTRODUCTION	101
	RESULTS	105
	DISCUSSION	108
	METHODS	112
	REFERENCES	116
4	PRACTICAL APPLICATIONS OF <i>PYROCOCCUS FURIOSUS</i> HYDROGENASE	131
5	DISCUSSION AND CONCLUSIONS	167
	REFERENCES	171

LIST OF TABLES

	Page
Table 1.1: Conserved sequence surrounding catalytic site interacting residues of [NiFe] hydrogenases	26
Table 2.1: Strains and plasmids used in this study	82
Table 2.2: Purification of recombinant <i>P. furiosus</i> SHI from <i>E. coli</i>	83
Table 3.1: Strains used in this study	120
Table 3.2: Purification of dimeric SHI from <i>Pf</i>	121
Table 3.3: Physical properties of dimeric SHI	122

LIST OF FIGURES

	Page
Figure 1.1: Anaerobic and aerobic reaction scheme of prokaryotes in a stagnant aquatic stratified system.....	3
Figure 1.2: Electron acceptor in iron sulfur cluster free hydrogenase, methenyltetrahydromethanopterin and active site structure	7
Figure 1.3: Catalytic site H-cluster of the [FeFe] hydrogenase and proposed maturation pathway of [FeFe] hydrogenase domains.....	11
Figure 1.4: Catalytic cycle of the [FeFe] hydrogenases	15
Figure 1.5: [NiFe] hydrogenase general structure and catalytic site	20
Figure 1.6: Catalytic cycle of [NiFe] Hydrogenase	23
Figure 1.7: Maturation of <i>E. coli</i> HycE, the catalytic subunit of Hyd3.....	32
Figure 1.8: HypC, HypD, and HypE modeling the CN ⁻ transfer for the formation of the [NiFe] site precursor Fe(CN) ₂ CO	35
Figure 1.9: Modified Embden-Meyerhof glycolytic pathway of <i>Pyrococcus furiosus</i>	43
Figure 1.10: Current opinion of hydrogen metabolism in <i>Pyrococcus furiosus</i>	46
Figure 1.11: Soluble hydrogenase I predicted cofactor content and maturation factors as predicted by homology to <i>E. coli</i>	49
Figure 2.1: Synthesis of <i>P. furiosus</i> soluble hydrogenase I (SHI) and the plasmid constructs used for recombinant production.....	84

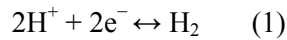
Figure 2.2: Synthesis of <i>P. furiosus</i> soluble hydrogenase I (SHI) and the plasmid constructs used for recombinant production	86
Figure 2.3: Analysis of <i>E. coli</i> promoters with a <i>lacZ</i> gene fragment β -galactosidase reporter assay	88
Figure 2.4: Plasmid construction for rSHI production in <i>E. coli</i>	90
Figure 2.5: Accessory proteins required for maturation of recombinant <i>P. furiosus</i> SHI <i>in vivo</i> and <i>in vitro</i>	92
Figure 2.6: Analysis of the <i>P. furiosus</i> maturation proteins required to produce active rSHI in <i>E. coli</i>	94
Figure 2.7: Properties of recombinant <i>P. furiosus</i> SHI.....	96
Figure 3.1: <i>Pyrococcus furiosus</i> heterotetrameric and dimeric soluble hydrogenase I.....	123
Figure 3.2: <i>pdaD</i> disruption with $P_{gdh}pyrF$	125
Figure 3.3: OE-SHI Dimer recombination plasmid and P_{slp} Dimer strain.....	127
Figure 3.4: Model of the pyruvate-oxidizing, hydrogen producing POR-SHI Dimer system	129
Figure 4.1: The synthetic metabolic pathway for conversion of polysaccharides and water to hydrogen and carbon dioxide.....	135
Figure 4.2: Proof-of-principle synthesis of (1S)-phenyl ethanol in a by-product free reaction mixture from hydrogen and soluble hydrogenase I from <i>Pyrococcus furiosus</i>	139
Figure 4.3: Temperature dependence of <i>Pf</i> SHI hydrogen-catalyzed $NADP^+$ reduction	144

Figure 4.4: Biological mechanism of dissimilative reduction of glycerol to 1,3-propanediol	148
Figure 4.5: Operon structure of 1,3-propanediol related genes in <i>Thermoanaerobacter</i> X514.....	151
Figure 4.6: <i>pdaD</i> suicide vector for <i>Tx</i> 514 PD gene integration on the chromosome of <i>Pf</i>	153
Figure 4.7: Model of inverted membrane vesicles catalyzing light dependent ATP synthesis via rhodopsin and ATP synthase.....	158
Figure 4.8: Sequence alignment of <i>Thermus aquaticus</i> Y51MC23 and <i>Salinibacter ruber</i> rhodopsin.....	161
Figure 4.9: <i>pdaD</i> suicide vector for <i>Taq</i> Y51 rhodopsin gene integration on the chromosome of <i>Pf</i>	164

CHAPTER 1

INTRODUCTION AND LITERATURE REVIEW

Organisms from all three kingdoms of life utilize hydrogen gas (H₂) in some form of metabolism. The biological enzyme responsible for activating hydrogen is hydrogenase, catalyzing the reversible reaction (Eqn 1):



The reducing and hydrogen rich atmosphere of early earth supports the hypothesis that the enzyme hydrogenase may have been one of the first enzymes to evolve [1]. The widespread distribution of hydrogenases across all domains of life demonstrates the importance and necessity of the reaction. It has been observed that abiotically derived hydrogen and CO₂ can support life in certain ecosystems referred to as “HyperSLIME” (hyperthermophilic subsurface lithoautotrophic microbial ecosystem) [2]. The implications of these communities are not limited to finding analogs of primitive life on earth but could also mimic that of extraterrestrial life. The atmosphere of Mars potentially could support subsurface life with an abundance of photochemically produced H₂ and CO₂ [3].

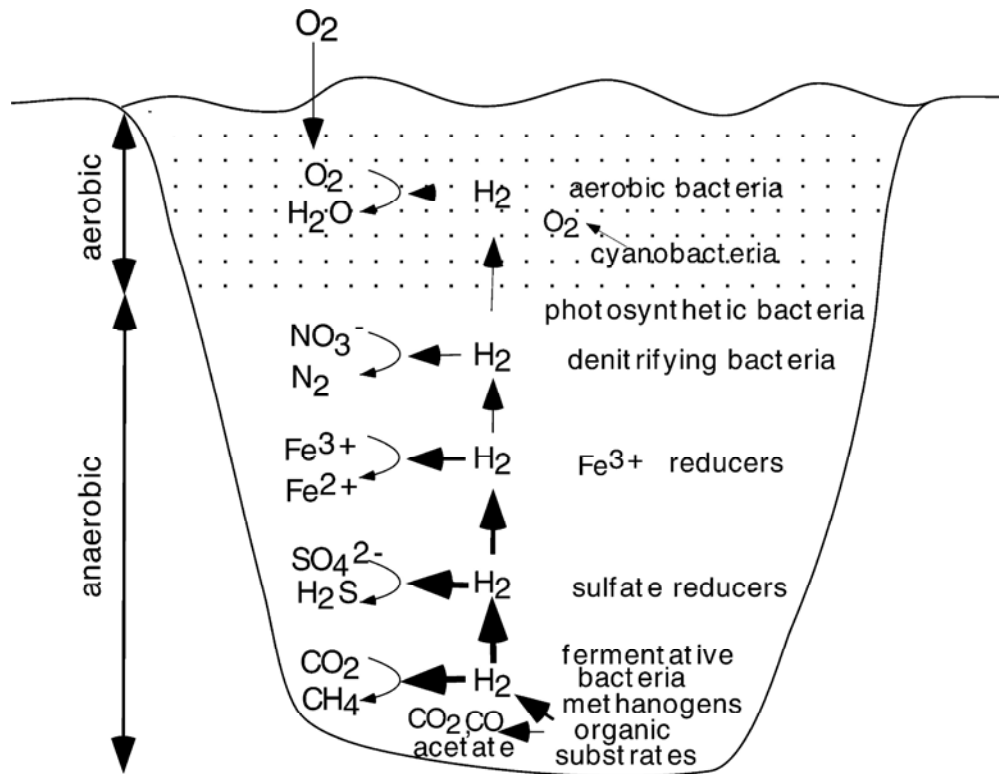
The activity and name hydrogenase was first described by Stephenson and Stickland in 1931 [4]. Hydrogenase enzymes are found in many species of bacteria, archaea and a few unicellular eukaryotes [5,6,7,8,9]. Most of the organisms able to metabolize hydrogen, though, belong to either the Bacterial or Archaeal domain of life. The utilization of hydrogen by microorganisms is usually defined by the redox

potential of the environment in which they inhabit. Prokaryotes able to evolve and activate molecular hydrogen include fermentative, photosynthetic, aerobic, anaerobic, autotrophic, and heterotrophic organisms. A few lower eukaryotes contain hydrogenase enzymes but are of a very limited distribution. Hydrogen is an energy rich molecule that releases over 100 kJ per gram when oxidized to water and as such can act as a source of low potential reductant (H_2/H^+ , $E_o' = -420\text{mV}$) for cellular energy generation and anabolic processes [10]. Figure 1.1 represents a general scheme of possible reactions that occur at different levels of a stagnant aquatic environment [11]. Hydrogen oxidation can be coupled with membrane electron transport to a variety of terminal electron acceptors such as fumarate, sulfate, carbon dioxide, and oxygen. The production of hydrogen is typical of organisms occupying anaerobic, low potential environments and is often used as a redox valve to release excess reductant. The synthesis of hydrogen in these organisms allows the regeneration of oxidized electron carriers and the continuation of energy generation via fermentation. H_2 is regarded as a trace gas, though, as little is released into the atmosphere. Organisms occupying more redox positive levels of the environment are positioned to efficiently utilize hydrogen and prevent the wasteful release of this energetic compound.

While the reaction hydrogenases catalyze is simple, the enzymes involved are extremely complex. Production of the enzymes is highly regulated on the transcriptional level and requires a complicated *in vivo* maturation process, and is inactivated by molecular oxygen. Three classes of hydrogenases are known, nickel-

Figure 1.1.

Anaerobic and aerobic reaction scheme of prokaryotes in a stagnant aquatic stratified system adapted from [11].



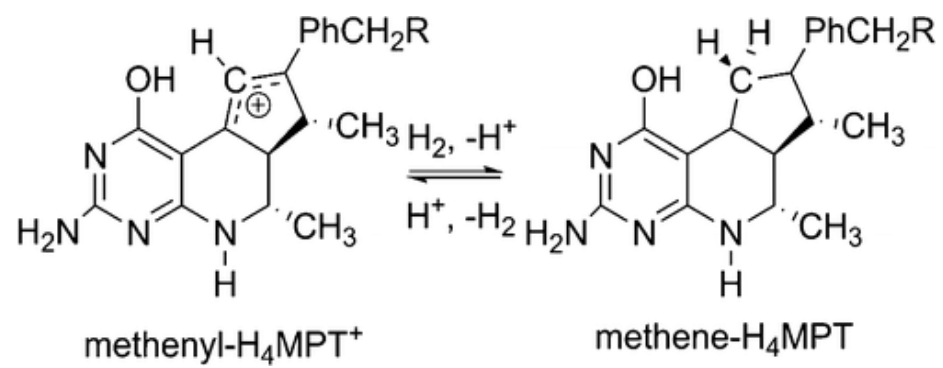
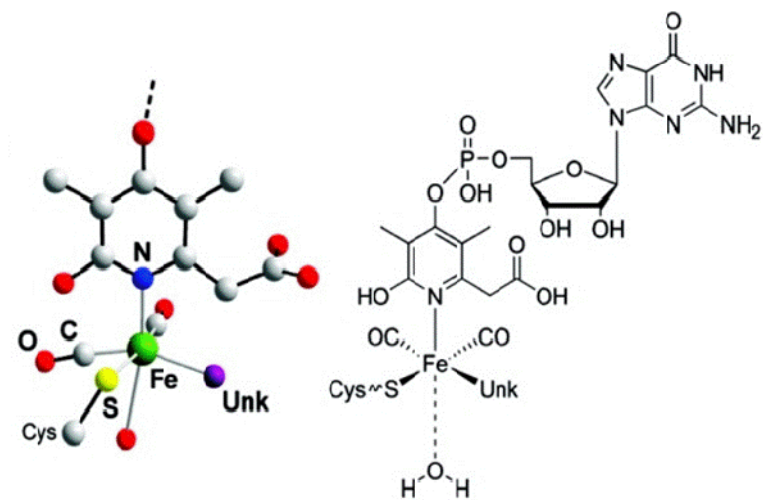
iron [NiFe], iron-only [FeFe], and iron sulfur free hydrogenase [Fe] (methylenetetrahydromethanopterin (methylene-H₄MPT) dehydrogenase) [12,13,14]. The three classes of hydrogenase, which are phylogenetically unrelated, all catalyze the reversible reduction of protons to hydrogen [15]. This evolution of enzymes that have different mechanisms for activating molecular hydrogen is one of the most compelling cases of convergent evolution. Though the reactions catalyzed by hydrogenases are reversible, they are usually biased to one direction (H₂ oxidation or H⁺ reduction) *in vivo*. Depending on their location the enzymes may be tuned for intracellular redox balancing by producing or disposing of equivalents of reductant and some involved in creating proton gradients for ATP synthesis. The hydrogenase enzymes are localized to the cytoplasm or periplasm in prokaryotes, either in a soluble or membrane bound form. In a limited number of unicellular eukaryotes hydrogenases are found localized to specialized subcellular compartments (e.g. chloroplasts in *Chlamydomonas reinhardtii*). Three general designations are used to describe these enzymes: membrane bound (MBH), soluble (SH), and regulatory (RH). MBH enzymes are usually involved in hydrogen oxidation and the SH family in proton reduction, although many exceptions are known. Regulatory hydrogenases do not actively participate in hydrogen metabolism but rather function as a sensor to regulate the expression of genes involved in H₂ oxidation. Herein the three classes of hydrogenase are described as pertaining to their structure, physiological function, and known maturation requirements for active site biosynthesis.

IRON SULFUR CLUSTER FREE HYDROGENASES

The [Fe] hydrogenases are found in only a few species of methanogenic Archaea and their expression is induced under nickel limited conditions [16]. The enzymes catalyze the reversible reduction of methenyltetrahydromethanopterin with H_2 to methylenetetrahydromethanopterin and a proton (Figure 1.2a [17]). The reduction of the methenyl-substrate with H_2 is an intermediary step in the biological conversion of carbon dioxide to methane. The [Fe] hydrogenase enzymes are not found in all methanogenic archaea, and this is most likely explained by the presence of two other enzymes, a F_{420} -reducing [NiFe]-hydrogenase (Frh) and a F_{420} -dependent methylene- H_4 MPT dehydrogenase (Mtd) [18]. The structure of a native [Fe] hydrogenase has not been determined as all crystals have been twinned precluding phasing of X-ray data (Rolf Thauer, unpublished results). A structure has been obtained by the reconstitution of an [Fe]-hydrogenase apoenzyme from *Methanothermobacter jannaschii* with an iron cofactor from *Methanothermobacter marburgensis*, which has allowed the crystallization of an active enzyme and its characterization by X-ray crystallography (Figure 1.2b) [12]. In the [FeFe] and [NiFe] hydrogenase H_2 is activated at the binuclear active site and electrons flow through a set of FeS clusters to the terminal electron acceptor. [Fe] hydrogenases, however, do not release electrons and it is thought that the carbocation substrate methenyl- H_4 MPT⁺ directly accepts a hydride from H_2 . Two possible mechanisms for this reaction have been proposed. Shima and Thauer hypothesize H_2 cleavage comes from a concerted action of the substrate, a strong hydride acceptor methenyl- H_4 MPT⁺, and the Lewis acid Fe(II) of the active site. This scheme would problematically lower the pK_a of the H_2

Figure 1.2

- A. Electron acceptor in iron sulfur cluster free hydrogenase,
methenyltetrahydromethanopterin**
- B. Active site structure (Unk, Unknown ligand) adapted from [18].**

A**B**

and deactivate it with respect as a hydride source. Tard suggests a more reasonable proposal that Fe(II) coordinates H₂ and a neighboring base heterolytically splits H₂ by abstracting a proton [18]. This mechanism involving Fe(II) would generate a hydride more suited for concerted or sequential transfer to the methenyl-H₄MPT⁺. A second pathway for H₂ oxidation by the [Fe] hydrogenase involves oxidative addition of H₂ to an Fe⁰ species generating a dihydride followed by removal of one dihydride by methenyl-H₄MPT⁺. Regeneration of the dihydride intermediate could occur via proton removal prior or concerted with H₂ ligation to the monohydride [18]. The precedent for both of these proposed chemical reactions have been well established [19]. This [Fe] hydrogenase is unique and a relative orphan in the grand scheme of hydrogen metabolism as it is present in only a few methanogens and performs the niche reaction of hydrogen oxidation using a very specialized electron carrier in nickel limited growth conditions.

IRON-IRON HYDROGENASES

[FeFe] hydrogenases are distributed throughout bacteria and a few eukaryotes, but are not present in Archaea [11]. The absence of [FeFe] hydrogenases in Archaea is not consistent with evolution and the current arrangement of the phylogenetic tree of life. A reasonable explanation for some eukaryotes possessing the genes encoding [FeFe] hydrogenase and their maturation factors is either lateral gene transfer or more likely endosymbiosis of a [FeFe]-hydrogenase-containing prokaryote by an early ancestor. Many of the [FeFe] hydrogenase are monomeric but dimeric, trimeric, and tetrameric enzymes have been described [20,21,22]. [FeFe] enzymes are cytoplasmic and generally function in the evolution of hydrogen coupled to the oxidation of

ferredoxin (Fd). Compared to the other families of hydrogenase, the [FeFe] enzymes are orders of magnitude more catalytically active but are easily and irreversibly inactivated by molecular oxygen [11]. Structures of the [FeFe] enzymes have been determined [21,23,24,25,26] and reveal a cysteinyl-coordinated binuclear active site bridged by a dithiolate ligand and bound to a 4Fe4S cubane cluster (H-cluster) (Figure 1.3a). The catalytic site contains the biologically unusual ligands cyanide (CN⁻) and carbon monoxide (CO). The identity of the bridging atom in the dithiolate ligand remains in contention though recent crystallographic data refinement suggests a dithiomethylamine ligand [27].

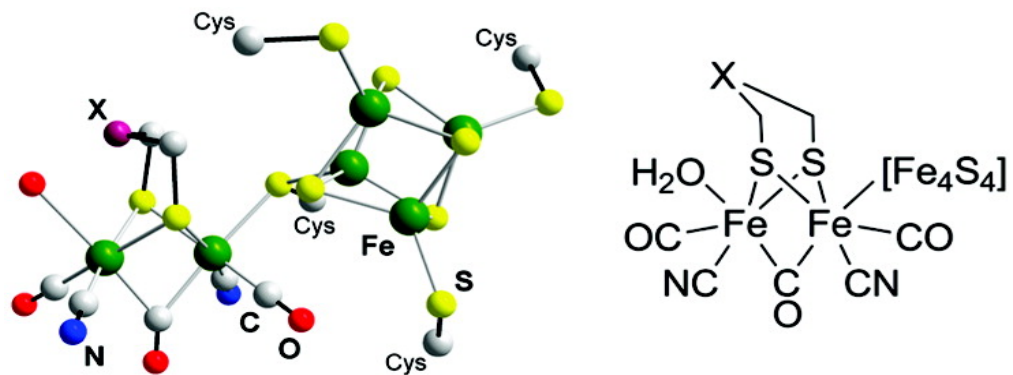
Although hydrogenases have been studied for the past 80 years only recently has great progress been realized. As with other complex metalloenzymes, such as nitrogenase, [FeFe] hydrogenases require a set of maturation factors for active site biosynthesis and insertion. It was demonstrated in *Chlamydomonas reinhardtii*, a unicellular green alga, that two proteins are required for the production of a functional hydrogenase, hydEF and hydG [28,29]. Using this information, researchers were successful in heterologous expression of a *C. reinhardtii* [FeFe] hydrogenase in *E. coli*, which contains no native [FeFe] enzyme [30]. This provided the model system in which to elucidate the mechanism and substrates necessary for [FeFe] H-cluster assembly. The maturation of the [FeFe] enzymes requires only three gene products (two of the hyd genes are fused in *C. reinhardtii*) for the assembly of a catalytically active hydrogenase. To investigate the mechanism of maturation of the H-cluster, King et al. expressed the maturation enzymes HydE, HydF, and HydG from *Clostridium acetobutylicum* with various other algal and bacterial [FeFe]

Figure 1.3.

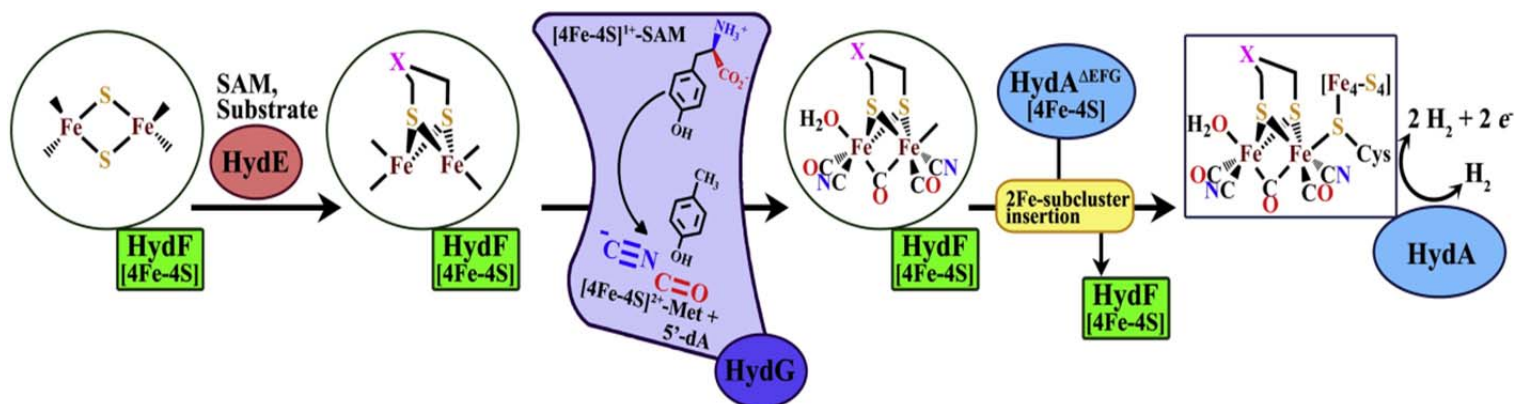
A. Catalytic site H-cluster of the [FeFe] hydrogenase

**B. Proposed maturation pathway of [FeFe] hydrogenase adapted from
[18,31].**

A



B



hydrogenases (HydA) [30]. The three maturation factors, HydE, HydF, and HydG, are common to all organisms expressing an [FeFe] hydrogenase [28]. Based on PFAM analysis HydE and HydG are members of the radical S-adenosylmethionine (AdoMet) enzyme family and HydF is predicted to have GTPase activity. All three proteins are also able to bind iron sulfur clusters based on work with these enzymes from the organism *Thermatoga maritima* [32,33]. *In vitro* work suggests that activation of HydA expressed without any of the three maturation factors (HydA^{ΔEFG}) only occurs with extracts of *E. coli* in which all three maturation factors were co-expressed [34]. Incubation of HydA^{ΔEFG} with extracts containing singly expressed HydE, HydF, or HydG failed to activate HydA, suggesting an activating component that is protein associated. To elucidate the mechanism of HydA activation, Peters and coworkers co-expressed all three Hyd maturation factors and independently purified each. By incubating HydA^{ΔEFG} with each individual Hyd purified from a Hyd^{EFG} background it was determined that HydF is able to act as a scaffold and transfer an activating component to HydA.

The general scheme of HydA H-cluster maturation is detailed in Figure 1.3b. With the development of *in vitro* maturation protocols for the [FeFe] hydrogenase it became possible to ask which specific maturases and precursors are responsible for the CO and CN⁻ ligands. Peters and coworkers provided the initial data suggesting that CO and CN⁻ synthesis utilizes tyrosine as a substrate [35]. A more in-depth study by the lab of Cramer and coworkers solidified the conclusion that functional groups of tyrosine are ultimately converted into the biologically unusual ligands cyanide and carbon monoxide [31]. Kuchenreuther et al. labeled each carbon of tyrosine

individually (^{13}C) and analyzed the *in vitro* matured enzyme with Fourier transform infrared spectroscopy (FTIR). The labeling studies demonstrated unequivocally that the CO moieties are derived from the carboxylate carbon and that CN^- originates from the amino substituent of tyrosine [31].

The mechanism of proton reduction and hydrogen oxidation by hydrogenase has been the subject of much research. In contrast with inorganic catalysts (e.g. platinum-based electrodes), hydrogenase heterolytically cleaves hydrogen [36]. The enzymes also catalyze the interconversion of para- (parallel nuclear spins) to ortho-dihydrogen [37]. A common characteristic of hydrogenase enzymes are the biologically unusual ligands CO and CN^- at the sulfur-bridged bimetallic active sites. These ligands are required to activate hydrogen at the catalytic center of hydrogenase. The [FeFe] hydrogenase has been extensively studied with regards to catalytic mechanism. Spectroscopic studies of the [FeFe] hydrogenase suggest that only two states of the active site can be stable intermediates of the catalytic cycle, considering the redox potential ranges in which the enzyme can catalyze H_2 turnover [38]. The two redox states are designated H_{ox} and H_{red} as outlined in Figure 1.4. H_{ox} is the redox state available for heterolytic cleavage of H_2 and H_{red} is responsible for proton reduction. There is a one electron difference between these two states, but the hydrogenase reaction requires two electrons; the FeS clusters must be responsible for accepting and transferring the additional electrons. In contrast to the [NiFe] hydrogenases, *vide infra*, there is no spectroscopic evidence of an intermediate with a hydride present on the [FeFe] catalytic site, though a hydride intermediate is expected

Figure 1.4.

Catalytic cycle of the [FeFe] hydrogenases adapted from [39].

to exist. The spectroscopic and structural studies of the [FeFe] hydrogenase begin to give clues to the mechanism of hydrogen activation at the 2Fe subcluster. The model generally accepted involves coordination of H₂O at the ligand exchangeable Fe of the H_{ox} state. Upon metal cluster reduction or presence of available H₂ as a coordinating group the water is displaced to form the hydride intermediate. Like other hydrogenases, [FeFe] enzymes are inhibited by CO in a competitive manner. Crystallographic investigations of CO inhibited enzymes revealed the CO moiety on the distal Fe [40,41]. Owing to the available binding ability of CO at this Fe, heterolytic H₂ bond cleavage is proposed to take place at this distal Fe site. FTIR studies of the *C. reinhardtii* hydrogenase revealed the bridging CO moiety of the H-cluster is present in both the H_{ox} and H_{red} state, further suggesting that H₂ activation takes place at the distal Fe [42]. Several groups have suggested that binding of H₂ at the distal Fe, which has the bridging CO group in *trans* position, favors heterolytic cleavage by increasing the acidity and allowing terminal hydride binding [41,43,44,45]. The cleavage of H₂ may be assisted by proton extraction by the putative amino group of the dithiolate ligand bridging the 2Fe site [24,46,47,48]. With this mechanism, simultaneous with H₂ heterolytic cleavage, an electron is donated to the iron-sulfur transport chain, leaving the putative hydride bound to the distal Fe [49]. This Fe(II)-Fe(II)-(H⁻) has the same electronic character as another predicted state, Fe(I)-Fe(I). This electron rich binuclear center is suggested to be the starting point for the reverse reaction, proton reduction [44,49,50,51].

[FeFe] hydrogenases, in terms of minimum subunit composition, are the simpler of the H₂ activating enzymes. The majority of [FeFe] enzymes are monomeric and

consists of ca. 350 residues containing the catalytic site, but across phylogenetic lines can vary greatly in size [13]. Many of the [FeFe] hydrogenase contain additional FeS clusters for electron transfer to the H-cluster and can be more than 800 residues. The core of the [FeFe] hydrogenases contain a highly conserved domain involved in coordinating the H-cluster. Conserved amino acids around this H-cluster domain include four cysteines, a few residues around the catalytic site, and those presumed to be involved in the H⁺ and H₂ channels to and from the buried active site [25,52]. Although the monomeric [FeFe] enzymes are in the majority, many other iron hydrogenases contain a variety of additional subunits. Known examples include the tetrameric NADP-reducing from *Desulfovibrio fructosovorans* and trimeric bifurcating from *Thermotoga maritima* [22,53]. In general, though, [FeFe] enzymes are biased to proton reduction and function as a redox valve to release excess electrons during fermentation.

NICKEL-IRON HYDROGENASES

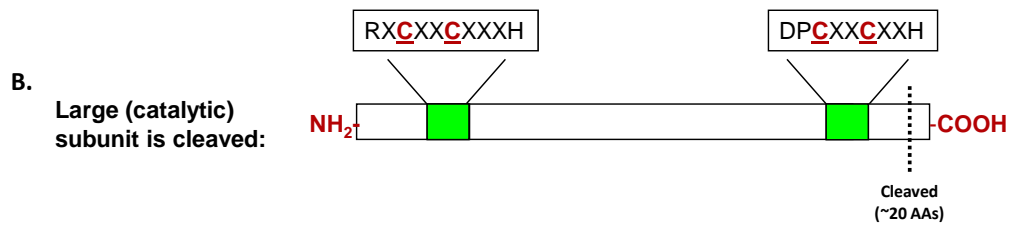
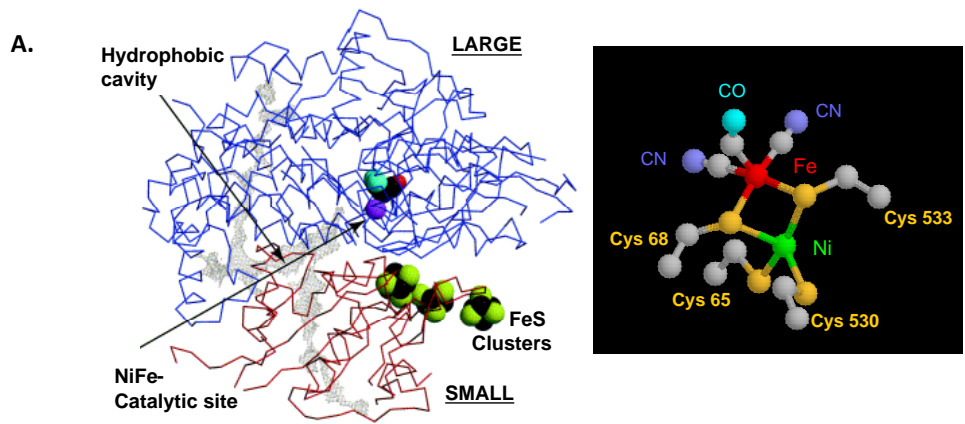
The majority of hydrogenases that occur in nature are of the [NiFe] variety and these are the focus of this research. These enzymes have also been well characterized and several crystal structures are available [54,55,56,57,58,59]. The [NiFe] enzymes are composed of at least two subunits; a large subunit (LSU) containing the active site and a small subunit (SSU) containing FeS clusters for trafficking electrons to or from the active site. The catalytic site is composed of a bimetallic Ni and Fe buried deep within the inter of the LSU (Figure 1.5a). The [NiFe] active site is coordinated by four cysteines in the LSU which are found in CxxC motifs on the N- and C-terminus of the protein. Two of the cysteines also coordinate the Fe atom which is modified

with two CN^- and one CO ligand (Figure 1.5b) [60,61,62]. These unlikely ligands are believed to maintain the Fe in a low spin state to facilitate the activation of hydrogen. Such ligands are also found on the [FeFe] hydrogenases [21], which have an active site geometry surprisingly similar to that of the [NiFe] enzymes. This is an evocative example of convergent evolution as two different systems arose which both require similar active site geometric structure, and cyanide and carbon monoxide ligands to activate hydrogen [20,25,63]. Evidence of [NiFe] enzymes that contain extra CN^- ligands on the Fe [64] as well as the Ni [65] has been demonstrated and appears to affect the enzyme's sensitivity to oxygen inactivation. Organometallic chemistry obviously plays an important role in the biological activation of hydrogen [63].

The [NiFe] hydrogenases are routinely purified under aerobic conditions – even from anaerobic organisms – and are catalytically inactive. The model for catalytic mechanistic studies is the [NiFe] hydrogenase from *Desulfovibrio vulgaris* MF as its structure has been determined to a very high resolution in the oxidized[66], reduced[67], and the CO-inhibited states [68]. The inactive states of the enzyme (termed Ni-A and Ni-B) are proposed to contain a bridging oxo-group (likely a peroxide or hydroperoxide molecule) between the nickel and iron atoms, although the exact identity is not known (Figure 1.6) [58,60,61,69,70]. Catalytic activity can be regenerated by incubating the oxidized enzyme in reducing conditions under an atmosphere of H_2 for several hours. The Ni-A state is designated unready-inactive and the Ni-B ready-inactive. The Ni-A state requires much longer incubation to obtain an active enzyme whereas the Ni-B state can be quickly reduced to a catalytically active form [71]. A few so-called oxygen-tolerant hydrogenases have

Figure 1.5.

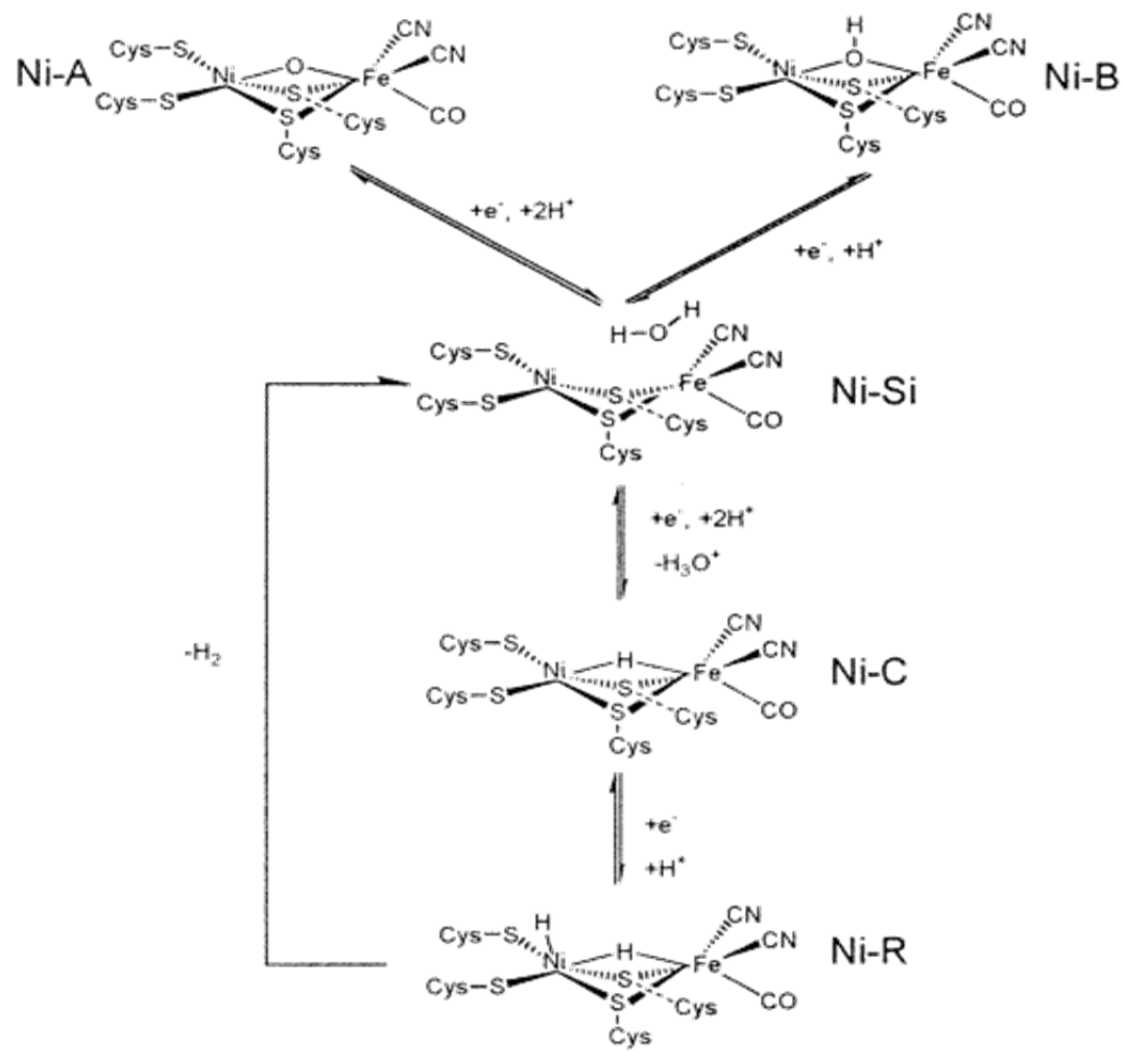
**[NiFe] hydrogenase general structure and catalytic site. Modified from
[57,58,60,61,69].**



been reported to not exhibit a Ni-A state and minimize the deleterious effects of molecular oxygen by only resting in the easily reactivated Ni-B state [72,73].

Recently the structures of two oxygen-tolerant hydrogenases (MBH from *Hydrogenovibrio marinus* and *Ralstonia eutropha* H16) were solved and revealed the presence of a novel 4Fe3S cluster [74,75]. This unprecedented cluster is proposed to not only be a component of electron transfer for the catalytic cycle, it may also donate two electrons and one proton for the reduction of O₂ in preventing the formation of an unready, inactive state of the enzyme [74]. The catalytic states of the [NiFe] active site were initially characterized by EPR analysis but this only provides insight into the paramagnetic states of the [NiFe] cluster. Introduction of Fourier transform infrared spectroscopy (FTIR) allows analysis of all redox conditions of the [NiFe] site by detecting signals from the CO and CN⁻ ligands of the Fe atom. Interestingly, the [FeFe] hydrogenase is the only other known metalloenzyme that exhibits these characteristic FTIR signals [70]. Upon one electron reduction of the Ni-A and Ni-B states, the catalytically inactive Ni-SU (silent unready) and Ni-SI (silent ready) EPR silent states are formed, respectively [39]. Further reduction of the Ni-SI state produces a third EPR active state, Ni-C, and is representative of the active enzyme [69,76,77,78,79]. The fully reduced and EPR silent state, Ni-R, is realized after an additional one electron reduction of the Ni-C state. Through compilation of these analyses in different redox states, the catalytic cycle of the [NiFe] site has been elucidated to a fair degree of accuracy (Figure 1.6). These results suggest a reaction mechanism that maintains the Fe in a low spin and low oxidation state through all reaction intermediates while the Ni switches formal charge between a diamagnetic Ni

Figure 1.6
Catalytic cycle of [NiFe] Hydrogenase From [80].



(II) and paramagnetic Ni (III) [71]. Heterolytic cleavage of hydrogen is predicted to take place at the redox active Ni ion [39].

Knowing that [NiFe] enzymes are ubiquitously distributed throughout the domains bacteria and archaea, it is not surprising they are the most structurally and functionally diverse class of hydrogenase. The classification of these enzymes originally was based on electron donor specificity, i.e. NAD, cytochromes, F_{420} , or ferredoxins, but it became exponentially difficult to classify enzymes with the advent of high throughput genome sequencing [11]. Despite the diversity of [NiFe] enzymes, all are based around a minimal dimeric structure consisting of at least a large catalytic subunit and small FeS-containing subunit for electron transfer to or from the active site. These subunits interact through a large contact surface and form a globular heteromeric complex. Two highly conserved regions exist in the large subunit around the two [NiFe] coordinating CxxC motifs, termed L1 and L2. Based on these sequences, nickel-iron enzymes can be divided into four groups as detailed in Table 1.

Group 1 [NiFe] enzymes are described as membrane-bound uptake hydrogenases and generally function to link the oxidation of hydrogen to electron acceptors such as NO^3^- , SO_4^{2-} , fumarate, and CO_2 (anaerobic respiration) or to O_2 (aerobic respiration) and conserve energy via a proton gradient [11]. These enzymes are located on the inner membrane, periplasmic facing, and connected to the quinone pool of the respiratory chain by a third subunit. Iterations on this basic structure are found across proteobacteria but the function remains conserved. Hydrogenase assembly is complex and as such the translocation of the enzyme to the periplasm must proceed

Table 1.

Group	Function	Length
1	Membrane-bound H ₂ uptake hydrogenases	S 268 - 552
		L 428 - 633
2a	Cyanobacterial uptake hydrogenases	S 284 - 384
		L 416 - 547
2b	H ₂ -sensing hydrogenases	S 258 - 347
		L 472 - 496
3a	F ₄₂₀ -reducing hydrogenases	S 216 - 298
		L 370 - 469
3b	Bifunctional (NADP) hydrogenases	S 237 - 282
		L 412 - 458
3c	Methyl-Viologen-reducing hydrogenases	S 287 - 366
		L ^a 418 - 496
3d	Bidirectional NAD(P)-linked hydrogenases	S 160 - 209
		L 471 - 507
4	Membrane-bound H ₂ evolving hydrogenases	S 135 - 277
		L 358 - 588

Group	Large subunit pattern
1	L1 [EGMQS]RxC[GR][IV]Cxxx[HT]xxx[AGS]x(0,4)[VANQD]
	L2 [AFGIKLMV][HMR]xx[HR][AS][AFLY][DN]PC[FILMV]xC[AGS]xH
2a	L1 PR[AIV]CGICx(1,3)Hx(0,2)Lxx[AST]
	L2 Vx[KR]S[FHY]DxCxVC[ST][TV][HK]
2b	L1 PR[IV]CGICS[IV][AS]Q[GS]xA
	L2 H[IV]VRSFDPCMVCT[AV]H
3a	L1 R[FIV]CG[ILV]C[PQ]x[APT]H[ACGT]x[AS][AGS]
	L2 R[ACS]YD[IP]C[AILV][AS]Cx(2,3)Hx[ILMV]
3b	L1 R[IV]C[AGS][FIL]Cxxx[HY]xx[AST][ANS]xx[AS][AILV]
	L2 R[ANS][FHY]DPCISC[AS][ATV]H
3c ^b	L1 Px[FILV][TV][ADPST]x[IV]CG[IV]CxxxHxx[AC][AS]xxA
	L2 E[FMV][AGLV][FIV]Rx[FY]DPCx[AS]C[AS][ST]Hx[AILV]
3d	L1 Ex[APV]xxxxRxCG[IL]Cxx[AS]Hx[IL][ACS][AGS][AGNSV][KR][ATV]xD:
	L2 DPC[IL]SC[AS][AST]H[ASTV]x[AG]xx[APV]
4	L1 C[GS][ILV]C[AGNS]xxH
	L2 [DE][PL]Cx[AGST]Cx[DE][RL]

Adapted from [15].

through either membrane targeting and translocation (Mtt) or twin-arginine translocation (Tat) machinery [81,82]. Protein transport is Sec-independent and provides fully folded enzyme transfer across the inner membrane. A conserved signal peptide (ca. 35-50 amino acids) is present on the small subunit and allows the so-called hitchhiker mechanism of transporting both the small and large catalytic subunit [11].

Group 2 encompasses the cyanobacterial uptake (subgroup 2a) and H₂ sensing [NiFe] enzymes (subgroup 2b). Two distinguishing features of this group include the small subunit lacking an N-terminal signal peptide and numerous identical SSU deletions as compared to group 1 enzymes. Group 2a cyanobacterial hydrogenases, generally designated as HupSL, are enzymes differentially regulated with nitrogenase and function to recapture the H₂ concomitantly released during N₂ fixation. Group 2b regulatory hydrogenases (RH) represent a unique set of H₂ sensors that function in transcriptional regulation of other uptake [NiFe] enzymes. These RH form multimeric complexes with kinases to create a hydrogen-dependent phosphorylation and signaling cascade mechanism. In *Ralstonia eutropha* H16 and the absence of hydrogen, the regulatory hydrogenase functions to activate a kinase, HoxJ, which subsequently phosphorylates HoxA inhibiting transcription of hydrogenase genes. In the presence of hydrogen, kinase activity is inhibited by the RH and genes associated with hydrogen oxidation are derepressed [83]. While these enzymes contain the usual [NiFe] catalytic site they are insensitive to oxygen. It has been hypothesized that a narrow gas channel precludes oxygen penetration of the buried catalytic site. Site-directed mutagenesis of *R. capsulatus* HupUV and *R. eutropha* HoxBC confirmed

that enlarging the gas channel by substituting amino acids with less bulky side chains conferred oxygen sensitivity [84,85].

Group 3 heteromultimeric cytoplasmic [NiFe] hydrogenases represent a set of enzymes where the dimeric hydrogenase module is associated with other subunits involved in binding redox active soluble cofactors (e.g. F₄₂₀, NAD(P)). The group is designated bidirectional due to the apparent ability to both oxidize hydrogen and generate reduced cofactor or oxidize cofactors and evolve molecular hydrogen *in vivo*. Many members of this group are found in the domain Archaea and also in bacteria and cyanobacteria. NAD(P)-linked hydrogenases from, *R. eutropha*, *Synechocystis* spp., and *P. furiosus* have been the focus of much research. The HoxYH enzyme from *R. eutropha* was the first NAD-dependent hydrogenase isolated and consists of the hydrogenase dimeric module and HoxFU diaphorase subunits. The Ni in the active site of this enzyme has an additional CN⁻ moiety bound that may contribute to oxygen tolerance [64]. The cyanobacterial bidirectional hydrogenase from photosynthetic *Synechocystis* PCC6803 is a pentameric enzyme (HoxEFUYH) able to reduce and accept electrons from NAD(P)H [86]. The cyanobacteria phyla that harbor both hydrogenase and photosynthetic components present an interesting system in which to possibly link the two reactions. In dark-adapted anaerobic cultures of *Synechocystis* PCC6803 a transient burst of hydrogen is observed upon illumination. The H₂ synthesis is most likely due to the sudden increase of NADPH production by the photosynthetically driven ferredoxin:NADP oxidoreductase. The production of hydrogen ceases shortly after dark to light transition due to production of molecular oxygen from photosystem II [86]. The cessation of hydrogenase activity

due to oxygen inactivation highlights the difficulty of working with and manipulating the enzymes especially when attempting to link non-physiological reactions. The SH from the hyperthermophilic Euryarchaeon *Pyrococcus furiosus* is a well-studied enzyme that recently presented itself as a model for engineering hydrogenases. Though belonging to the bidirectional group, the tetrameric NAD(P) linked hydrogenase appears to function *in vivo* only to oxidize hydrogen for the production of NADPH [87]. The recent development of genetics in *P. furiosus* has allowed for the facile manipulation of the *Pf* chromosome [88]. Overexpression of SHI was reported and represents a new model system in which to investigate these enzymes from hyperthermophiles [89].

Group 4 hydrogenases are a unique class of membrane bound [NiFe] multimeric complexes as some of the enzymes exclusively catalyze proton reduction, a reaction normally catalyzed by the [FeFe] hydrogenases. Because many of the group 4 enzymes pump a proton or sodium ion along with H₂ evolution, they are referred to as energy-converting hydrogenase (Ech) [15]. The first enzyme described of this group, *E. coli* hydrogenase-3 (Hyd3), is linked to a formate dehydrogenase and forms a large formate hydrogenlyase complex (FLH-1) catalyzing the production of H₂ and CO₂ from formate [90]. In addition to the required large and small subunit the group 4 hydrogenases contain at least four other subunits, two hydrophilic proteins, and two integral membrane proteins [91]. Although the LSU and SSU of the Ech hydrogenases share little homology other than the sequences surrounding the conserved CxxC motifs, the partner subunits share a high degree of homology with NADH:quinone oxidoreductase, also known as complex I [92]. Complex I catalyzes

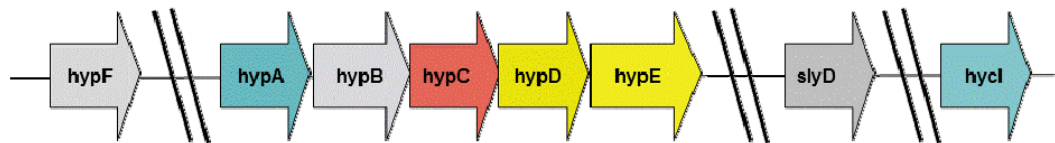
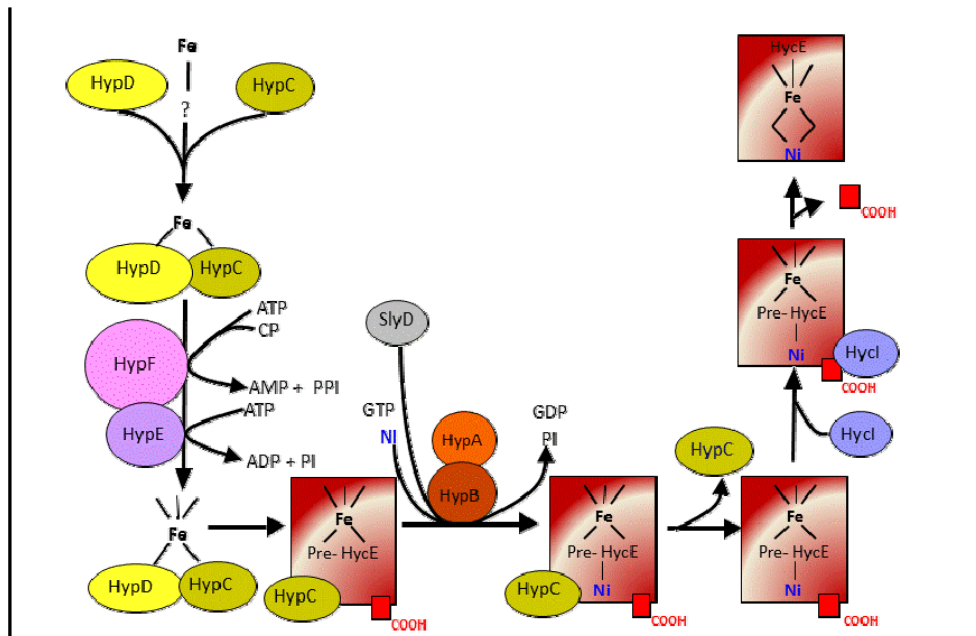
the oxidation of NADH and electron transfer to ubiquinone or menaquinone and concomitantly pumps protons or sodium ions across a membrane [93]. The close homology of these two complexes suggests that Ech type [NiFe] enzymes may be the ancestral origin of complex I [94]. A unique aspect of the Ech hydrogenases able to function reversibly *in vivo* is the lack of a C-terminal tail. The maturation of hydrogenases, described below in detail, usually involves the proteolytic cleavage of the C-terminus of the catalytic subunit as the final processing step in converting apoenzyme to holoenzyme. For an unknown reason, many Ech hydrogenases from methanogens and a few bacteria (e.g. *Methanosarcina barkeri*, *Rhodospirillum rubrum*, and *Carboxydotherrmus hydrogenoformans*) lack this C-terminus similar to that of regulatory hydrogenases. Many of the characterized Ech hydrogenases that have a strong bias for proton reduction and do not act reversibly *in vivo* (e.g. *Pf* MBH, *E. coli* Hyd3) in general do contain the typical C-terminal extension characteristic of [NiFe] hydrogenases. The lack of hydrogen oxidation, though, may be due to complexing with other large multimeric enzymatic complexes that would also have to function in reverse (e.g. *Pf* monovalent cation/proton antiporter (MRP), *E. coli* formate lyase), and this may be prohibitive for the reaction.

An area of research that has received much attention is the maturation of the [NiFe] hydrogenases. In proteobacteria, the genes that encode hydrogenase structural and maturation genes are clustered and in some cases include the regulatory genes responsible for controlling expression. The lab of August Böck has elucidated the maturation mechanism of Hyd3 from *E. coli* through a number of elegant studies (Figure 1.7). The Hyd3 system has become the model for [NiFe] maturation and

requires at least eight gene products for the proper assembly of the active site and correct folding of the catalytic subunit [95,96]. The maturation factors required for processing of hycE (catalytic subunit of HYD3 Figure 1.7) are HypA, HypB, HypC, HypD, HypE, HypF, HycI and SlyD. The hyp nomenclature from [97] represents “**h**ydrogenase **p**leiotropic” and indicates that a lesion in any one of these genes abolishes all hydrogenase activity from *E. coli*, which contains three characterized hydrogenase enzymes. The first step in hydrogenase maturation is the assembly of a $\text{Fe}(\text{CN})_2\text{CO}$ moiety. Iron is sequestered by HypC-HypD through a yet unknown mechanism and serves as a scaffold for addition of CN^- and CO. The order of CN^- and CO ligand addition to the Fe is not known but it has been shown that the biological source of CN^- is carbamoyl phosphate (CP) [98]. HypF, a carbamoyltransferase, catalyzes the transfer of CP onto the C-terminal cysteine of HypE as a thio-carboxamide in an ATP dependent reaction [99,100]. The thio-carboxamide of HypE is further dehydrated in an ATP dependent manner to a thiocyanate moiety [101]. A recent x-ray structure of HypC, HypD, and HypE from *Thermococcus kodakaraensis* has shed light on the possible mechanism of CN^- transfer [102]. The structures indicate that the HypC and HypD proteins form a complex that coordinate a mononuclear iron by HypD Cys38 and the only HypC cysteine, Cys2 (Figure 1.8). Watanabe et al. also propose a mechanism by which the CN^- transfer may occur, but this is not supported by any biochemical data [102]. It is not entirely clear when the CO addition to the Fe occurs but it must be within the same few steps surrounding CN^- addition. It was demonstrated in two different

Figure 1.7

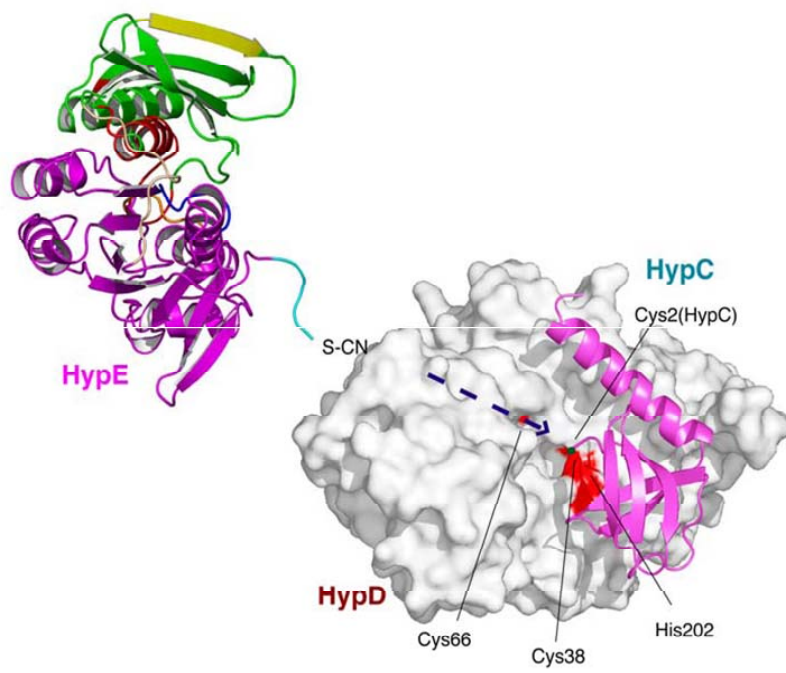
Maturation of *E. coli* HycE, the catalytic subunit of Hyd3. Adapted from [103].



systems that CO does not originate with carbamoyl phosphate. It was previously thought that the supposed low potential [FeS] cluster of HypD (the only Hyp gene product containing FeS clusters) may catalyze a reduction of $\text{CO}_2 \rightarrow \text{CO}$ but this is unlikely taking into account ^{13}C labeling studies [104,105,106]. It has been demonstrated that cultures of *Ralstonia eutropha* grown under ^{13}CO will produce the [NiFe] active site with a ^{13}C labeled CO ligand [106]. This suggests that the mechanism of CO ligand addition may include a short-lived “free” CO intermediate. However, very few biological reactions produce CO (incomplete combustion of organic compounds [107] heme degradation [108], methionine metabolism [109], fatty acid oxidation in plants [110], aromatic amino acid metabolism by bacteria [111], and more recently radical SAM cleavage of tyrosine [31]) and the actual source of the CO ligand remains an enigma. The most recent study by the group of Friedrich and Lenz concluded that the mechanism of CO synthesis is different than [FeFe] hydrogenases and it must come from metabolism [112]. As shown in Figure 1.7, $\text{Fe}(\text{CN})_2\text{CO}$ synthesis on the HypC-HypD scaffold is followed by dissociation of HypD and transfer of the immature metal site onto apo-hycE [113]. Nickel is subsequently delivered to the pre-hycE $\text{Fe}(\text{CN})_2\text{CO}$ subunit by the zinc metalloprotein HypA [114,115]. HybB, a metal binding and GTP-hydrolyzing enzyme, is also required for nickel insertion [116]. It has been demonstrated that the hydrogenase-deficient phenotype of HypA and HypB mutants can be complemented with high concentrations of nickel in the growth media [117,118].

Figure 1.8

HypC, HypD, and HypE modeling the CN⁻ transfer for the formation of the [NiFe] site precursor Fe(CN)₂CO from [102].



This implies that HypA and HypB may function only to improve the kinetics of metal insertion. HypB may also act as a switch that triggers the release of the Hyp proteins complexed with hycE upon successful nickel insertion [119]. A third gene, the peptidyl-prolyl *cis/trans* isomerase SlyD, has been implicated in improving nickel insertion efficiencies. It has not been demonstrated in *E. coli* that either HypA or HypB bind nickel; SlyD is a good candidate for the physiological supplier of Ni to the maturing hydrogenase [120]. The final step in processing the hycE protein is a C-terminal cleavage by the peptidase HycI. This step is dependent upon the presence of nickel and only occurs after Fe(CN)₂CONi is properly inserted into HycE [121,122]. Although HycI acts as a peptidase, common protease inhibitors are unable to prevent the C-terminal cleavage event, suggesting a novel mechanism of proteolysis [123]. It is proposed that the cleavage of the C-terminus brings about a major conformational change that “seals” the [NiFe] active site deep within the protein [124].

The focus of this thesis is the [NiFe] hydrogenases of thermophilic anaerobes, specifically those of the Euryarchaeon *Pyrococcus furiosus*. The following section details the criteria of thermophile classification, metabolic strategies employed by this genre for energy generation and unique adaptations anoxic microbes growing at elevated temperatures. The hydrogen-dependent metabolism of *Pf* is described with emphasis on the characteristics of the hydrogenases encoded this thermophilic Archaeon.

THERMOPHILIC ANAEROBIC METABOLISM

Bacteria and Archaea that grow at an optimal growth temperature ($T_{\text{opt}} > 50^{\circ}\text{C}$) and do not require oxygen for growth are described as thermophilic anaerobes

[125,126,127]. These organisms that exhibit extreme growth characteristics are of great interest for basic and applied science research. Having extreme growth characteristics translate to these organism's proteins also having extreme stabilities [128]. This is desirable from an industrial and biotechnological perspective as most chemical reactions proceed faster at higher temperatures and stability in non-aqueous media is beneficial [129]. Many thermophilic anaerobes are the focus of research because it is assumed they are the closest microorganisms to those responsible for the origin of life [130]. Indicators of biological life have been dated to 3.8 billion years ago (Ga) and fossils of microbial communities dated to 3.5 Ga, however oxygen accumulation in the atmosphere happened later, 2.1-2.3 Ga [131]. In addition to early life evolving anoxically, it is widely accepted that early organisms evolved at elevated temperatures. Some researchers disagree with this theory of a thermophilic origin of life and suggest that low temperature life evolved and a rapid selection of thermophiles occurred during the late bombardment [132]. This evolution, especially rapid adaptation, from mesophilic to thermophilic life is generally considered improbable and most posit that life originated around 80°C on clay or iron-sulfur mineral surfaces in shallow pools [133].

Though the first forms of life no longer exist, natural thermal environments similar to the conditions of early earth when life presumably began do exist [134]. Many of these environments are devoid of oxygen for a number of anaerobic factors: low O₂ solubility at elevated temperatures, hyper salinity, reducing gas infusion (H₂ and H₂S), and O₂ consumption by surface microbes [125]. By definition, anaerobes populating these environments are unable to use O₂ as a terminal electron acceptor,

even if they are able to survive in the presence of oxygen [135]. Many of these anaerobic thermophiles can tolerate exposure to atmospheric levels of oxygen especially at suboptimal growth temperatures or in the absence of metabolizable substrates [136,137]. In addition to substrate level phosphorylation, anaerobes are able to respire without oxygen and realize energy generation through electron transport driven ATP formation with a variety of terminal electron acceptors such as CO_2 , CO , NO_3^- , NO_2^- , NO , N_2O , SO_4^{2-} , SO_3^{2-} , $\text{S}_2\text{O}_3^{2-}$, S^0 , Fe(III) , Mn(IV) , and Mo(VI) [138,139]. Thermophiles by definition thrive at elevated temperatures, and are characterized by their optimal temperature (T_{opt}), maximal temperature (T_{max}), and the range over which the organisms continue to double [135]. Organisms with a T_{opt} of 50°C - 64°C are classified as moderate thermophiles, T_{opt} of 65°C - 79°C as extreme thermophiles, and $T_{\text{opt}} \geq 80^\circ\text{C}$ as hyperthermophiles [125,126,140]. Bacteria and Archaea able to grow above 35°C - 40°C are considered temperature-tolerant thermophiles [141]. Some thermophiles are able to grow over a very large temperature range, such as *Methanothermobacter thermautotrophicus* (22°C - 75°C) [135]. Conversely, other thermophilic anaerobes have very narrow temperature ranges in which growth is possible, such as *Anaerolinea thermolinosa* [142] (42°C - 55°C) and *Anaerolinea thermophila* [143] (50°C - 60°C). Hyperthermophiles with a $T_{\text{opt}} \geq 80^\circ\text{C}$ were first reported by Stetter and isolated from hot vents at Vulcano Island of the coast of Sicily, Italy, in 1981 [144]. Many of these hyperthermophiles are found at deep-sea vents or deep in hot spring channels and sediments, with the increased pressure allowing water to stay in liquid form well above 100°C [135,145].

The current record for T_{\max} is a *Methanopyrus kandleri* strain capable of growing under increased pressure at 122°C [146].

The extreme temperature in which thermophiles thrive is not the only similarity they may share with early forms of life; the mechanisms of carbon assimilation and cellular energy generation are also of great interest. The metabolic diversity of thermophilic anaerobes is quite varied but this is not surprising as they inhabit some of the most unique environments on earth. Many are chemoorganoheterotrophic, using organic compounds for carbon and energy, but a variety of other metabolic approaches such as chemolithoautotrophy, chemolithoheterotrophy, photoheterotrophy, and photoautotrophy are observed [135]. The mechanism of thermophilic chemorganoheterotrophic growth is further characterized by carbon source utilization and include glycolytic, cellulolytic, lipolytic, and peptidolytic metabolisms. Among the glycolytic thermophilic anaerobes, the Embden-Meyerhof (EM) and Entner-Doudoroff (ED) pathways have been discovered, but a number of modifications have been observed particularly within the domain Archaea [147]. Primary fermentation metabolites include acetate, lactate, ethanol, CO₂, and H₂. Some archaeal glycolytic pathways deviate from the classical EM pathway by the presence of several novel enzymes and enzyme families, catalyzing, e.g., the phosphorylation of glucose and fructose-6-phosphate, isomerization of glucose-6-phosphate, and oxidation of glyceraldehyde-3-phosphate [148,149]. Notable exception to these pathways include the euryarchaeon *Picrophilus torridus*, which was recently described to possess a strict nonphosphorylative Entner-Doudoroff pathway that involves a novel 2-keto-3-deoxygluconate-specific aldolase [150]. The most

abundant renewable natural plant fiber is cellulose and its degradation and subsequent conversion to biofuels, such as ethanol and butanol, by thermophilic anaerobic is the subject of intense research. The first hyperthermophilic organism capable of degrading cellulose was relatively recently isolated, the archaeon *Desulfurococcus fermentans* [151]. Of equally important interest is the metabolism of xylanolytic thermophilic anaerobes, as xylan, a component of plant hemicellulose, is the second most abundant renewable polysaccharide in biomass [135]. Thermophilic organisms possessing enzymes capable of breaking down the recalcitrant material found in plant biomass are of great interest as industrial scale hydrolysis would proceed faster and more efficiently at elevated temperatures [152]. Some thermophilic anaerobes are able to survive lithotrophically by catalyzing the oxidation of a gaseous component of deep-sea hydrothermal vents CO, by the equation $\text{CO} + \text{H}_2\text{O} \rightarrow \text{CO}_2 + \text{H}_2$. Acetogens can assimilate carbon dioxide utilizing the Wood-Ljungdahl pathway by the reaction $3\text{H}_2 + \text{CO}_2 \rightarrow \text{acetate}$ [153]. In addition to inorganic sources, some high temperature anaerobes are able to harvest light energy and convert it to chemical energy. Two biological mechanisms for the utilization of light energy are known, (bacterio)-chlorophyll and rhodopsins, though no anaerobes are known to contain rhodopsin [154,155]. The required cofactor of rhodopsin, retinal, is derived from the oxidative cleavage of beta-carotene, a reaction not possible in anaerobic metabolism and the reason for exclusion of this mechanism from anaerobes. Moderately thermophilic phototrophic-based metabolism has been observed but there are no known hyperthermophilic phototrophs, most likely due to the labile nature of the photosystems [138].

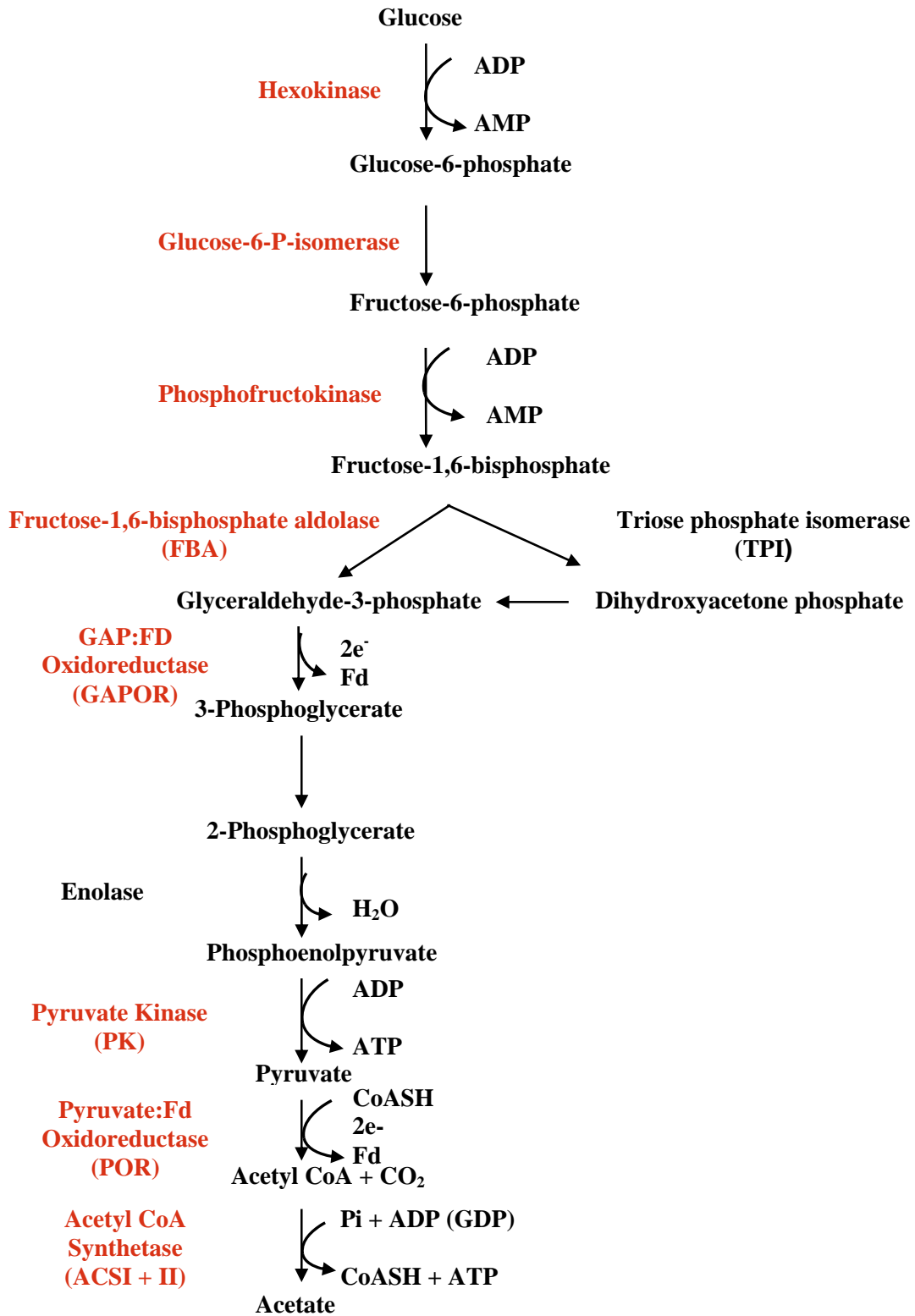
A variety of inorganic terminal electron acceptors define a large class of the thermophilic anaerobes. Sulfur in particular is utilized by a majority of thermophiles and Amend and Shock suggest the most common energy-yielding reaction for these organisms may be the reduction of elemental sulfur by the mechanism: $H_2 + S^{\circ} \rightarrow H_2S$ [138]. The anaerobic reduction of metals, such as Fe(III), are distributed in nearly all known high temperature environments [156,157]. Mn(IV) and Mo(VI) reduction is also known to be coupled to energy generation [158,159,160,161]. Other metals are known to be reduced by thermophilic anaerobes, such as Co(III), Cr(VI), and U(VI), but are most likely part of detoxification mechanisms [135,162].

PYROCOCCUS FURIOSUS METABOLISM AND HYDROGENASES

Pyrococcus furiosus (*Pf*), a euryarchaeon that grows optimally at 100°C, is a model for the study of hyperthermophilic physiology and metabolism. *Pf* was first isolated from geothermally heated marine sediments off the coast of Vulcano, Italy by Stetter and coworkers [163]. *Pf* is a strict anaerobe that grows heterotrophically using carbohydrates (starch, glycogen and cellobiose) or peptides (in the presence of sulfur (S°)) and produces organic acids, CO_2 and H_2 as end products. It preferentially releases excess reductant as H_2S rather than producing H_2 when grown in the presence of elemental sulfur (S°). Although *Pf* is able to ferment various disaccharides and complex carbohydrates as carbon source, it is unable to utilize monosaccharides. Through characterization of glycolytic enzymes in *Pf* and ^{13}C NMR spectroscopy it was determined that a modified Embden-Meyerhof (EM)

Figure 1.8

Modified Embden-Meyerhof glycolytic pathway of *Pyrococcus furiosus*.

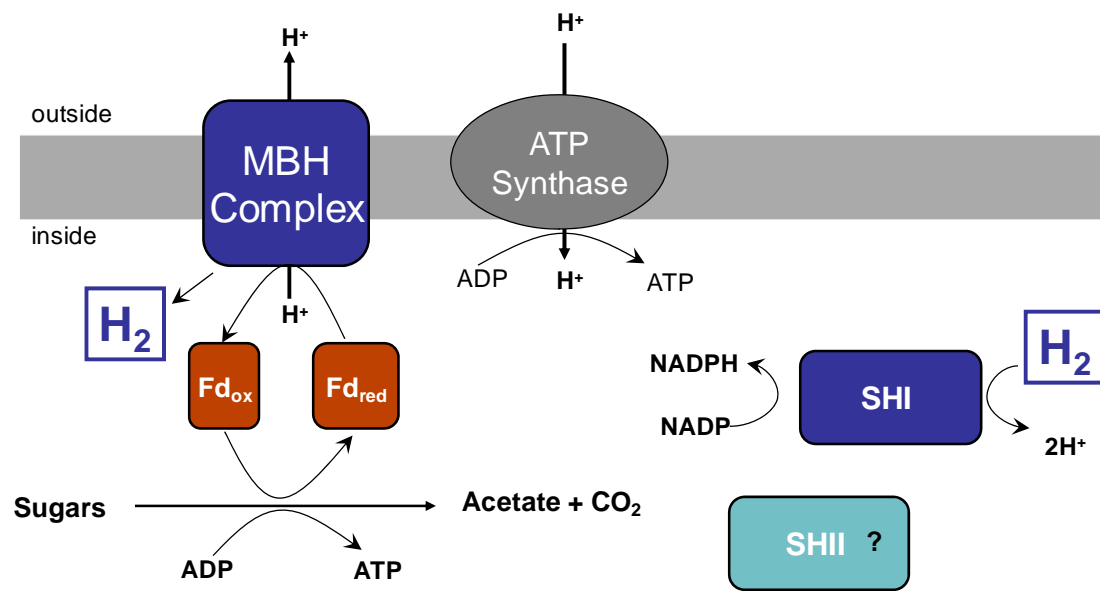


pathway is utilized (Figure 1.9) [164,165,166,167]. *Pf* produces only reduced ferredoxin (Fd_{red}) rather than NADH from the oxidation of glucose [168] and the two reactions responsible for this are glyceraldehyde:ferredoxin oxidoreductase (GAPOR, [166]) and pyruvate: ferredoxin oxidoreductase (POR, [169]). Other unusual features of the EM pathway in *Pf* include ADP- rather than ATP-dependent hexokinase and phosphofructokinase [167]. Fd_{red} produced from the oxidation of glucose predominantly has two fates depending on growth conditions, proton reduction generating hydrogen or in the presence of sulfur, S° reduction to H_2S , both of which are proposed to generate an ion gradient for energy conservation [170,171]. The focus of this thesis is hydrogen metabolism and the hydrogenases encoded by *Pf*.

Pf has three operons that contain genes with homology to [NiFe] hydrogenases; two cytoplasmic enzymes consisting of four subunits and a membrane bound hydrogenase with 14 putative subunits. The two soluble enzymes, termed soluble hydrogenase I (SHI) and soluble hydrogenase II (SHII), utilize NAD(P)(H) as the physiological electron carrier [172,173,174,175]. The membrane bound hydrogenase (MBH) accepts electrons from Fd_{red} and is the enzyme responsible for evolving hydrogen during growth [176]. It has also been demonstrated that the MBH complex pumps sodium ions concomitantly with the oxidation of ferredoxin and evolution of hydrogen. The proton motive force created by this ion gradient can be used to generate ATP via an ATP synthase [170]. The role of the soluble hydrogenases is speculated to be in the recycling of hydrogen produced by the MBH.

Figure 1.9

Current opinion of hydrogen metabolism in *Pyrococcus furiosus*.

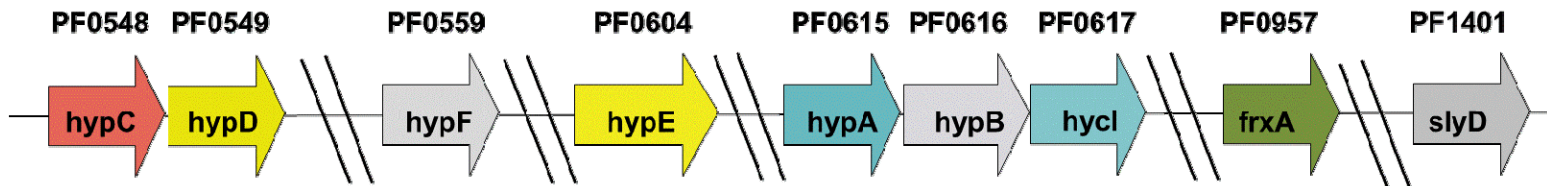
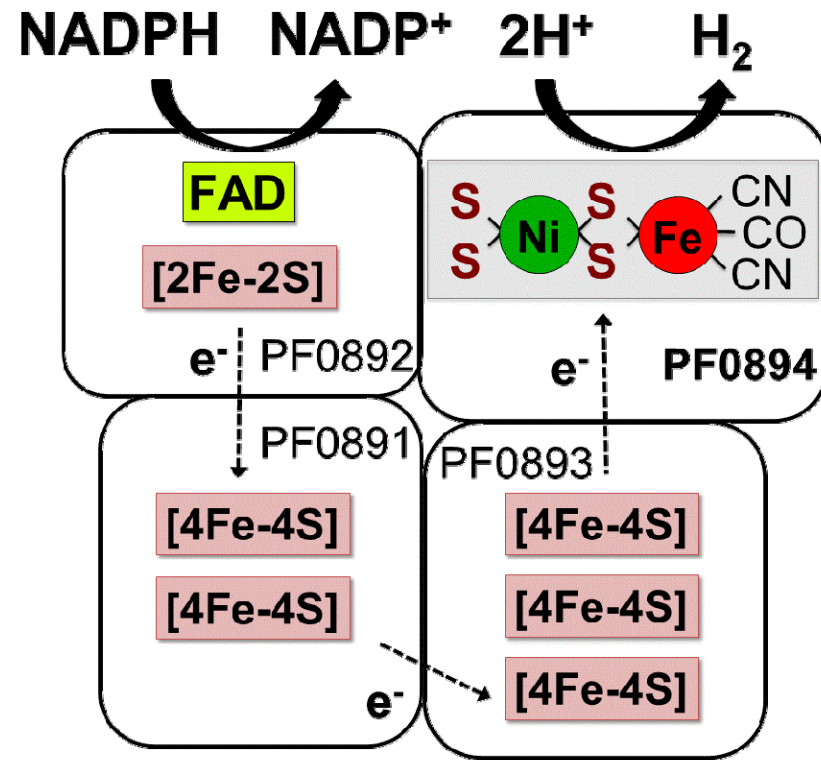


Although the SHI and SHII enzymes are able to efficiently reduce S° to H_2S with H_2 or NADPH *in vitro*, microarray analysis show that the enzymes are not expressed when *Pf* is grown in the presence of sulfur [177,178]. The most convincing evidence for the *in vivo* role of the soluble hydrogenase I come from *in vitro* activity ratios of $H_2 \rightarrow NADP$ and $NADPH \rightarrow H_2$. The soluble enzymes catalyze the uptake of hydrogen and reduction of the physiological electron carrier NADP about 10 times more efficiently than hydrogen evolution from reduced coenzyme [87,179].

The genome sequence of *Pf* is sequenced [179] and the genes encoding hydrogenases have been identified using N-terminal sequencing data from purified proteins [172,175]. In particular, the SHI is encoded by four genes (PF0891-0894) encoded by a single operon. The large subunit (LSU) and small subunit (SSU) characteristic of [NiFe] hydrogenases is encoded by genes PF0894 and PF0893, respectively (Figure 1.10) [172]. One of the additional subunits is predicted to contain FeS clusters (PF0891) and the other is predicted to be the flavin adenine dinucleotide (FAD)-containing diaphorase subunit (PF0892). SHI is extremely stable at high temperatures and in the presence of oxygen at moderate temperatures. The SHI activity has a $t_{1/2}$ at $90^{\circ}C$ of approximately 12 hours and $t_{1/2}$ after exposure to ambient oxygen (~20%) of about 6 hours [172]. Although SHI utilizes NADP(H) as a coenzyme at an optimal temperature of $100^{\circ}C$, assays are routinely carried out at $80^{\circ}C$ with the artificial electron donor/acceptor methyl viologen (MV) [180]. Assays are performed at $80^{\circ}C$ for convenience and hydrogen evolution using reduced MV catalyzes a reaction about 30-fold greater than the rate of NADPH oxidation.

Figure 1.10

Soluble hydrogenase I predicted cofactor content and maturation factors as predicted by homology to *E. coli*.



To produce an active hydrogenase, the genome of *Pf* must encode the maturation proteins processing [NiFe] hydrogenases. Homologs of the *E. coli* enzymes exist for seven of the eight accessory genes; HypA (Ni insertion, PF0615), HypC and HypD (Fe insertion (PF0548 and PF0549), HypE and HypF (CO/CN⁻ synthesis, PF0604 and PF0559), HycI (C-terminal peptidase PF0617), and SlyD (Ni insertion PF1401). An obvious homolog to HypB does not exist in *Pf*. The processing genes in *Pf* are not arranged in a single operon as most are in *E. coli* (Figure 1.10) but are broken into five different transcriptional units. Interestingly, *E. coli* contains three hydrogenases, all three membrane-bound, that all have a specific C-terminal protease involved in the last step of hydrogenase maturation. *Pf* also contains three hydrogenases but contains only one gene with apparent homology to [NiFe] peptidases.

5. PROPOSED RESEARCH

It has been demonstrated that by using enzymes of the pentose phosphate pathway, starch phosphorylase, and NADPH-utilizing *Pf* SHI, one can evolve hydrogen with a surprisingly high efficiency and yield [181]. Though promising, no system for expression of a recombinant hydrogenase in large quantities in a genetically tractable host is available. Much research has also been done to assess the possibility of linking hydrogenase enzymes to the low potential electrons generated during photosynthesis [182,183,184]. One major problem is the generation of oxygen during the water splitting reaction of photosystem II and the oxygen sensitivity characteristic of most hydrogenases. It is of major interest and importance to investigate the mechanism of such oxygen sensitivity. In order to facilitate this investigation and ultimately engineer a hydrogenase enzyme without this O₂

inactivation, it will be necessary to have a system in which to produce mutants that can be screened on a large and high-throughput scale. Chapter 2 describes the first heterologous expression of a [NiFe] hydrogenase in *E. coli* yielding preparative amounts of enzyme. With the advent of genetics it became possible to directly manipulate the hydrogenases of *Pf* in the native organism. Chapter 3 describes the novel over-expression of a dimeric form of soluble hydrogenase I of *Pf*.

CHAPTER 2
HETEROLOGOUS EXPRESSION AND MATURATION OF AN NADP-
DEPENDENT [NIFE]-HYDROGENASE:
A KEY ENZYME IN BIOFUEL PRODUCTION¹

¹ Robert C. Hopkins, Junsong Sun, Francis E. Jenney, Jr., Patrick McTernan, and Michael W. W.

Adams. 2010. *PLoS One*. 2010 May 6;5(5):e10526.

Reprinted here with permission of the publisher.

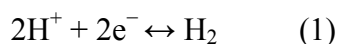
ABSTRACT

Hydrogen gas is a major biofuel that is metabolized by a wide range of microorganisms. Microbial hydrogen production is catalyzed by hydrogenase, an extremely complex, air-sensitive enzyme that utilizes a binuclear nickel-iron [NiFe] catalytic site. Production and engineering of recombinant [NiFe]-hydrogenases in a genetically-tractable organism, as with metalloprotein complexes in general, has met with limited success due to the elaborate maturation process that is required, primarily in the absence of oxygen, to assemble the catalytic center and functional enzyme. We report here the successful production in *Escherichia coli* of the recombinant form of a cytoplasmic, NADP-dependent hydrogenase from *Pyrococcus furiosus*, an anaerobic hyperthermophile. This was achieved using novel expression vectors for the co-expression of thirteen *P. furiosus* genes (four structural genes encoding the hydrogenase and nine encoding maturation proteins). Remarkably, the native *E. coli* maturation machinery will also generate a functional hydrogenase when provided with only the genes encoding the hydrogenase subunits and a single protease from *P. furiosus*. Another novel feature is that their expression was induced by anaerobic conditions, whereby *E. coli* was grown aerobically and production of recombinant hydrogenase was achieved by simply changing the gas feed from air to an inert gas (N₂). The recombinant enzyme was purified and shown to be functionally similar to the native enzyme purified from *P. furiosus*. The methodology to generate this key hydrogen-producing enzyme has dramatic implications for the production of hydrogen and NADPH as vehicles for energy storage and transport, for engineering

hydrogenase to optimize production and catalysis, as well as for the general production of complex, oxygen-sensitive metalloproteins.

INTRODUCTION

From the human economic perspective, molecular hydrogen (H₂) is an ideal form of transportable energy. It is superior to current forms such as gasoline as it is less toxic, safer to use, and has an approximately three-fold higher energy yield per kilogram[1]. A number of problems must be surmounted before a 'hydrogen economy' is a reality, however, including the economic production and transportation of H₂ [2,3]. At present H₂ is generated from fossil fuels by steam reforming processes and by electrolysis of water using electricity typically produced from fossil fuels [1,2,3]. Biological H₂ production is an attractive, and renewable, alternative for human needs. The gas is generated by microorganisms from all three domains of life, and for some, H₂ provides an excellent source of low potential reducing power (H₂/H⁺, E_o' = -420mV) for growth and biosynthesis [4,5]. Microorganisms have evolved elegant and efficient mechanisms for H₂ metabolism. All are based on the enzyme hydrogenase, which catalyzes the reversible reduction of protons (Eqn. 1):



Many microorganisms obtain energy by metabolically coupling H₂ oxidation to a variety of terminal electron acceptors such as fumarate, sulfate, carbon dioxide, and oxygen [4,6]. The production of H₂ is typical of organisms occupying anaerobic environments and is used as a means of disposing of excess reductant from oxidative metabolism.

Hydrogenases catalyze H₂ production using a binuclear metal center active site consisting of either [NiFe] or [FeFe] [6,7]. The [FeFe]-hydrogenases usually have high catalytic rates but are extremely sensitive to irreversible inactivation by oxygen,

much more so than the [NiFe]-enzymes [4]. In contrast to [FeFe]-hydrogenases, which are limited to certain bacteria and a few unicellular eukaryotes, [NiFe]-hydrogenases are widespread in both bacteria and archaea. Although these two classes of hydrogenase are not phylogenetically related, the geometry of the catalytic sites is highly similar [7], and both contain the unusual biological ligands carbon monoxide (CO) and cyanide (CN) which serve to modulate their electronic structure and facilitate catalysis [8].

All [NiFe]-hydrogenases are comprised of at least two subunits, one of which (the large subunit, or LSU) contains the [NiFe] catalytic site, while the other (the small subunit, or SSU) contains three iron-sulfur (FeS) clusters. These clusters transfer electrons from an external electron donor to the [NiFe] active site in the LSU for reduction of protons. The assembly of the [NiFe] site and maturation of the enzyme requires the concerted reactions of multiple gene products. The facultative anaerobe *E. coli* contains three membrane-bound hydrogenases, and elegant studies by Böck and coworkers have shown that the assembly of one of them (HYD3) requires the participation of eight accessory proteins (encoded by *hypA-hypF*, *hycI*, and *slyD*, Fig. 2.1a) [9]. The final step of hydrogenase maturation requires a specific protease (HycI) that removes a peptide of ≤ 20 residues from the C-terminal of the LSU, allowing the protein to fold around the [NiFe] active site [12]. In contrast, it appears that only three maturation proteins are required for the production of a functional [FeFe]-hydrogenase [13].

In the present study we demonstrate for the first time the heterologous expression in a genetically-tractable organism (*E. coli*) of a functional [NiFe]-hydrogenase enzyme, that from a model hyperthermophilic microorganism, *Pyrococcus furiosus* (*Pf*), which grows optimally at 100°C [14]. Previous attempts to heterologously produce [NiFe]-hydrogenases have involved related host organisms and/or have met with limited success. For example, *Desulfovibrio gigas* hydrogenase produced in *D. fructosovorans* exhibited only low activity [15], and transfer of the entire H₂ uptake (*hup*) gene cluster (~18 kb) from *Rhizobium leguminosarum* led to functional expression in only some closely-related species [16]. A functional, NAD-dependent [NiFe] hydrogenase from a gram-positive organism, *Rhodococcus opacus*, was produced in the gram-negative *Ralstonia eutropha* [17], and the membrane bound hydrogenase of *Ralstonia eutropha* was produced in *Pseudomonas stutzeri* using a broad-host-range plasmid containing the *hyp* genes and a regulatory hydrogenase-histidine kinase system [18]. This H₂-sensing, regulatory hydrogenase of *R. eutropha* has also been heterologously produced in *E. coli* but this does not require the proteolytic processing involved in maturation of the [NiFe]-hydrogenase enzymes [19]. While previous attempts to heterologously produce a recombinant [NiFe]-hydrogenase in *E. coli* have been unsuccessful [20,21], our system employs a novel set of compatible vectors modified with an anaerobically-induced *E. coli* hydrogenase promoter, P_{hya}, and minimally requires a single processing gene from *Pf*. It therefore appears that the *E. coli* processing enzymes can assemble functional (and soluble) [NiFe]-hydrogenase enzyme from phylogenetically distant organisms, even

from a completely different domain of life, including those growing at extreme temperatures.

Pf grows by fermenting carbohydrates to organic acids, CO₂ and H₂ [14]. It contains three [NiFe]-hydrogenases; two are cytoplasmic enzymes consisting of four subunits, and the third is a membrane-bound hydrogenase (MBH) of fourteen subunits. The two cytoplasmic enzymes, termed soluble hydrogenase I (SHI) and hydrogenase II (SHII), utilize NADP(H) as the physiological electron carrier [15]. MBH accepts electrons from reduced ferredoxin (Fd_{red}) and is the enzyme responsible for evolving hydrogen during growth, while SHI and SHII are thought to be involved in the recycling of hydrogen produced by MBH [16]. Herein we demonstrate heterologous production of functional *Pf* SHI.

RESULTS

Pf SHI is encoded by four genes (PF0891-0894) in a single operon, with the catalytic LSU encoded by PF0894 and SSU encoded by PF0893[22]. One of the additional subunits is predicted to contain two FeS clusters (PF0891) while the other (PF0892) is predicted to contain another FeS cluster and flavin adenine dinucleotide (FAD), and to interact with NAD(P)(H). SHI purified from *P. furiosus* biomass is extremely stable at high temperatures ($t_{1/2}$ for loss of activity \sim 2 hours at 100°C) and in the presence of oxygen ($t_{1/2} \sim$ 6 hours at 23°C in air)[11].

The four structural genes encoding *Pf* SHI (PF0891-PF0894) were coexpressed in *E. coli* under anaerobic conditions with eight processing genes identified in the *Pf* genome (*hypCDABEF*, *hycI* and *slyD*), based on sequence similarity to the processing genes identified in *E. coli*. These include PF0617, which is the homolog of the *E. coli* peptidase (HycI) involved in C-terminal processing of one of its three hydrogenases, termed HYD3. However, the C-terminal region of *Pf* SHI is more similar to the catalytic subunit of another *E. coli* hydrogenase, HYD2, rather than to HYD3, and HYD2 is processed by another protease (HybD) [23]. A search of the *Pf* genome revealed a gene (PF0975), annotated as ferredoxin oxidoreductase A (*frxA*), which shows 47% sequence similarity to *E. coli* HybD. This was included as the ninth *Pf* gene to be coexpressed in *E. coli* under anaerobic conditions.

A series of four compatible vectors based on the DUET vector system (Novagen) had been modified previously to contain GATEWAY™ recombination sites (Invitrogen) [24], which allows coexpression of as many as eight separate genes or operons under the control of T7 promoters. This cloning approach also inserts 19 amino acids (GSITSLYKKAGSENYFQGG, ~ 2.0 kDa) at the N-terminus of the first gene of the operon in each plasmid. Since the standard T7 promoter does not function in *E. coli* under anaerobic conditions, four different promoters were investigated for anaerobic heterologous expression of the *Pf* genes in *E. coli*. Three were native *E. coli* hydrogenase promoters that are anaerobically-induced (*hya*, *hyb*, and *hyc*, [25,26,27]), while the fourth (*hyp*, [28]) induces expression of *E. coli* hydrogenase-processing genes. Expression of the *lacZ* gene by these four promoters (Fig. 2.2) and several of the *Pf hyd* genes, including *hypCDAB* and *hycI*, were examined using RT-PCR (data not shown). The *hya* promoter (P_{hya}) was induced by anaerobiosis and gave the highest level of expression. The T7 promoters on all expression vectors were therefore replaced with P_{hya} (Fig. 2.3). One vector (pDEST-C3A) was further modified to include the tRNA genes from plasmid pRIL (Stratagene), which is typically required for efficient expression of *Pf* genes in *E. coli* due to differing codon usage, creating the plasmid pC3A-RIL. The complete list of expression vectors used in this study is given in Table 2.1.

To facilitate detection of heterologously-produced *Pf* SHI, all four vectors (Fig. 2.1b) were co-transformed into an *E. coli* strain MW1001 lacking the catalytic subunits of its own hydrogenases ($\DeltahyaB \DeltahybC \DeltahycE$) [31]. Strain MW1001 produces no H₂ during anaerobic growth, and cell extracts have no detectable

hydrogenase activity at either 37 or 80°C (using the standard assay of methyl viologen (MV)-linked H₂ evolution *vide infra*). However, cell-free extracts of anaerobically-grown *E. coli* MW1001 containing the four vectors encoding *Pf* SHI and the *Pf* hydrogenase processing genes did show hydrogenase activity at 80°C (Fig. 2.4a), which must therefore arise from recombinant *Pf* hydrogenase I.

In order to determine the minimum number of *Pf* genes needed for assembly of an active form of SHI in *E. coli*, different *Pf* accessory genes and plasmids were omitted from the complete heterologous expression system (Fig. 2.4a and Fig. 2.5). The results show that maximal recombinant production of functional SHI, as measured by the specific activity in the cell-free extract at 80°C, requires, in addition to the structural genes (PF0891-PF0894), coexpression of only the plasmid containing *frxA* (PF0975) (Fig. 2.4a). FrxA is, therefore, the protease required to process SHI by removing the four C-terminal –VVRL residues (Fig. 2.1a). Low activity was detected if HycI was present, but there was no activity if both proteases were absent, showing that *E. coli* proteases cannot process SHI. The *E. coli* processing enzymes HypABCD and HypEF appear to assemble a functional SHI whose catalytic subunit (PF0894) lacks C-terminal processing. This was confirmed both *in vivo* (Fig. 2.5) and using an *in vitro* assay (Fig. 2.4b) where extracts from *E. coli* cells expressing either only the four structural genes for SHI or only *frxA* were mixed and SHI activity was measured after incubation at 80°C. As expected, much lower SHI activity was obtained if *hycI* replaced *frxA*. Surprisingly, unprocessed SHI (where PF0894 lacks C-terminal cleavage) appears to be stable in *E. coli*, which will be of great utility to

those interested in studying the mechanism of assembly of the [NiFe] site. The minimal expression system in *E. coli* therefore contains five *Pf* genes encoding only SHI and FrxA.

Recombinant *Pf* SHI (rSHI) was purified from *E. coli* strain MW4W (Fig. 2.6a, Table 2.2) to a final specific activity of 100 U mg⁻¹, which is comparable to that of the native enzyme purified from *P. furiosus* biomass (Fig. 2.6b). The hydrogenase was obtained as a homogeneous protein of MW ~ 150,000 Da (based on size-exclusion chromatography, data not shown), also similar to that of the native enzyme, and contained the four different protein subunits (Fig. 2.6a) [11]. Comparison of the properties of the recombinant and native enzymes (Fig. 2.6b) demonstrate that rSHI is similar in specific activity, affinity for NADPH (apparent K_m), stability upon oxygen exposure, and metal content. The only significant difference is the lower stability of rSHI at 90°C. This was not due to the additional N-terminal residues (~2 kDa) on one of the subunits (PF0891, due to the Gateway cloning strategy) since the properties of the wild-type form of rSHI, obtained by recloning PF0891-PF0894 to include only the wild-type amino acid sequence (pET-A-SHI, Fig. 2.7), and that of Gateway-tagged and wild-type rSHI were virtually identical (data not shown).

DISCUSSION

The ability of recombinant *Pf* SHI to accept electrons from the physiological electron carrier NADPH[22] is of some significance since this requires a properly processed, mature, and folded enzyme containing the FAD- (PF0892) and the FeS-containing (PF0891 and PF0892) subunits, in addition to catalytic LSU (PF0894) and SSU (PF0893). In contrast, electrons from the low potential artificial electron donor MV, which was used in all of the routine assays of hydrogenase activity, can theoretically be donated to any of the FeS clusters in the enzyme. The results (Fig. 2.6b) demonstrate that rSHI can accept electrons from NADPH as efficiently as the native enzyme, indicating that it is functionally folded and contains all cofactors.

Like other hydrogenases, *Pf* SHI is much more active with an artificial redox dye (methyl viologen) than with its physiological electron carrier ([33], see Figure 2.6), nevertheless, the specific activity of H₂ production from NADPH by *Pf* SHI is more than 6-fold higher than that reported for an NADH-dependent hydrogenase [33]. While the recombinant form of SHI is as active as the native enzyme at 80°C, it is not as thermostable (Figure 2.6). Interestingly, the native enzyme gives rise after SDS-electrophoresis to a protein band of ~80 kDa, in addition to the four subunits. This band retains hydrogenase activity and is thought to represent a highly stable SDS-resistant residual form of the holoenzyme ([15], and Lane 1 of Figure 2.6). The lack of this additional band in the recombinant preparations (Figure 2.6) suggests that assembly of the recombinant hydrogenase is not completely correct, even though its catalytic activity indicates that it is functionally assembled. It is possible that

holoenzyme assembly to the native-like form of SHI represents a kinetic problem, as speculated with other recombinant hydrogenases [15], since all known *Pf* accessory genes are present in the recombinant host.

The availability of a system to produce rSHI provides a ready supply of the enzyme as well as the opportunity to generate mutant forms with desired characteristics. For example, it was recently demonstrated that a combination of NADPH-utilizing *Pf* SHI, obtained from native *Pf* biomass, with enzymes of the pentose phosphate pathway and starch phosphorylase, evolved H₂ *in vitro* from starch with surprisingly high efficiency and yield [34]. Similarly, attempts have been made to link hydrogenase to the low potential reductant generated by photosynthesis, thereby constructing a light-driven H₂-production system [35,36]. A major problem is the generation of oxygen by photolysis of water, which inhibits the oxygen-sensitive hydrogenase. A functional expression system for hydrogenase provides the tools needed to engineer a hydrogenase enzyme resistant to O₂ inactivation, as well for optimizing output of H₂. Directed evolution techniques can now be utilized to generate [NiFe]-hydrogenases with tailored catalytic activity, oxygen sensitivity, and potentially even changing coenzyme specificity. There are also broader implications for heterologous production of complex, heteromeric metalloproteins. If *E. coli* does not possess homologs of the required accessory genes for any candidate metalloprotein complex, coexpression of multiple genes involved in multiprotein complex assembly is now possible even under anaerobic conditions, and even for complex metalloproteins from extremophiles. While expression of stable

hyperthermophilic proteins in *E. coli* is well-documented (e.g., see[37]), it is surprising that at least some of them, such as the *Pf* protease, are functional at 37°C, in this case to efficiently process *Pf* SHI in *E. coli*. The ability to heterologously produce and engineer a soluble hydrogenase, particularly one as thermostable and as relatively oxygen-insensitive as *Pf* SHI, makes this enzyme an excellent model system for future basic and also applied studies (e.g., [38]).

METHODS

Strains and growth conditions

Escherichia coli strain MW1001 (*lacI^rrrnB_{T14}ΔlacZ_{WJ16}hsdR514ΔaraBAD_{AH33}ΔrhaBAD_{LD78}ΔhyaBΔhybCΔhycE*) [31] was a generous gift from Dr. Thomas K. Wood (Department of Civil and Environmental Engineering, Texas A & M University). *E. coli* strains were routinely grown in 2X YT [39] medium containing Ampicillin 50μg/mL, Chloramphenicol 20μg/mL, Streptomycin 25μg/mL, Kanamycin 25μg/mL, supplemented with 1mM MgSO₄. For anaerobic expression, an overnight culture was used to inoculate (1% vol/vol) 1L of medium in a 2.8L baffled Fernbach flask, and the culture was grown at 37°C shaking at 150 rpm under N₂ for 3-5 hours to an OD_{600nm} ~ 0.8. Cultures were then decanted into 1L bottles and 100μM FeCl₃, 25μM NiSO₄ and 56 mM glucose were added. The bottles were sealed with 43mm Straight Plug stoppers (Wheaton, Millville, NJ) under N₂, and incubated at 37°C with shaking at 120 rpm for 12-16 hours. For larger scale fermentations (15 L), cultures were grown aerobically as described above and were decanted into a carboy (20 L) and sealed under N₂. The culture was allowed to grow anaerobically to induce expression and maturation of the recombinant hydrogenase for 14 hours. Cells were harvested by centrifugation at 10,000 x g for 5 min. The cell pellets were flash frozen in liquid nitrogen and stored at -80°C before use. Molecular biology techniques were performed as described [39], and unless otherwise indicated, chemicals were obtained from Sigma-Aldrich (St. Louis, MO). All molecular biology reagents were utilized following the manufacturer's protocols and were obtained from New England Biolabs (Ipswich, MA), except for Pfu DNA polymerase (Stratagene,

La Jolla, CA) and the reagents for GATEWAY™ recombination (Invitrogen, Carlsbad, CA).

Purification of recombinant *P. furiosus* SHI

All purification steps were performed under strictly anaerobic conditions. Frozen cell pellets were resuspended in Buffer A (50 mM Tris, 2 mM sodium dithionite (J.T. Baker, Phillipsburg, NJ), pH 8.0) containing 0.5 mg/mL lysozyme (Sigma) and 50 µg/mL deoxyribonuclease I (Sigma) in a ratio of 3 mL/g wet weight cells. The resuspended cells were incubated with stirring at room temperature under an atmosphere of argon for one hour and sonicated on ice with a Branson Sonifer 450 for 30 minutes (output 6.0, 50% duty cycle). Cell lysates were heated to 80°C for 30 minutes, cooled to room temperature, and centrifuged (Beckman L90K ultra centrifuge 45Ti rotor at 100,000 x g for 1hr). The supernatant was collected and loaded onto a DEAE anion exchange column (66mL; GE Healthcare, Piscataway, NJ) equilibrated in Buffer A. The column was washed with 5 volumes of Buffer A and the proteins were eluted with a gradient of 0 to 500 mM NaCl in Buffer A over 20 column volumes and collected in 25 ml fractions in an anaerobic chamber. Fractions containing hydrogenase activity were pooled and Buffer A containing 2.0 M ammonium sulfate was added to a final concentration of 0.8 M. The sample was then loaded on to a column of Phenyl Sepharose (45 ml; GE Healthcare) equilibrated in Buffer C (Buffer A containing 0.8M (NH₄)₂S₀₄). The column was washed with 5 volumes of Buffer C and eluted with a 20 column volume gradient from 0.8-0 M (NH₄)₂S₀₄ in Buffer A collected in 20 ml fractions. Fractions containing

hydrogenase activity were combined and concentrated anaerobically by ultrafiltration (PM-30 kDa MWCO membrane, Millipore, Billerica, MA), and applied to a gel filtration column (Superdex S-200 26/60 GE Healthcare) equilibrated with Buffer D (Buffer A containing 300 mM NaCl) and eluted anaerobically in 2 mL fractions over 1.5 column volumes. Native *P. furiosus* SHI was isolated as previously described [40]. The results of the procedure are summarized in Table 2.2.

Hydrogenase assays

Hydrogen production by *E. coli* cultures was routinely measured by removing 100 μ l from the culture headspace with a gas-tight syringe (Hamilton Co, Reno, NV) and injecting into a Shimadzu GC8 gas chromatograph equipped with a washed molesieve 5A 80/100 (6' x 1/8" x 0.085") column. Hydrogenase activity was routinely determined by H₂ evolution from methyl viologen (1 mM) reduced by sodium dithionite (10 mM) at 80°C as described previously [40], except the buffer was 100 mM EPPS, pH 8.4. For the physiologically-relevant hydrogen evolution assay, methyl viologen and sodium dithionite were replaced by NADPH (1 mM). One unit of hydrogenase specific activity is defined as 1 μ mole of H₂ evolved min⁻¹ mg⁻¹. Oxygen sensitivity assays were performed by exposing samples to air at 25°C. Thermal stability assays were measured by anaerobic incubation of the hydrogenase samples (0.06 mg/ml in 100mM EPPS buffer, pH 8.4, containing 2 mM sodium dithionite) at 90°C. Residual enzyme activities were measured using the MV-linked H₂-evolution assay.

Construction of lacZ reporter anaerobic expression plasmids

Four *E. coli* anaerobic promoters, P_{hya}, P_{hyb}, P_{hyc} and P_{hyp} (Fig. 2.2) were inserted into the plasmid pLX1 between *EcoRI* and *XmaI* sites to construct plasmids pLXA, pLXB, pLXC and pLXP. pLX1 was constructed from plasmid pSB2019 [32] by replacing a green fluorescent protein gene between *XmaI* and *SalI* with the N-terminal sequence of lacZ. Plasmids containing lacZ under control of these promoters were transformed into *E. coli* DH10B cells. β -galactosidase activity in extracts of anaerobically-grown cells was analyzed (Spectra MAX 190 96 well microplate reader) using a modified Miller assay [29]. The specific activity of β -galactosidase is expressed as units per mg of total protein in the cell-free extract.

Construction of anaerobic expression vectors

A series of four vectors were constructed by Horanyi et al. [24] in which the GATEWAY™ recombination cassette from Invitrogen was combined with the four compatible expression vectors of the Novagen (EMD Chemicals, San Diego, CA) DUET vector system (Table 2.1). The four original DUET vectors, as well as the four GATEWAY-modified versions (pDEST-C3A, pDEST-C11A, pRSF-ACG, and pET-ACG), were further modified to replace the native T7 promoter, which is not functional under anaerobic growth conditions [41]. The *hya* promoter [42] (see Fig. 2.3) was amplified from genomic DNA purified from the *E. coli* strain MG1655 using the primers (JS1 5'-CTCGAATTCCTTCTCTTTTACTCGTTTAG, JS2 5'-CACCCATATCGCACGTCTCTCTCC). The PCR product was then treated with T4 polynucleotide kinase, and ligated to plasmid pDEST-C3 digested with *EcoI*CR1

to create pDEST-C3A; the entire cassette containing P_{hya} and Gateway cloning sites was amplified with primers (JS1 and JS3 5'-GCCGCAAGCTTAGCAGCCGGAT , the cassette was digested with *EcoRI* and *HindIII*, then ligated with the similarly digested plasmids (pCDFDuet1, pRSFDuet1 and pET23) to create pDEST-C11A, pRSF-ACG and pET-ACG respectively. A 813 bp DNA fragment containing three tRNA genes from plasmid pRIL [43] was amplified using the primers JS4 (5'-CGCGGATCCGTCACCCTGGATGCTGTAC) and JS5 (5'-AAGTACGAGCTCAGGTCGCAGACGTTTTGCA), and cloned into pDEST-C3A between *BamHI* and *SacI* to create the plasmid pC3A-RIL (Table 2.1).

Cloning of the *P. furiosus* genes encoding SHI and the hydrogenase maturation proteins

The *P. furiosus* SHI structural genes (PF0891-PF0894) were amplified using purified *P. furiosus* genomic DNA (DSM 3638, **Genbank Accession number AE009950**) as the template. The entire four-gene operon was amplified with the primers (PF0891-attB1-TEV: 5'-GGGGACAAGTTTGTACAAAAAAGCAGGCTCAGAAAACCTGTATTTTCAGG GAGGAAGGTATGTTAAGTTACCCAAGG and PF0894-attB2-TEV: 5'-GGGGACCACTT TGTACAAGAAAGCTGGGTCTCCTCCCTGAAAATACAGGTTTTCTAAAGT CTAACCACGTGGACTGAG). The 4164 bp PCR product was crossed into the GATEWAY entry vector pDONR/Zeo using the manufacturer's protocol, resulting in the entry vector pDONR-SHI, and subsequently used to cross into the modified

GATEWAY expression vector pET-SHI. The plasmid pET-A-SHI was constructed to produce “tagless” recombinant *P. furiosus* SHI. P_{hya} without the downstream GATEWAY tag was amplified by primer pair Pa-SacF (CTCGAATTCCTTCTCTTTTACTCGTTTAG) and Pa-HindR (TGAGGAAGCTTATCGATGGTACCGCGGCATGCATATGGCACGTCTCTCCTCCTTGCG), the pET-A plasmid was made by inserting the *HindIII/EcoRI* digested PCR product into the similarly treated pETDuet-1(Novagen). The tagless Pf SHI gene was amplified with primer pair 0891-NdeF (GATAGGTTCCATATGAGGTATGTTAAGTTACCCAAGGA) and 0894-KpnR (ATAGGGTACCTTAAAGTCTAACCACGTGGACTGAGC), the *NdeI/KpnI* digested PCR product was inserted into similarly treated pET-A to produce pET-A-SHI. To make the expression vector pC11A-CDABI, the *Pf hypCD* operon (PF0548-PF0549) was first amplified with primers PF0548-attB1-TEV (5'-GGGGACAAGTTTGTACAAAAAAGCAGGCTCAGAAAACCTGTATTTTCAGG GAGGATGCCTTGCAATCCCAGGGAAAG) and CD-ABI-R (5'-CTTACTATTGCATCTGCCAACGCCCATTCGTGCATTTTCCACCTCCTACAT CAGGGCGCCATATTTGTAAA). This 1460 bp *hypCD* PCR product was used as the forward primer to join and amplify the *hypABI* operon (PF0615 – PF0617) creating the artificial *hypCDABI* operon with the reverse primer PF0617-attB2-TEV (5'-GGGGACCACTTTGTACAAGAAAGCTGGGTCTCCTCCCTGAAAATACAGGT TTTCTAAGAAAGCTCAAGACTTTCATAA). A fused *hypEF* operon (PF0604 and PF0559) was obtained with the same strategy by PCR that employed the primer

PF0604-attB1-TEV (5'-
GGGGACAAGTTTGTACAAAAAAGCAGGCTCAGAAAACCTGTATTTTCAGG
GAGGAGAAGAATAATTAGGGAGGTAA and the primer EF-fusion (5'-
GTGAATTCTATAAGCTTTCATTCTCTCCCCAGATACATTTTCCACCTCCTA
ACAAACTCTAGGAACGGGATCAC). The resulting 1025 bp PCR product of
PF0604 was used as the forward primer along with the reverse primer PF0559-attB2-
TEV (5'-
GGGGACCACTTTGTACAAGAAAGCTGGGTCTCCTCCCTGAAAATACAGGT
TTTCTACATCAGGGCGCCATATTTGTAA) to generate the 3428 bp artificial
hypEF operon. The fused *P.furiosus slyD* (PF1401) and *frxA* (PF0975) genes were
cloned by the same PCR method with the primers PF1401-attB1-TEV (5'-
GGGGACAAGTTTGTACAAAAAAGCAGGCTCAGAAAACCTGTATTTTCAGG
GAGGAAAAGTAGAGAAAGGAGATGTCA), the fusion primer SlyD-FrxA-F (5'-
GAGGAGAGTGAGTCTAAAGCGGAAGAATCTTAAGAGGTGGAAAGTGAGT
AACTTTTAACTTTCCTT) and the reverse primer frxA-attB2 (5'-
GGGGACCACTTTGTACAAGAAAGCTGGGTCTCCTATTACTCACCTTCCCT
AATTATTGAC).

It was not possible to transform all four plasmids simultaneously into *E. coli* strains, so routinely one plasmid was transformed, and competent cells made from these cells to transform the next plasmid, and this process repeated as needed.

Metal and Proteomic Analyses

Nickel and iron were measured using a quadrupole-based ICP-MS (7500ce, Agilent Technologies, Tokyo, Japan), equipped with a MicroMist Nebulizer (Agilent Technologies). Proteins were separated using native- or SDS-PAGE gradient gel electrophoresis (4-20% Criterion gels; Biorad, Hercules, CA) and stained with Coomassie Brilliant. Gel bands of interest were cut out, processed and digested for 16 h at 37 °C according to the manufacturer's protocol provided with the recombinant porcine trypsin used for the in-gel protein digest (Roche Applied Science, Indianapolis, IN). The peptides were purified with C-18 reversed-phase NuTip® cartridges according to the manufacturer's instructions (Glygen Corp., Columbia, MD). Approximately 1 µL of purified peptides and 1 µL of ProteoMass Peptide & Protein MALDI-MS Calibration Kit standard (Sigma) were spotted onto a MTP 384 Massive MALDI target (Bruker Daultonics, Billerica, MA). The target was analyzed using a Bruker Daultonics Autoflex MALDI-TOF mass spectrometer (Billerica, MA) following calibration with the standard. The mass list was generated by the SNAP peak detection algorithm using a signal-to-noise threshold of four following baseline correction of the spectra. Proteins were identified by searching the mass list against the National Center for Biotechnology Information (NCBI) annotation of the *P. furiosus* genome (NC_003413) using Mascot's Peptide Mass Fingerprint tool (version 2.1, Matrix Science Ltd., Boston, MA). The searches were conducted using a peptide mass tolerance of 1.0, variable modifications of Carbamidomethylation (C) and Oxidation (M), and a maximum of one missed cleavage. Proteins with a $p < 0.05$

(corresponding to a Mascot protein score of greater than 46) were considered significant.

Acknowledgements

This research was supported by a grant (DE-FG02-05ER15710) from the Chemical Sciences, Geosciences and Biosciences Division, Office of Basic Energy Sciences, Office of Science, U.S. Department of Energy.

REFERENCES

1. Armstrong FA, Belsey NA, Cracknell JA, Goldet G, Parkin A, et al. (2009) Dynamic electrochemical investigations of hydrogen oxidation and production by enzymes and implications for future technology. *Chem Soc Rev* **38**: 36-51.
2. Sigfusson TI (2007) Pathways to hydrogen as an energy carrier. *Philos Transact A Math Phys Eng Sci* **365**: 1025-1042.
3. Edwards PP, Kuznetsov VL, David WI (2007) Hydrogen energy. *Philos Transact A Math Phys Eng Sci* **365**: 1043-1056.
4. Vignais PM, Billoud B (2007) Occurrence, classification, and biological function of hydrogenases: an overview. *Chem Rev* **107**: 4206-4272.
5. Ogata H, Lubitz W, Higuchi Y (2009) [NiFe] hydrogenases: structural and spectroscopic studies of the reaction mechanism. *Dalton Trans* **37**: 7577-7587.
6. Vignais PM, Colbeau A (2004) Molecular biology of microbial hydrogenases. *Curr Issues Mol Biol* **6**: 159-188.
7. Fontecilla-Camps JC, Volbeda A, Cavazza C, Nicolet Y (2007) Structure/function relationships of [NiFe]- and [FeFe]-hydrogenases. *Chem Rev* **107**: 4273-4303.
8. Pierik AJ, Roseboom W, Happe RP, Bagley KA, Albracht SP (1999) Carbon monoxide and cyanide as intrinsic ligands to iron in the active site of [NiFe]-hydrogenases. NiFe(CN)₂CO, Biology's way to activate H₂. *J Biol Chem* **274**: 3331-3337.
9. Blokesch M, Paschos A, Theodoratou E, Bauer A, Hube M, et al. (2002) Metal insertion into NiFe-hydrogenases. *Biochem Soc Trans* **30**: 674-680.

10. Böck A, King PW, Blokesch M, Posewitz MC (2006) Maturation of hydrogenases. *Adv Microb Physiol* **51**: 1-71.
11. Bryant FO, Adams MW (1989) Characterization of hydrogenase from the hyperthermophilic archaeobacterium, *Pyrococcus furiosus*. *J Biol Chem* **264**: 5070-5079.
12. Rossmann R, Maier T, Lottspeich F, Böck A (1995) Characterisation of a protease from *Escherichia coli* involved in hydrogenase maturation. *Eur J Biochem* **227**: 545-550.
13. Posewitz MC, King PW, Smolinski SL, Smith RD, Ginley AR, et al. (2005) Identification of genes required for hydrogenase activity in *Chlamydomonas reinhardtii*. *Biochem Soc Trans* **33**: 102-104.
14. Fiala G, Stetter KO (1986) *Pyrococcus furiosus* sp. nov. represents a novel genus of marine heterotrophic archaeobacteria growing optimally at 100C. *Arch Microbiol* **145**: 56-61.
15. Rousset M, Magro V, Forget N, Guigliarelli B, Belaich JP, et al. (1998) Heterologous expression of the *Desulfovibrio gigas* [NiFe] hydrogenase in *Desulfovibrio fructosovorans* MR400. *J Bacteriol* **180**: 4982-4986.
16. Bascones E, Imperial J, Ruiz-Argueso T, Palacios JM (2000) Generation of new hydrogen-recycling *Rhizobiaceae* strains by introduction of a novel *hup* minitransposon. *Applied and Environmental Microbiology* **66**: 4292-4299.
17. Porthun A, Bernhard M, Friedrich B (2002) Expression of a functional NAD-reducing [NiFe] hydrogenase from the gram-positive *Rhodococcus opacus* in the gram-negative *Ralstonia eutropha*. *Arch Microbiol* **177**: 159-166.

18. Lenz O, Gleiche A, Strack A, Friedrich B (2005) Requirements for heterologous production of a complex metalloenzyme: the membrane-bound [NiFe] hydrogenase. *J Bacteriol* **187**: 6590-6595.
19. Lenz O, Zebger I, Hamann J, Hildebrandt P, Friedrich B (2007) Carbamoylphosphate serves as the source of CN(-), but not of the intrinsic CO in the active site of the regulatory [NiFe]-hydrogenase from *Ralstonia eutropha*. *FEBS Lett* **581**: 3322-3326.
20. English CM, Eckert C, Brown K, Seibert M, King PW (2009) Recombinant and *in vitro* expression systems for hydrogenases: new frontiers in basic and applied studies for biological and synthetic H₂ production. *Dalton Trans*: 9970-9978.
21. Shirshikova GN, Khusnutdinova AN, Postnikova OA, Patrusheva EV, Butanaev AM, et al. (2009) Expression of Ni-Fe hydrogenase structural genes derived from *Thiocapsa roseopersicina* in *Escherichia coli*. *Doklady Biochemistry and Biophysics* **425**: 124-126.
22. Ma K, Weiss R, Adams MW (2000) Characterization of hydrogenase II from the hyperthermophilic archaeon *Pyrococcus furiosus* and assessment of its role in sulfur reduction. *J Bacteriol* **182**: 1864-1871.
23. Menon NK, Robbins J, Vartanian MD, Patil D, Peck HD, et al. (1993) Carboxy-Terminal Processing of the Large Subunit of [NiFe] Hydrogenases. *FEBS Letters* **331**: 91-95.

24. Horanyi P, Griffith J, Wang BC, Jenney FE (2006) Vectors and Methods for High Throughput Co-Expression. In: Office USP, editor. Patent Number 7,582,475 USA.
25. Menon NK, Chatelus CY, Dervartanian M, Wendt JC, Shanmugam KT, et al. (1994) Cloning, sequencing, and mutational analysis of the *hyb* operon encoding *Escherichia coli* hydrogenase 2. J Bacteriol **176**: 4416-4423.
26. Menon NK, Robbins J, Wendt JC, Shanmugam KT, Przybyla AE (1991) Mutational analysis and characterization of the *Escherichia coli hya* operon, which encodes [NiFe] hydrogenase 1. J Bacteriol **173**: 4851-4861.
27. Sawers RG, Ballantine SP, Boxer DH (1985) Differential expression of hydrogenase isoenzymes in *Escherichia coli* K-12: evidence for a third isoenzyme. J Bacteriol **164**: 1324-1331.
28. Lutz S, Jacobi A, Schlenz V, Bohm R, Sawers G, et al. (1991) Molecular characterization of an operon (*hyp*) necessary for the activity of the three hydrogenase isoenzymes in *Escherichia coli*. Mol Microbiol **5**: 123-135.
29. Miller JH (1972) Experiments in molecular genetics. [Cold Spring Harbor, N.Y.]: Cold Spring Harbor Laboratory. xvi, 466 p. p.
30. Dougherty WG, Carrington JC, Cary SM, Parks TD (1988) Biochemical and mutational analysis of a plant virus polyprotein cleavage site. EMBO J **7**: 1281-1287.
31. Maeda T, Sanchez-Torres V, Wood TK (2007) *Escherichia coli* hydrogenase 3 is a reversible enzyme possessing hydrogen uptake and synthesis activities. Appl Microbiol Biotechnol **76**: 1035-1042.

32. Qazi SN, Rees CE, Mellits KH, Hill PJ (2001) Development of gfp Vectors for Expression in *Listeria monocytogenes* and Other Low G+C Gram Positive Bacteria. *Microb Ecol* **41**: 301-309.
33. Schneider K, Schlegel HG (1976) Purification and properties of soluble hydrogenase from *Alcaligenes eutrophus* H 16. *Biochim Biophys Acta* **452**: 66-80.
34. Zhang YH, Evans BR, Mielenz JR, Hopkins RC, Adams MW (2007) High-yield hydrogen production from starch and water by a synthetic enzymatic pathway. *PLoS ONE* **2**: e456.
35. Esper B, Badura A, Rogner M (2006) Photosynthesis as a power supply for (bio-)hydrogen production. *Trends Plant Sci* **11**: 543-549.
36. Prince RC, Kheshgi HS (2005) The photobiological production of hydrogen: potential efficiency and effectiveness as a renewable fuel. *Crit Rev Microbiol* **31**: 19-31.
37. Jenney FE, Jr., Adams MW (2008) The impact of extremophiles on structural genomics (and vice versa). *Extremophiles* **12**: 39-50.
38. Mertens R, Greiner L, van den Ban ECD, Haaker HBCM, Liese A (2003) Practical applications of hydrogenase I from *Pyrococcus furiosus* for NADPH generation and regeneration. *Journal of Molecular Catalysis B-Enzymatic* **24-5**: 39-52.
39. Sambrook J, Russell DW (2001) *Molecular cloning : a laboratory manual*. Cold Spring Harbor, N.Y.: Cold Spring Harbor Laboratory Press.

40. Ma K, Adams MW (2001) Hydrogenases I and II from *Pyrococcus furiosus*.
Methods Enzymol **331**: 208-216.
41. Oxeer MD, Bentley CM, Doyle JG, Peakman TC, Charles IG, et al. (1991) High-Level Heterologous Expression in *Escherichia coli* Using the Anaerobically-Activated Nirb Promoter. Nucleic Acids Research **19**: 2889-2892.
42. King PW, Przybyla AE (1999) Response of *hya* expression to external pH in *Escherichia coli*. Journal of Bacteriology **181**: 5250-5256.
43. Schenk PM, Baumann S, Mattes R, Steinbiss HH (1995) Improved high-level expression system for eukaryotic genes in *Escherichia coli* using T7 RNA polymerase and rare Arg tRNAs. Biotechniques **19**: 196-198, 200.

Table 2.1. Strains and plasmids used in this study.

Strains and plasmids	Genotype	Source
Strains		
<i>E. coli</i> MW1001	<i>lacI</i> ^q <i>rrnB</i> _{T14} Δ <i>lacZ</i> _{WJ16} <i>hsdR514</i> Δ <i>araBAD</i> _{AH33} <i>ΔrhaBAD</i> _{LD78} <i>ΔhyaB</i> <i>ΔhybC</i> <i>ΔhycE</i>	24
<i>E. coli</i> DH10B	<i>F</i> ⁻ <i>endA1</i> <i>recA1</i> <i>galE15</i> <i>galK16</i> <i>nupG</i> <i>rpsL</i> <i>ΔlacX74</i> Φ 80 <i>lacZ</i> Δ M15 <i>araD139</i> Δ (<i>ara,leu</i>)7697 <i>mcrA</i> Δ (<i>mrr-hsdRMS-mcrBC</i>) λ ⁻	Invitrogen
<i>E. coli</i> MW4W	MW1001 strain with plasmids: pC11A2-CDABI /pC3AR2-SF/pRA2-EF/pEA2-SH1	This study
Plasmids		
a. lacZ reporter plasmids		
pSB2019	Amp ^R P _{xyIA} -GFP	31
pLXA	Amp ^R P _{hya} -lacZ	This study
pLXB	Amp ^R P _{hyb} -lacZ	This study
pLXC	Amp ^R P _{hyc} -lacZ	This study
pLXP	Amp ^R P _{hyp} -lacZ	This study
b. Destination and Expression plasmids		
pDEST-C1	Cloning vector, Sm ^R	32
pDEST-C11A2	Cloning vector, Sm ^R	This study
pC11A2-CDABI	Expression vector, Sm ^R	This study
pDEST-C3	Cloning vector, Cm ^R	32
pDEST-C3A	Cloning vector, Cm ^R	This study
pRIL	Express tRNA <i>argU/ileY/leuW</i> , Cm ^R	Stratagene
pC3A-RIL*	Cloning vector, Cm ^R	This study
pC3AR2-slyD*	Expression vector, Cm ^R	This study
pC3AR2-SdFa*	Expression vector, Cm ^R	This study
pET-CAG2	Cloning vector, Amp ^R	This study
pEA2-SH1	Expression vector, Amp ^R	This study
pET-A-SH1	Expression vector, Amp ^R	This study
pRSFDuet-1	Cloning vector, Kan ^R	Novagen
pRSF-CAG2	Cloning vector, Kan ^R	This study
pRA2-EF	Expression vector, Kan ^R	This study

* Contain tRNA genes *argU/ileY/leuW*

Table 2.2. Purification of recombinant *P. furiosus* SHI from *E. coli*.

Step ^a	Activity (U)	Protein (mg)	Specific Activity (U mg ⁻¹)	Yield (%)	Purification (Fold)
Cell Extract (CE)	1183	37260	0.03	100	1
Heat Treated CE	1287	2381	0.5	109	17
DEAE	789	573	1	67	43
PS	237	45	5	20	166
S-200	80	0.8	100	7	3150

^a*E. coli* cells were lysed, and the cell-free extract (CE) was heated to 80°C for 30 min to remove heat labile *E. coli* proteins and yield the Heat Treated CE. The recombinant hydrogenase was purified by three chromatography steps using Diethylaminoethyl Sepharose anion exchange (DEAE), Superdex 200 size exclusion (S-200), and Phenyl Sepharose hydrophobic exchange (PS). Activity was measured by the methyl viologen-linked H₂ evolution assay at 80°C, where 1 U is 1 μmole H₂ evolved min⁻¹.

Figure 2.1. Synthesis of *P. furiosus* soluble hydrogenase I (SHI) and the plasmid constructs used for recombinant production. (a) Maturation pathway for the [NiFe] catalytic site of *P. furiosus* SHI is based on that proposed for *E. coli* hydrogenase 3 [10]. HypE and HypF generate thiocyanate in an ATP-dependent process from carbamoyl phosphate (CP). The source of the CO ligand is unknown. The HypCD complex binds the iron atom containing the CN and CO ligands and donates it to the catalytic subunit (PF0894). The Ni atom is provided by the HypAB-SlyD complex in a GTP-dependent reaction. The Ni and Fe atoms in the [NiFe] site are coordinated to PF0894 by the S atoms of four of its Cys residues (indicated by S). Activation of PF0894 requires cleavage of four C-terminal residues (-VVRL) catalyzed by a newly identified peptidase, FrxA (and to a much lesser extent by HycI). It is not known how the biosynthesis of PF0894 is coordinated with that of the other three subunits (PF0891, PF0892 and PF0893) to give catalytically-active SHI. The predicted cofactor content of mature heterotetrameric SHI [11] is shown together with their roles in the reversible production of hydrogen gas from NADPH. The abbreviations used are: CP, carbamoyl phosphate; CO, carbonyl ligand; CN, cyano ligand; FAD, flavin adenine dinucleotide. (b) The expression plasmids utilized for production of SHI in *E. coli* strain MW4W. The antibiotics refer to the selective marker on each plasmid: Amp, Ampicillin; Sm, Streptomycin; Kan, Kanamycin; Cam, Chloramphenicol.

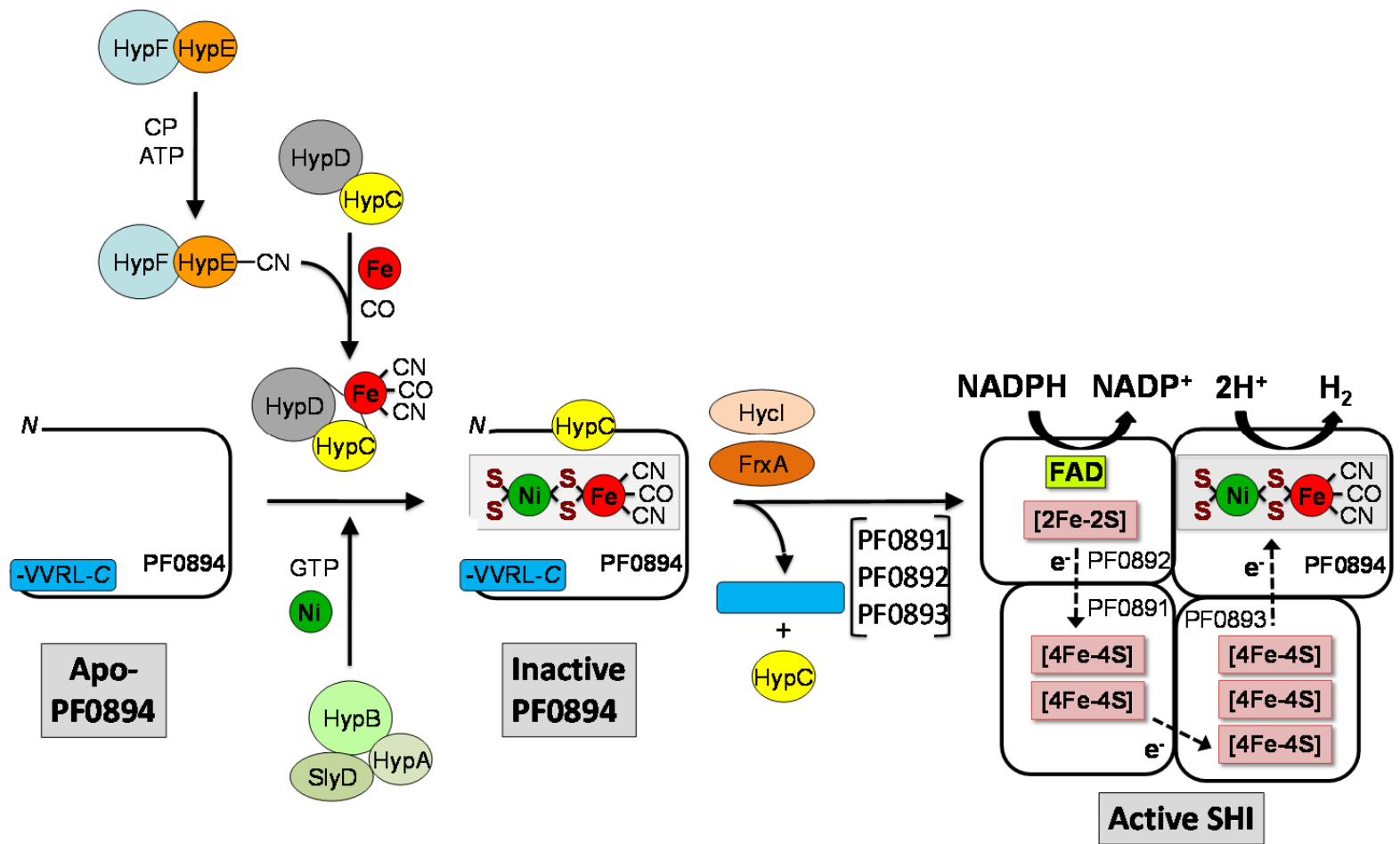


Figure 2.2. Analysis of *E. coli* promoters with a *lacZ* gene fragment β -galactosidase reporter assay. Plasmids were transformed into DH10B. The specific activity of *lacZ* was measured by a modified Miller [29] assay calculated as $200(\text{OD}_{420-t1}-\text{OD}_{420-t2}) \text{ min}^{-1}\text{mg}^{-1}$, where t1 and t2 are the start and end time points, respectively.

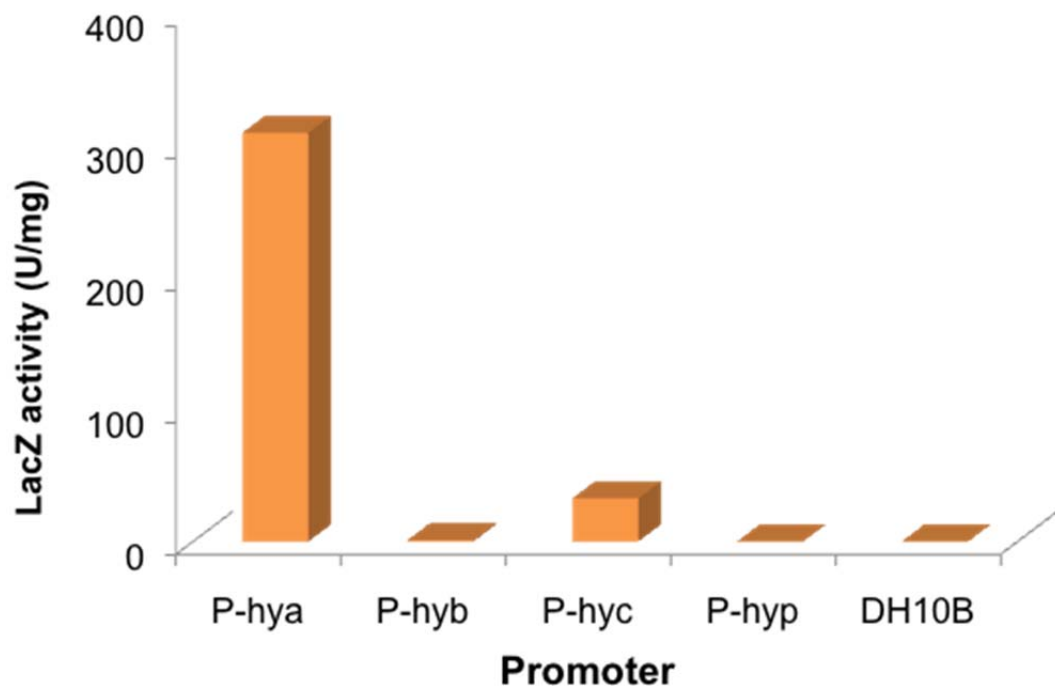
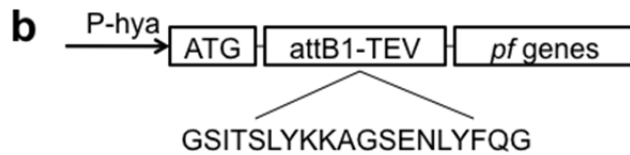


Figure 2.3. Plasmid construction for rSHI production in *E. coli*. P_{hya} was cloned into a set of patented plasmids constructed by inserting Invitrogen Gateway cassettes into Novagen Duet plasmids [24]. **(a)** Sequences of *E. coli* anaerobic promoter P_{hya} , attB1 and TEV protease recognition site sequence and their encoded peptide sequence [30]. **(b)** Elements constructed in the final expression plasmids: P_{hya} promoter, N-terminus of the first protein in the operon derived from the Gateway recombination cloning site (attB1) including a TEV protease site [30] and *P. furiosus* genes. **(c)** Artificial Shine-Dalgarno sequences inserted between *P. furiosus* fused ORFs in plasmids pC11A2-CDABI, pC3AR2-SdFa and pRA2-EF.

a P_{hya} promoter with Gateway attB1/TEV sequence:

CTCGAATTCCTTCTCTTTTACTCGTTTAGCAACCGGCTAAACATCCCCACCGC
 CCGGCCAAAAGAAAAATAGGTCCATTTTTATCGCTAAAAGATAAATCCACACA
 GTTTGTATTGTTTTGTGCAAAAGTTTCACTACGCTTTATTAACAATACTTTCTG
 GCGACGTGCGCCAGTGCAGAAGGATGAGCTTTCGTTTTTCAGCATCTCACGT
 GAAGCGATGGTTTGCCTTGCTACAGGGACGTCGCTTGCCGACCATAAGCGC
 CCGGTGTCCTGCCGGTGTGCGCAAGGAGGAGAGACGTGC

start codon *Gateway Tag + TEV site:* GSITSLYKKAGSENYFQGG
 GAT**ATG**GGGTGGGGCTCGATCACAAGTTTGTACAAAAAAGCAGGCTCAGAAA
 ACCTGTATTTTCAGGGAGGA



c
 ORF1.....TAA**gaggtggaaa**ATG.....ORF2

Figure 2.4. Accessory proteins required for maturation of recombinant *P. furiosus* SHI *in vivo* and *in vitro*. (a) Recombinant SHI (rSHI) was expressed in the presence of different *Pf* processing genes and the resulting *E. coli* cell-extracts were assayed at 80°C. The bars indicate methyl viologen-linked specific activity expressed as U mg⁻¹ or μmol H₂ evolved min⁻¹ mg⁻¹. FrxA but not SlyD is necessary to produce high amounts of active hydrogenase. (b) Processing of rSHI in cell-free extracts of *E. coli* by FrxA and HycI of *P. furiosus*. An *E. coli* cell-extract containing rSHI (PF0891-0894) as the only expressed *Pf* genes, was added to another cell-extract containing only either *FrxA* or *HycI* as the only expressed *Pf* genes. The mixtures were incubated for 30 min at the indicated temperature and the specific activity was determined at 80°C by the methyl viologen-linked assay.

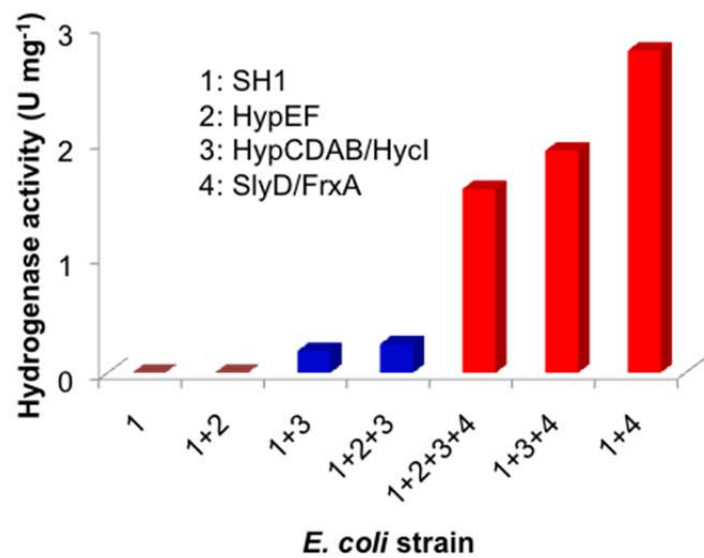
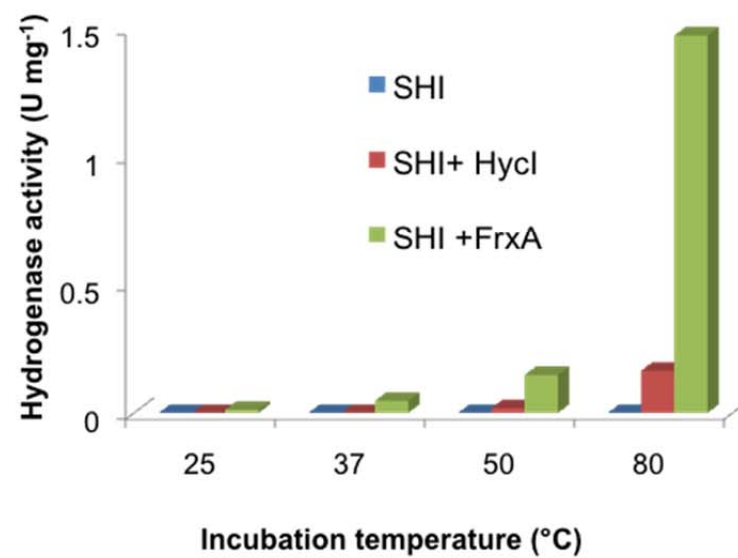
a**b**

Figure 2.5. Analysis of the *P. furiosus* maturation proteins required to produce active rSHI in *E. coli*. The specific activities are shown for rSHI in cell extracts of *E. coli* resulting from the co-expression of different *Pf* processing genes in *E. coli* MW1001. Bars indicate MV-linked specific activity ($\mu\text{mol H}_2 \text{ evolved min}^{-1} \text{ mg}^{-1}$). All cell extracts were heated for 30 min at 80°C prior to assay.

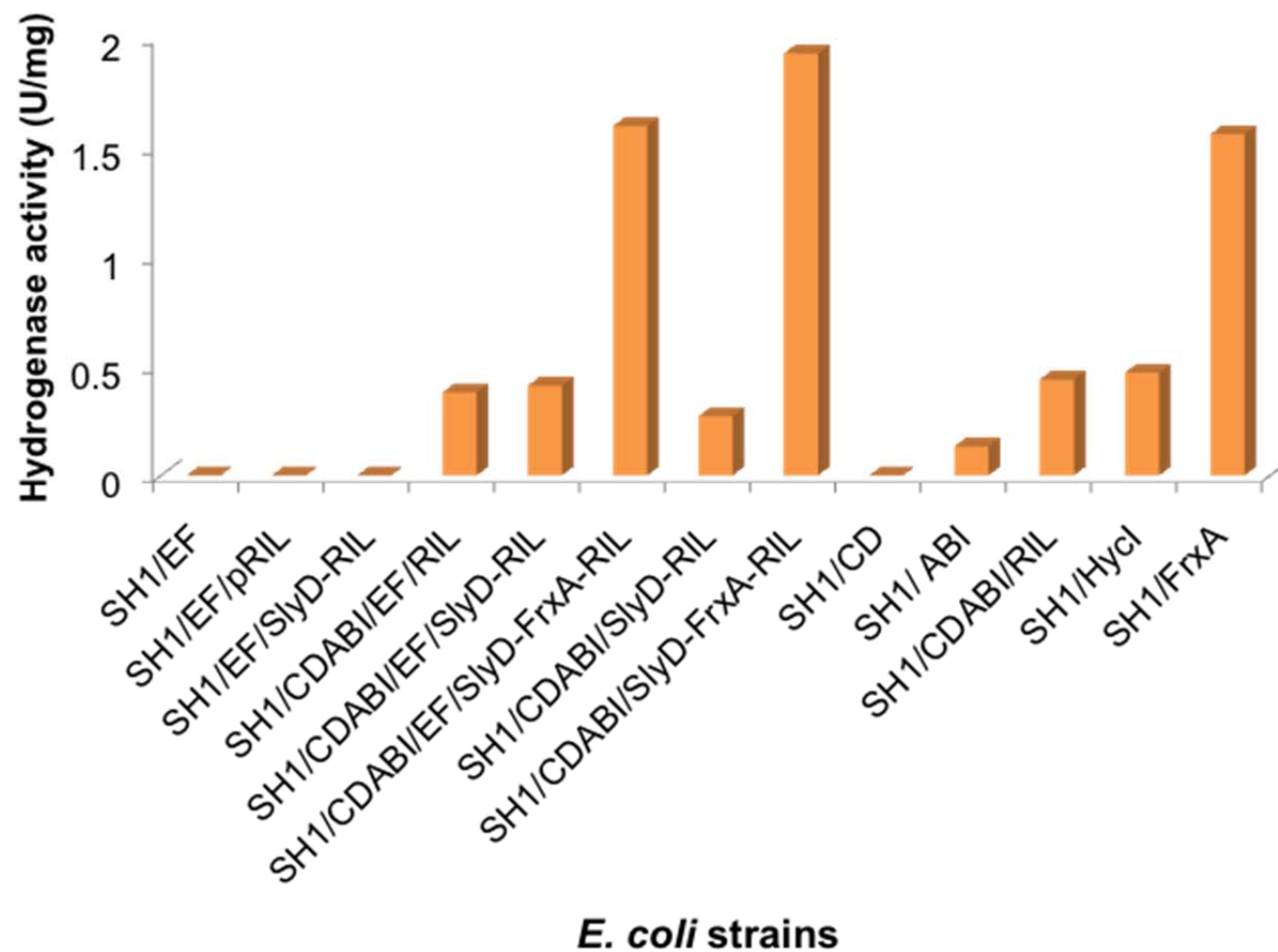
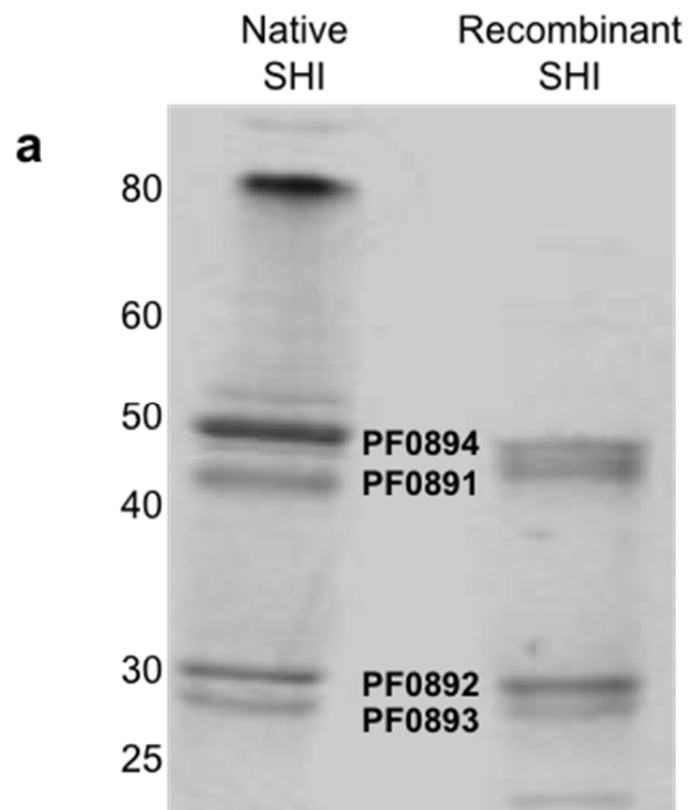


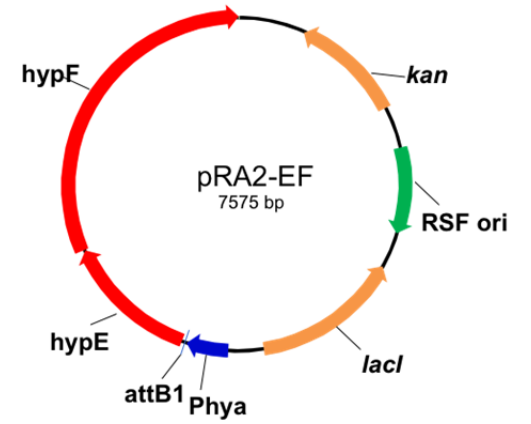
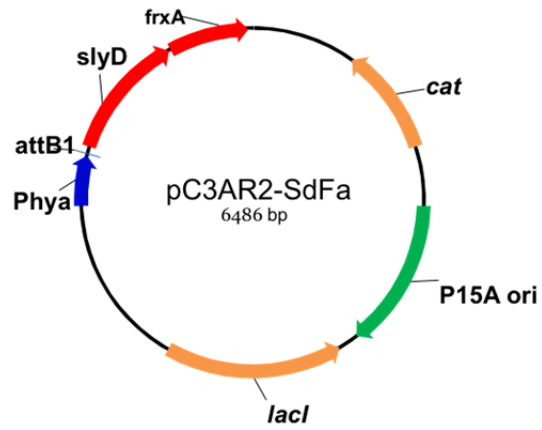
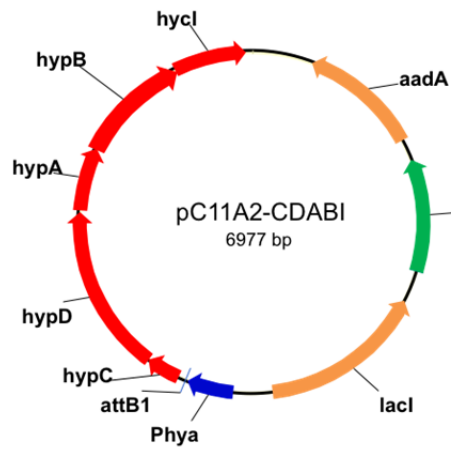
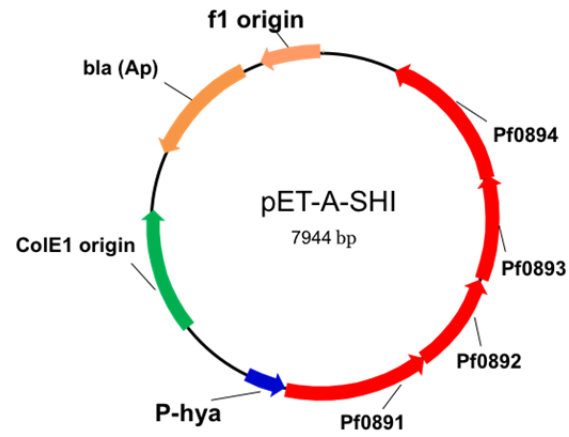
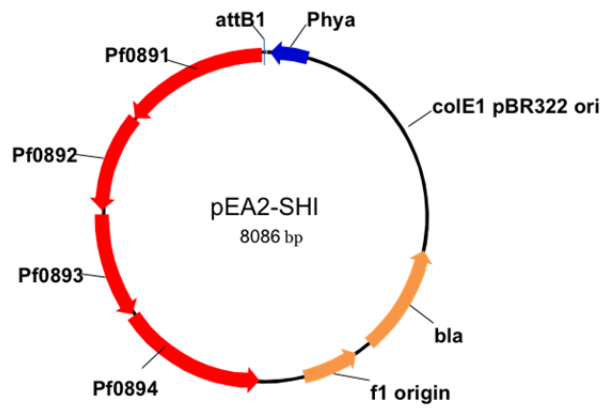
Figure 2.6. Properties of recombinant *P. furiosus* SHI. (a) Gel electrophoresis (SDS-PAGE) analysis of native and recombinant SHI. Bands representing the four subunits of the SHI are indicated, all of which were confirmed by MALDI-TOF analysis (data not shown). The high molecular weight band in the native protein, not seen in the recombinant version, represents undenatured tetrameric protein [11]. Recombinant PF0891 is approximately 2 kDa larger than the native protein due to the N-terminal extension (see Fig. 3). Molecular weight markers (kDa) are indicated. (b) Physical and catalytic properties of rSHI and the native hydrogenase purified from *P. furiosus* biomass. Hydrogen evolution was measured using either methyl viologen (MV) or NADPH as the electron donor at 80°C.



b

Property	Native SHI	Recombinant SHI
Activity, MV-linked (U/mg)	163	89
Activity, NADPH-linked (U/mg)	1	1
NADPH, K_m (μ M)	30	7
Metal content (Ni:Fe)	1:25	1:32
Stability at 90°C ($t_{1/2}$, hr)	30	1
Stability in air (23°C, $t_{1/2}$, hr)	25	20

Figure 2.7. Maps of expression plasmids. Plasmid pEA2-SHI and pET-A-SHI were used to express rSHI in *E. coli*, and pET-A-SHI was used to generate SHI with a Gateway sequence and TEV recognition site attached to the N-terminal of PF0891 subunit. The plasmid pC11A2-CDABI contains the operons *hypCD* and *hypAB, hycI* from *P. furiosus*. The operons *hypCD* and *hypAB, hycI* of *P. furiosus* were linked by an intergenic region shown in Figure 3c. The Gateway sequence is located at the N-terminus of the HypC protein. The plasmid pC3AR2-SdFa has *slyD* and *frxA* of *P. furiosus* cloned behind P_{hya}, the recombinant SlyD has the N-terminal Gateway sequence/TEV site. Plasmid pRA2-EF was constructed to co-express HypE/HypF, the same linker as in the plasmid pC11A2-CDABI or pC3AR2-SdFa, is inserted between *hypE* and *hypF* gene, and HypE contains the N-terminal Gateway sequence.



CHAPTER 3
HOMOLOGOUS EXPRESSION OF A SUBCOMPLEX OF *PYROCOCCUS*
***FURIOSUS* HYDROGENASE**
THAT INTERACTS WITH PYRUVATE FERREDOXIN
OXIDOREDUCTASE¹

¹ R. Christopher Hopkins, Junsong Sun, Francis E. Jenney, Jr., Sanjeev K. Chandrayan, Patrick M.

McTernan, and Michael W. W. Adams. 2011. *PLoS One*. 2011. 6(10):e26569.

Reprinted here with permission of the publisher.

ABSTRACT

Hydrogen gas is an attractive alternative fuel as it is carbon neutral and has higher energy content per unit mass than fossil fuels. The biological enzyme responsible for utilizing molecular hydrogen is hydrogenase, a heteromeric metalloenzyme requiring a complex maturation process to assemble its O₂-sensitive dinuclear-catalytic site containing nickel and iron atoms. To facilitate their utility in applied processes, it is essential that tools are available to engineer hydrogenases to tailor catalytic activity and electron carrier specificity, and decrease oxygen sensitivity using standard molecular biology techniques. As a model system we are using hydrogen-producing *Pyrococcus furiosus*, which grows optimally at 100°C. We have taken advantage of a recently developed genetic system that allows markerless chromosomal integrations via homologous recombination. We have combined a new gene marker system with a highly-expressed constitutive promoter to enable high-level homologous expression of an engineered form of the cytoplasmic NADP-dependent hydrogenase (SHI) of *P. furiosus*. In a step towards obtaining 'minimal' hydrogenases, we have successfully produced the heterodimeric form of SHI that contains only two of the four subunits found in the native heterotetrameric enzyme. The heterodimeric form is highly active (150 units mg⁻¹ in H₂ production using the artificial electron donor methyl viologen) and thermostable (t_{1/2} ~ 0.5 hour at 90°C). Moreover, the heterodimer does not use NADPH and instead can directly utilize reductant supplied by pyruvate ferredoxin oxidoreductase from *P. furiosus*. The SHI heterodimer and POR therefore represent a two-enzyme system that oxidizes

pyruvate and produces H₂ *in vitro* without the need for an intermediate electron carrier.

INTRODUCTION

The supply of cost-effective fossil fuels is finite, and for decades a major focus of research has been renewable energy generation [1]. Energy sources of the future must be abundant and carbon neutral with minimal impact on the environment. Driven by powerful new molecular biology tools, biofuel research has dramatically increased in the past decade, however, significant effort is still necessary to develop an economically viable, sustainable, and renewable energy supply [2,3,4]. As an energy carrier, hydrogen is attractive as it is non-toxic and has three times the energy of gasoline per unit mass [5]. Currently hydrogen is produced by steam reforming of natural gas or electrolysis of water, both of which are either non-renewable or inefficient on a large scale [5,6,7]. For sustainable and renewable production of hydrogen an abundant source of energy, such as sunlight, must be utilized. Photobiological production of hydrogen is an appealing solution but many problems remain in coupling oxygenic photosynthesis with the enzymatic production of hydrogen [3].

The ability to metabolize hydrogen is distributed across all three domains of life and is catalyzed by the hydrogenase enzymes [8]. Regardless of their source, these enzymes are usually highly regulated on the transcriptional level, require a complicated *in vivo* maturation process, and are inactivated by molecular oxygen. Two major classes of phylogenetically unrelated hydrogenases are known, nickel-iron (NiFe) and iron-iron (FeFe) [9,10], and these catalyze the reversible interconversion of hydrogen, two protons and two electrons (Eqn. 1). These enzymes have been

investigated for almost 80 years [11] but it has only recently become possible to manipulate or redesign the enzymes using standard molecular biology approaches [12,13]. The FeFe enzymes have a limited distribution in the microbial world and although they typically have high catalytic rates of hydrogen production they are very sensitive to irreversible inactivation by molecular oxygen [9]. NiFe hydrogenases are ubiquitous in bacteria and archaea and function physiologically in both hydrogen oxidation and evolution [8]. They are much more resistant to molecular oxygen, and as such may be better targets for engineering, notwithstanding their lower catalytic turnover rates as compared to FeFe hydrogenases (5-10%) [10,14]. In order to link these enzymes to energetic biological processes, and exploit their ability to generate molecular hydrogen, it will be necessary to tailor catalytic activity, further reduce oxygen sensitivity, and even change coenzyme specificity.



As a model organism we are investigating the hyperthermophilic archaeon *Pyrococcus furiosus* (*Pf*), an obligate anaerobe that ferments simple and complex sugars to produce organic acids, CO₂, and (in the absence of elemental sulfur) H₂ [15]. *Pf* has three operons that encode NiFe hydrogenases; two cytoplasmic enzymes consisting of four subunits and a membrane bound hydrogenase (MBH) with 14 putative subunits [16,17]. The two soluble enzymes, soluble hydrogenase I (SHI) and soluble hydrogenase II (SHII), utilize NAD(P)(H) as the physiological electron carrier [18,19]. *Pf* SHI is a heterotetrameric enzyme consisting of the typical large

(LSU PF0894) and small (SSU PF0893) subunits along with two additional subunits predicted to contain FeS clusters (PF0891) and a flavin in the form of FAD (PF0892) (Figure 3.1a). *Pf* SHI is a remarkably stable enzyme having a $t_{1/2}$ at 90°C of approximately 12 hours and $t_{1/2}$ after exposure to air of about 6 hours [18].

Recently, a genetic system was developed for *Pf* allowing the markerless disruption or integration of genes onto the chromosome [20]. This system marks a significant turning point in the ability to use *Pf* as a model organism. A host strain (COM1) was generated via the deletion of *pyrF* (orotidine 5'-monophosphate decarboxylase) which allows subsequent gene knockouts and marker excision. Using this strategy, knockout mutants of each of the two cytoplasmic hydrogenases, *shI* $\beta\gamma\delta\alpha$ (soluble hydrogenase I), and *shII* $\beta\gamma\delta\alpha$ (soluble hydrogenase II) were constructed [20]. Expanding on this technique we utilize here a marked knock-in strategy to introduce an expression cassette into the *Pf* chromosome for homologous overexpression. To drive transcription of recombinant genes in *Pf* the promoter region of the gene encoding the S-layer protein (PF1399) was chosen. Based on microarray data ([21]) PF1399 is a high level, constitutively-expressed gene whose promoter will allow universal expression regardless of growth condition.

As a first step towards the production of 'minimal' hydrogenases, the goal of this work was to engineer a form of SHI that contained only two (LSU and SSU) rather than four subunits. This has been reported the enzyme for some *Ralsonia* species but this was achieved by dissociation of the native tetrameric hydrogenase using PAGE

and not by genetic manipulation [22]. In addition, we wished to take advantage of a new auxotrophic marker system for manipulating chromosomal DNA in the related organism *Thermococcus kodakarensis* [23,24]. It was shown that the deletion of an essential gene *pdaD* (TK0149 arginine decarboxylase) could be complemented with addition of the polyamine precursor agmatine, a metabolite not found in complex growth media. Based on this work, we have devised a simple method of integrating genes of interest onto the chromosome of *Pf* using agmatine prototrophy as a marker and report herein on the expression and characterization of an active, stable heterodimeric subcomplex of *Pf* SHI.

RESULTS

Construction of a *Pf* strain overexpressing dimeric hydrogenase via an agmatine selection. It was recently reported that agmatine is essential for the growth of the hyperthermophilic archaeon *Thermococcus kodakarensis* [23], a close relative of *Pf* that grows at a lower temperature (T_{opt} 85°C versus 100°C for *Pf*). Agmatine is derived from the decarboxylation of arginine and is a precursor for polyamine synthesis. In addition, it was recently discovered to be an essential conjugate of tRNA^{Ile} for AUA decoding in archaea [25]. Disruption of *Pf pdaD* (PF1623 arginine decarboxylase) with the P_{gdh} *pyrF* cassette (Figure 3.2) exhibited auxotrophy for agmatine and this allowed selection in the complex media used for *Pf* as yeast extract and casein both lack agmatine. This departure from defined media in growing and selection of *Pf* genetic mutants greatly simplifies the process of transformation.

A plasmid pSPF300 was designed to allow simple integrations on the *Pf* chromosome at the *pdaD* locus and includes a multiple cloning site after the P_{slp} promoter for cloning of genes for homologous (or heterologous) expression in *Pf*. To investigate if *Pf* SHI can exist as a dimeric enzyme, the LSU and SSU (PF0893-0894) were cloned into the homologous recombination plasmid pSPF300 with the addition of an N-terminal His₉-tag (on PF0893) generating plasmid pSPF302 (Figure 3.3). Linearized pSPF302 was successfully used to transform *Pf* and integrate the P_{slp} *shIδα* overexpression construct onto the *Pf* chromosome (Table 3.1).

Purification and characterization of homologously expressed dimeric hydrogenase. *Pf* cells harboring the P_{slp} *shIδα* overexpression construct (*Pf* strain P_{slp}

Dimer) were used for purification. The overexpressed (OE-SHI) dimer was purified to homogeneity (Figure 3.1b) with a final specific activity of 106 U mg⁻¹ (MV-linked hydrogen evolution) (Table 3.2), which is comparable to that obtained with the heterotetrameric enzyme [18]. Although only two subunits are expected from the purified enzyme complex, a persistent contaminant of approximately 8 kDa could not be separated from OE-SHI Dimer (Figure 3.1b). MALDI-TOF/TOF analysis revealed this to be PF1542, a gene annotated as snRNP (small nuclear ribonucleoprotein) that functions to mediate RNA-RNA interactions [26]. Size exclusion analysis of OE-SHI Dimer using a calibrated Superdex S200 column indicated the complex migrated at an apparent M_r of 88,000 daltons, in agreement with the trimer weight of PF0893-0894 and PF1542 (Table 3.3). As shown in Table 3.3, the OE-SHI Dimer was much less thermostable and more sensitive to oxygen exposure. As expected in the absence of the FAD-containing subunit PF0892, the OE-SHI Dimer was unable to evolve hydrogen from NADPH. Surprisingly, however, the OE-SHI Dimer was able to accept electrons from pyruvate via POR (Table 3.3). It has been previously reported that native *Pf* SHI cannot accept electrons from Fd_{red} using the POR-linked electron transfer system [27] and this was confirmed for our native SHI enzyme used in this study. Usually electrons derived from pyruvate are transferred from POR to the membrane bound hydrogenase via the cytoplasmic redox protein Fd [28]. In the *in vitro* assay OE-SHI Dimer was able to accept electrons directly from POR and the presence of Fd had no significant effect on activity. Native SHI is predicted to contain one [2Fe-2S] and five [4Fe-4S] clusters in addition to the NiFe active site (23 Fe total) while OE-SHI Dimer should

only contain three 4Fe4S and the NiFe site (13 Fe total; Figure 3.1a). Accordingly, metal analysis showed that native SHI has a nickel to iron ratio of 1:25 while the OE-SHI Dimer ratio is 1:10 (Table 3.3).

DISCUSSION

The recent development of a genetic system in *Pf* [20] enables the deletion and homologous expression of genes, together with the tagging of proteins to facilitate purification. Moreover, the initial method using the *pyrF* deletion strain was limited by the use of defined media, as the standard complex media contain contaminating uracil (which overcomes the selection). The construction of the pSPF300 homologous recombination vector for integration at the *pdaD* locus provides a simple method for manipulating genes in *Pf* even in rich media. The pSPF300 vector includes the 1kb regions for recombination, *pdaD* with native promoter (as marker), a high level, constitutive promoter (P_{slp}) for the gene of interest, and a multiple cloning site containing four unique restriction sites. For routine overexpression of genes in *Pf* the agmatine auxotrophy based marker system and pSPF300 recombination vector provides a facile selection method.

Utilizing the *pdaD* marker system an N-terminal His₉ dimeric version (PF0893-PF0894) of the heterotetrameric SHI (PF0891-PF0894) was cloned onto the chromosome of *Pf* to generate strain P_{slp} Dimer (Figure 3.3) in a strain (Δ SHI) lacking the native enzyme. The Δ SHI deletion strain has already been characterized [20] and this was chosen as the parent strain since it might not be possible to introduce a dimeric SHI into *Pf* if the native SHI operon is still intact. Based on microarray data the promoter (P_{slp}) for the gene (PF1399) encoding the highly expressed S-layer protein was used to drive transcription of a minimal form of the SHI enzyme. A phenotype was not observed for the P_{slp} Dimer strain but this is not surprising as other

hydrogenase deficient mutants of *Pf* also exhibited no obvious phenotype [20]. OE-SHI Dimer was able to accept electrons directly from POR *in vitro* and the possibility exist that the dimeric could short-circuit the path of electrons from POR to the membrane bound hydrogenase. Since this would bypass the creation of a proton motive force and the conservation of energy during metabolism one would expect a severe retardation of growth. *P_{slp}* Dimer exhibited similar growth to wild-type *Pf* and it appears *in vivo* the flow of electrons remains unchanged.

OE-SHI Dimer was purified to near homogeneity utilizing a two-step ion-exchange and nickel sepharose 6 purification protocol (Figure 3.1b; Table 3.2). The persistent contamination of OE-SHI Dimer with PF1542 was unexpected as they do not share any similarity in predicted function. A subsequent size exclusion column was also unable to separate the proteins but the complex migrated at the expected M_r for a heterotrimer (Table 3). This suggests that OE-SHI Dimer and PF1542 form a stable complex but the reason for this association is not known. In combination with the N-terminal His tag and high constitutive expression, this protocol greatly simplifies purification and provides a superior yield of enzyme. For comparison, the original report of SHI purification [18] reported 11 mgs of pure enzyme obtained from 450 g *Pf* cells; OE-SHI Dimer was purified from 330 g cells for a final yield of 53 mgs, a more than ten-fold increase in yield.

The OE-SHI Dimer was markedly less stable than native SHI, but this is not unexpected as the absence of two partner subunits of the normally heterotetrameric

enzyme would destabilize the complex. Although the heterodimeric enzyme appears less stable than native SHI after exposure to air and incubation at 90°C (under the same conditions of buffer and protein concentration, Table 3), the enzyme is still very robust as compared to mesophilic hydrogenases. The activity of the purified dimer with the redox dye MV was comparable to that of native SHI. As expected the OE-SHI Dimer lacked the ability to accept electrons from NADPH since the FAD-containing subunit PF0892 (and FeS-cluster containing subunit PF0891) are absent. Surprisingly, however, the OE-SHI Dimer was able to accept electrons directly from pyruvate ferredoxin oxidoreductase (POR), a reaction that native SHI cannot catalyze, and yet interestingly OE-SHI dimer cannot accept electrons from ferredoxin, the physiological electron acceptor of POR. Hence we have engineered a form of SHI that by chance directly interacts with native POR. This results in a two enzyme system that oxidizes pyruvate and produces H₂ without the need for an intermediate electron carrier, such as ferredoxin or NAD(P). As shown in Figure 3.4, POR contains thiamine pyrophosphate and three [4Fe-4S] clusters and oxidizes pyruvate to acetyl CoA [29]. Presumably there is direct electron transfer between the iron-sulfur clusters of the two enzymes (Figure 3.4).

One of the goals in engineering hydrogenases is to change coenzyme specificity, and this was achieved in this case by simply deleting two subunits. Activities with physiological-relevant electron carriers such as NADPH are usually much less than that measured with the artificial electron donor MV, as is evident with native SHI (Table 3). Consequently, while the OE-SHI Dimer and the native SHI had

comparable MV-linked hydrogen evolution activities, the OE-SHI Dimer exhibited only five-fold less activity with a physiological electron donor, in this case the enzyme POR, compared to native SHI and its true physiological partner, NADPH (Table 3). The expression of an active, dimeric form of SHI from *Pf* is a critical step towards engineering minimal hydrogenases. In conjunction with the genetic tools now available, the hydrogenase of *Pf* provides a robust model system for further engineering enzymes that will have utility in biohydrogen generating systems.

METHODS

Strains and growth conditions. Molecular biology techniques were performed as previously described [30]. *Pf* strains used in this study are listed in Table 1. *Pyrococcus furiosus* (DSM 3638) was cultured on liquid and solid support medium as previously described [20] with the addition of 4mM agmatine (Sigma Chemical, St. Louis, MO) as necessary for genetic selections.

***P. furiosus* genetics.** *Pf* strain Δ SHI [20] was used as the parent for this study. For markerless deletion of *pdaD* (PF1623, arginine decarboxylase) 1kb DNA flanking regions upstream and downstream of PF1623 were cloned around the P_{gdh} *pyrF* cassette (Figure 3.2) obtained from plasmid pGLW021 [20] using overlapping PCR. Transformation and selection of knockout *Pf* strains were performed as previously described [20] to generate strain Δ SHI Δ *pdaD*.

For homologous overexpression of genes in *Pf* a promoter region (200bp upstream PF1399) was selected based on microarray data to drive transcription. Across a wide range of conditions ([21]), PF1399 is constitutively expressed at a high level. Strains with disrupted *pdaD* were selected with defined medium lacking uracil and supplemented with 4 mM agmatine. For simple integrations on the *Pf* chromosome using agmatine prototrophy as a marker the plasmid pSPF300 was constructed. An *NspI* fragment was deleted from plasmid pSET152 removing the integrase gene to generate pSET-NS. From this pSPF101 was constructed by inserting the P_{gdh} *pyrF* cassette into *PstI/NheI* digested pSET-NS, which removes the OriT region, to produce pSPF101. The 200 bp upstream region from PF1399 (P_{slp} , promoter region

for S Layer Protein) and a multiple cloning site were inserted into *SacII/SphI* digested pSPF101 to generate pSPF102. A 1.1 kb upstream region of PF1623 was cloned into *Sal/NheI* pSPF102 making pSPF107. A 1.83 kb fragment containing intact PF1623 operon (0.73 kb) and 1.1 kb of its downstream region was amplified by PCR and cloned into *AscI/SphI* digested pSPF107 generating pSPF300. To construct a homologous recombination vector for the expression of dimeric hydrogenase, a cassette with 9X His tagged PF0893-0894 fused behind P_{slp} was first produced by overlap PCR, *SacII/KpnI* treated PCR product was then ligated with same enzymes treated pSPF300 to make pSPF302 (Figure 3.3). Transformation of *Pf* strain Δ SHI with *AscI/PmeI* linearized pSPF302 was performed and recombinant strains selected as previously described [20] to generate strain P_{slp} Dimer (Figure 3.3).

Large scale growth and protein purification. Native *Pf* SHI enzyme was purified from wild type *P. furiosus* DSM3638 as previously described [16]. *Pf* strain P_{slp} Dimer was grown in a 600L fermenter essentially as previously described [31] with the addition of 10 μ M uracil. Harvested cells were flash frozen in liquid nitrogen and stored at -80°C . All purification steps were performed using strict anaerobic technique under an atmosphere of argon. Cell-free lysate was prepared from the P_{slp} Dimer strain (330 g, wet weight) and DEAE (Diethylaminoethyl) anion exchange chromatography (GE Healthcare, Piscataway, NJ) performed as previously described [16]. Fractions eluting from DEAE anion exchange chromatography containing hydrogenase activity were pooled and loaded onto a 5 mL Ni Sepharose 6 Fast Flow column (GE Healthcare) equilibrated in 50 mM sodium phosphate, 300 mM sodium

chloride, 2 mM dithiothreitol, pH 8.0 (Buffer A). A linear 20 column volume gradient of 0-500 mM imidazole in buffer A was applied to the column and resulting fractions were analyzed for hydrogenase activity (Table 3.2). Apparent M_r was measured using a calibrated Superdex S200 sizing column (GE Healthcare).

Enzymatic assays and physical properties. Hydrogenase activity was routinely determined by H_2 evolution from methyl viologen (MV) (1 mM) reduced by sodium dithionite (10 mM) at 80°C as described previously [16], except the buffer was 100 mM EPPS, pH 8.4. One unit of hydrogenase specific activity is defined as 1 μ mole of H_2 evolved $\text{min}^{-1} \text{mg}^{-1}$. For a physiologically relevant assay, methyl viologen and sodium dithionite were replaced by NADPH (1 mM) as described [16]. To investigate altered coenzyme specificity, physiological hydrogen evolution assays were performed as previously described [27]. Oxygen sensitivity assays were performed by exposing samples to air at 25°C. Thermal stability assays were measured by anaerobic incubation of the hydrogenase samples at 90°C. Residual enzyme activities were measured using the MV-linked H_2 -evolution assay. Metal content of enzyme samples was measured as previously described [12].

:

Acknowledgements

This research was supported by grants (DE-FG05-95ER20175 and DE-FG02-05ER15710) from the Chemical Sciences, Geosciences and Biosciences Division, Office of Basic Energy Sciences, Office of Science, U.S. Department of Energy.

Author Contributions

Conceived and designed the experiments: RCH JS FEJ MWA. Performed the experiments: RCH JS SKC PM. Analyzed the data: RCH JS SKC PM FEJ MWA. Contributed reagents/materials/analysis tools: RCH JS SKC PM. Wrote the paper: RCH JS FEJ MWA.

REFERENCES

1. Dorian JP, Franssen HT, Simbeck DR (2006) Global challenges in energy. *Energy Policy* **34**: 1984-1991.
2. Wackett LP (2010) Engineering microbes to produce biofuels. *Curr Opin Biotechnol* **In Press**.
3. McKinlay JB, Harwood CS (2010) Photobiological production of hydrogen gas as a biofuel. *Curr Opin Biotechnol* **21**: 244-251.
4. Pfromm PH, Amanor-Boadu V, Nelson R (2010) Sustainability of algae derived biodiesel: A mass balance approach. *Bioresour Technol* **102**: 1185-1193.
5. Sigfusson TI (2007) Pathways to hydrogen as an energy carrier. *Philos Transact A Math Phys Eng Sci* **365**: 1025-1042.
6. Armstrong FA, Belsey NA, Cracknell JA, Goldet G, Parkin A, et al. (2009) Dynamic electrochemical investigations of hydrogen oxidation and production by enzymes and implications for future technology. *Chem Soc Rev* **38**: 36-51.
7. Edwards PP, Kuznetsov VL, David WI (2007) Hydrogen energy. *Philos Transact A Math Phys Eng Sci* **365**: 1043-1056.
8. Vignais PM, Billoud B (2007) Occurrence, classification, and biological function of hydrogenases: an overview. *Chem Rev* **107**: 4206-4272.
9. Vignais PM, Colbeau A (2004) Molecular biology of microbial hydrogenases. *Curr Issues Mol Biol* **6**: 159-188.
10. Fontecilla-Camps JC, Volbeda A, Cavazza C, Nicolet Y (2007) Structure/function relationships of [NiFe]- and [FeFe]-hydrogenases. *Chem Rev* **107**: 4273-4303.

11. Stephenson M, Stickland LH (1931) Hydrogenase: a bacterial enzyme activating molecular hydrogen: The properties of the enzyme. *Biochem J* **25**: 205-214.
12. Sun J, Hopkins RC, Jenney FE, McTernan PM, Adams MW (2010) Heterologous expression and maturation of an NADP-dependent [NiFe]-hydrogenase: a key enzyme in biofuel production. *PLoS One* **5**: e10526.
13. King PW, Posewitz MC, Ghirardi ML, Seibert M (2006) Functional studies of [FeFe] hydrogenase maturation in an *Escherichia coli* biosynthetic system. *J Bacteriol* **188**: 2163-2172.
14. Vincent KA, Parkin A, Armstrong FA (2007) Investigating and exploiting the electrocatalytic properties of hydrogenases. *Chem Rev* **107**: 4366-4413.
15. Fiala G, Stetter KO (1986) *Pyrococcus furiosus* sp. nov. represents a novel genus of marine heterotrophic archaeobacteria growing optimally at 100C. *Arch Microbiol* **145**: 56-61.
16. Ma K, Adams MW (2001) Hydrogenases I and II from *Pyrococcus furiosus*. *Methods Enzymol* **331**: 208-216.
17. Sapra R, Verhagen MF, Adams MW (2000) Purification and characterization of a membrane-bound hydrogenase from the hyperthermophilic archaeon *Pyrococcus furiosus*. *J Bacteriol* **182**: 3423-3428.
18. Bryant FO, Adams MW (1989) Characterization of hydrogenase from the hyperthermophilic archaeobacterium, *Pyrococcus furiosus*. *J Biol Chem* **264**: 5070-5079.

19. Ma K, Weiss R, Adams MW (2000) Characterization of hydrogenase II from the hyperthermophilic archaeon *Pyrococcus furiosus* and assessment of its role in sulfur reduction. *J Bacteriol* **182**: 1864-1871.
20. Lipscomb GL, Stirrett K, Schut GJ, Yang F, Jenney FE, Jr., et al. (2011) Natural competence in the hyperthermophilic archaeon *Pyrococcus furiosus* facilitates genetic manipulation: construction of markerless deletions of genes encoding the two cytoplasmic hydrogenases *Appl and Environ Microbiol* **77**: 2232-2238.
21. Schut GJ, Brehm SD, Datta S, Adams MW (2003) Whole-genome DNA microarray analysis of a hyperthermophile and an archaeon: *Pyrococcus furiosus* grown on carbohydrates or peptides. *J Bacteriol* **185**: 3935-3947.
22. Grzeszik C, Ross K, Schneider K, Reh M, Schlegel HG (1997) Location, catalytic activity, and subunit composition of NAD-reducing hydrogenases of some *Alcaligenes* strains and *Rhodococcus opacus* MR22. *Arch Microbiol* **167**: 172-176.
23. Fukuda W, Morimoto N, Imanaka T, Fujiwara S (2008) Agmatine is essential for the cell growth of *Thermococcus kodakaraensis*. *FEMS Microbiol Lett* **287**: 113-120.
24. Santangelo TJ, Cubonova L, Reeve JN (2010) *Thermococcus kodakarensis* genetics: TK1827-encoded beta-glycosidase, new positive-selection protocol, and targeted and repetitive deletion technology. *Appl Environ Microbiol* **76**: 1044-1052.

25. Ikeuchi Y, Kimura S, Numata T, Nakamura D, Yokogawa T, et al. (2010) Agmatine-conjugated cytidine in a tRNA anticodon is essential for AUA decoding in archaea. *Nat Chem Biol* **6**: 277-282.
26. Thore S, Mayer C, Sauter C, Weeks S, Suck D (2003) Crystal structures of the *Pyrococcus abyssi* Sm core and its complex with RNA. Common features of RNA binding in archaea and eukarya. *J Biol Chem* **278**: 1239-1247.
27. Silva PJ, van den Ban EC, Wassink H, Haaker H, de Castro B, et al. (2000) Enzymes of hydrogen metabolism in *Pyrococcus furiosus*. *Eur J Biochem* **267**: 6541-6551.
28. Sapro R, Bagramyan K, Adams MW (2003) A simple energy-conserving system: proton reduction coupled to proton translocation. *Proc Natl Acad Sci* **100**: 7545-7550.
29. Charon MH, Volbeda A, Chabriere E, Pieulle L, Fontecilla-Camps JC (1999) Structure and electron transfer mechanism of pyruvate:ferredoxin oxidoreductase. *Curr Opin Struct Biol* **9**: 663-669.
30. Sambrook J, Russell DW (2001) *Molecular Cloning : A Laboratory Manual*. Cold Spring Harbor, NY: Cold Spring Harbor Laboratory Press. 2100 p.
31. Verhagen MF, Menon AL, Schut GJ, Adams MW (2001) *Pyrococcus furiosus*: large-scale cultivation and enzyme purification. *Methods Enzymol* **330**: 25-30.

Table 3.1

Strain	Genotype	Originating Strain	Source
DSM	Wild Type	DSM3638	15
Δ SHI	Δ <i>pyrF</i> Δ <i>shI</i> β γ δ α	COM1	20
Δ SHI Δ <i>pdaD</i>	Δ <i>shI</i> β γ δ α Δ <i>pdaD::pyrF</i>	Δ SHI	This study
P_{slp} Dimer	Δ <i>shI</i> β γ δ α P_{slp} <i>shI</i> δ α	Δ SHI Δ <i>pdaD</i>	This study

Table 3.2

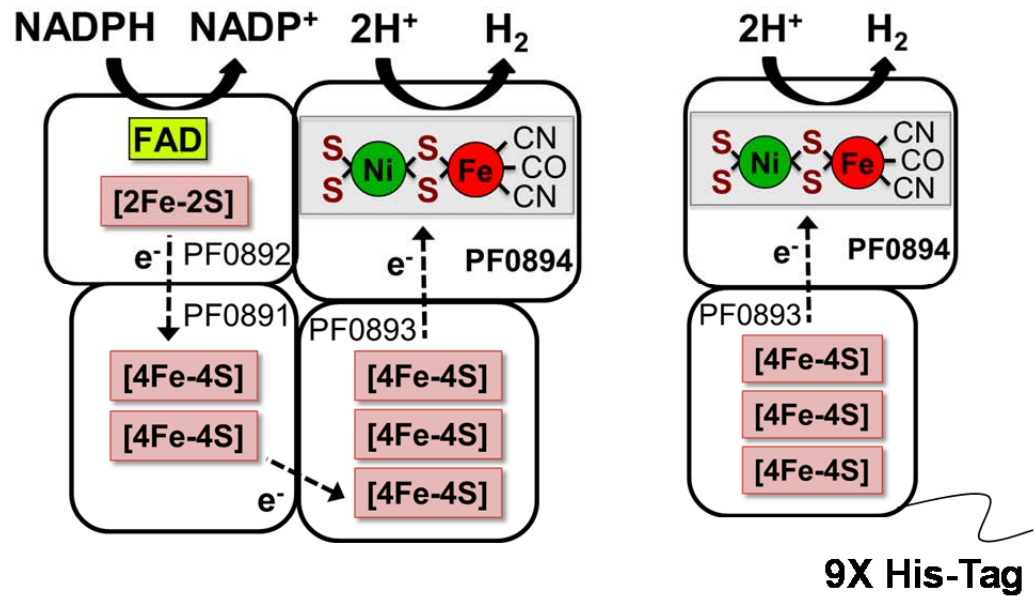
Step	Total Units ($\mu\text{mol min}^{-1}$)	Total Protein (mg)	Specific Activity (U mg^{-1})	Yield (%)	Purification (-fold)
Cytoplasm	15300	5110	3	100	1
DEAE Sepharose	14660	2740	5	96	2
Nickel Sepharose 6	5560	53	106	36	35

Table 3.3

Property	Native SHI [12]	OE-SHI Dimer
Activity, MV-Linked (U mg ⁻¹)	163	145
Activity, NADPH-linked (U mg ⁻¹)	1	0
Activity, POR-linked (U mg ⁻¹)	0	0.2
Metal Content (Ni:Fe)	1:25	1:10
Apparent M _r (Daltons)	155,000	88,000
Stability at 90°C (t _{1/2} , hr)	30	0.5
Stability in air (23°C, t _{1/2} , hr)	25	4

Figure 3.1. *Pyrococcus furiosus* heterotetrameric and dimeric soluble hydrogenase I. (a) Model of predicted cofactor contents of the heterotetrameric form of *Pf* SHI (taken without modification from Sun et al. [10]) and of the heterodimeric form of SHI that was produced (PF0893-PF0894) in this study that lacks PF0891 and PF0892. In the dimeric form, PF0893 is modified with an N-terminal His₉ tag. The abbreviations used are: CO, carbonyl ligand; CN, cyanide ligand; FAD, flavin adenine dinucleotide; NADP, nicotinamide adenine dinucleotide phosphate. (b) SDS-PAGE of purified heterotetrameric (*left lane*) and heterodimeric form of SHI (*right lane*) with molecular masses indicated in kDa.

a



b

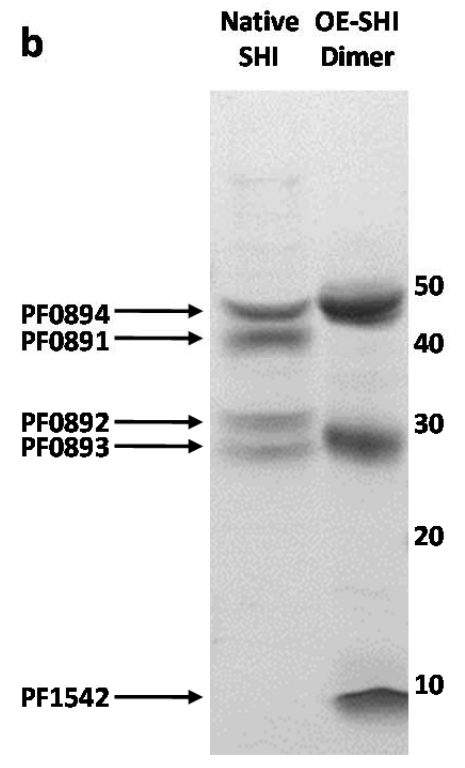


Figure 3.2. *pdaD* disruption with P_{gdh} *pyrF*. The 1kbp upstream and downstream regions for the *pdaD* locus (PF1399) were cloned around the P_{gdh} *pyrF* cassette [20]. Using previously described transformation methods the *Pf* chromosome was disrupted at *pdaD* generating a uracil prototroph and agmatine auxotroph [20].

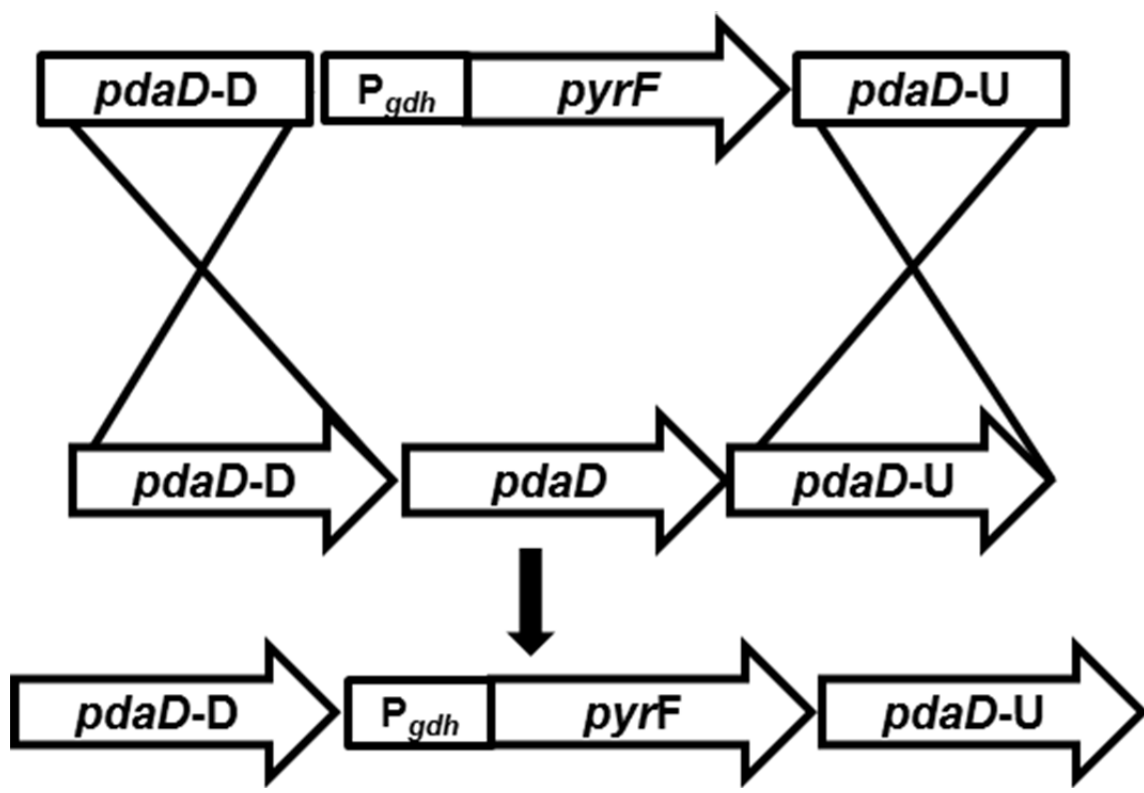
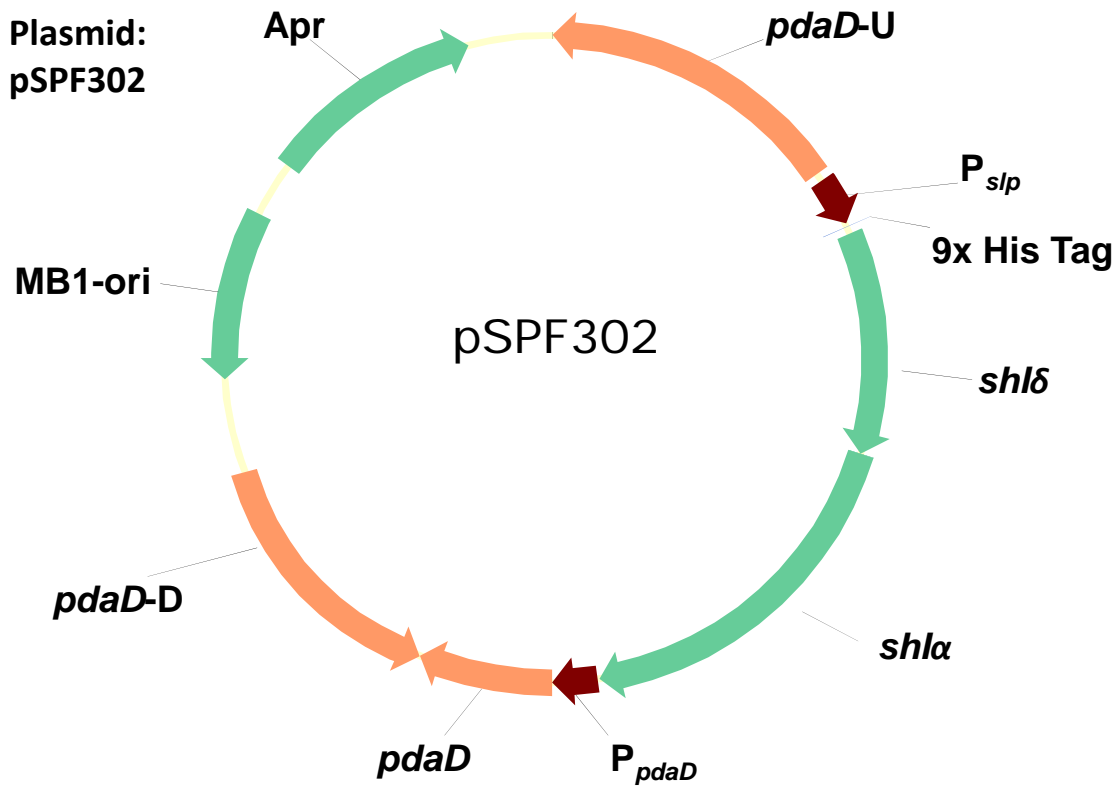


Figure 3.3. OE-SHI Dimer recombination plasmid and P_{slp} Dimer strain.

Plasmid pSPF302 was constructed for the integration of P_{slp} *shI*Δα onto the *Pf* chromosome at the *pdaD* locus. After homologous recombination P_{slp} Dimer strain contains the dimeric SHI construct under control of the constitutive promoter P_{slp} and the *pdaD* with its native promoter.

Plasmid:
pSPF302



Pf strain:
 P_{slp} Dimer

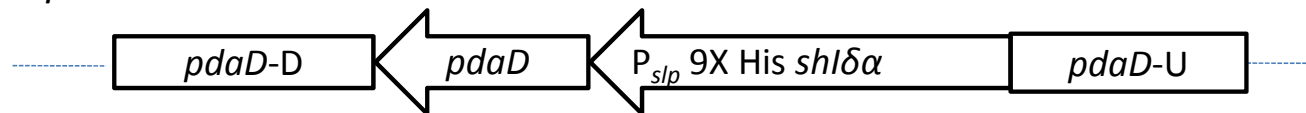
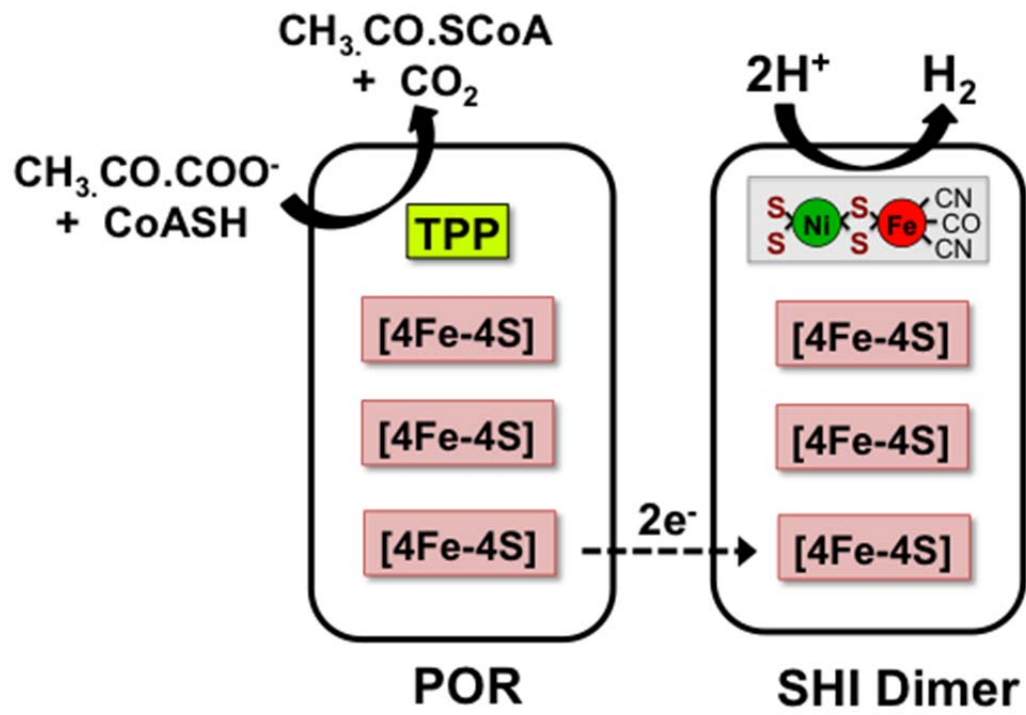


Figure 3.4. Model of the pyruvate-oxidizing, hydrogen producing POR-SHI Dimer system. The abbreviations are: POR, pyruvate ferredoxin oxidoreductase; SHI Dimer, heterodimeric form of SHI (PF0894+PF0893). TPP represents thiamine pyrophosphate.



CHAPTER 4
PRACTICAL APPLICATIONS OF HYDROGENASE AND GENETIC
ENGINEERING IN *PYROCOCCUS FURIOSUS*

The function of enzymes in bioprocesses has been known for some time, dating back to ancient Greece where they were unknowingly applied in baking, brewing, alcohol production, cheese fermentation, etc. [185]. With the increase of knowledge in enzyme isolation and characterization, the potential applications in industrial processes have increased exponentially. Thermostable enzymes, which are isolated almost exclusively from thermophilic hosts, have a number of commercial applications due to their intrinsic stability [186]. Performing enzymatic reactions at elevated temperatures facilitates higher reaction rates and process yields because of a decrease in viscosity, an increase in the diffusion coefficient of substrates, an increase in the solubility of substrates and products, and a favorable equilibrium displacement in endothermic reactions [185]. Early applications of thermophilic enzymes were almost exclusively amylases used in the starch industry [187], but the advent of the polymerase chain reaction underlined the indispensable nature of this class of enzyme [188,189].

Thermostability and optimal activity at high temperatures are innate properties of proteins isolated from thermophilic microorganisms. Because most proteins from mesophilic sources are inactive as such extreme temperatures, the mechanism of high-temperature stability has been of interest to the scientific community. The amino acid sequences of these enzymes reveal nothing novel, as many of the hyperthermophilic and mesophilic proteins exhibit high similarity, three-dimensional

structures that are superimposable, and perform the same catalytic mechanisms [190]. A survey of thermophilic enzymes expressed in *E. coli* revealed less than 10% exhibited properties and stabilities different from the natively isolated enzyme [190]. The fact that these enzymes remain thermostable after expression in mesophilic hosts suggest that the gene sequence is responsible for stability, though only few amino acid substitutions are observed [191]. General differences noted between some mesophilic and thermophilic enzymes are a higher instance of hydrophobic cores in thermostable proteins which may confer the increased stability [190,192,193]. No specific rules, though, for thermostability or generalizations can be derived from a systemic analysis of homologous mesophilic and thermophilic enzymes. Some studies employing site-directed mutagenesis of mesophilic proteins observed improved thermostability by substituting hydrophobic amino acids in core positions [194].

There are many advantages when working with hyperthermophilic organisms and their enzymes. In addition to facilitating higher reaction rates, the risk of contamination with mesophilic microorganisms decreases greatly at high temperatures and the enzymes are much more amenable to the harsh reactions conditions used in industrial settings. Extreme enzyme stability at room temperature allows for simple purification and manipulation protocols. Most thermophiles are poor hosts for obtaining large amounts of enzyme and the proteins are typically expressed in mesophilic organisms. Convenience is realized from this strategy as thermophilic enzymes expressed in mesophilic host are purified to near homogeneity

using a high temperature treatment (70°C-80°C) for up to 60 minutes. This level of purity is usually sufficient for most commercial applications.

The application of heat-stable enzymes in industry is well established. In addition to starch-degrading enzymes and polymerases, enzymes used commercially include proteases, xylanases, lipases, cellulases, and chitinases [185,191]. Although the enzymes produced by thermophiles are applied to many processes, rarely are the natively-isolated proteins or thermophilic organism itself utilized on a large scale. This is mainly due to the general lack of genetically-tractable thermophiles, and the low density fermentation for thermophiles, which yield insufficient biomass for protein extraction. Recently, however, genetic manipulation using standard molecular biology tools of some model hyperthermophiles was accomplished [88,195]. The application of these genetic tools can be used for far more than a gene knockout-phenotype searching approach. With thermophiles containing many novel enzymes, the opportunity presents itself to engineer a thermophilic organism directly for over-expression of proteins difficult to heterologously express and possibly metabolically engineer the organism itself for applied purposes. This chapter will describe the projects in progress involving hydrogenase and genetic engineering of *Pyrococcus furiosus*.

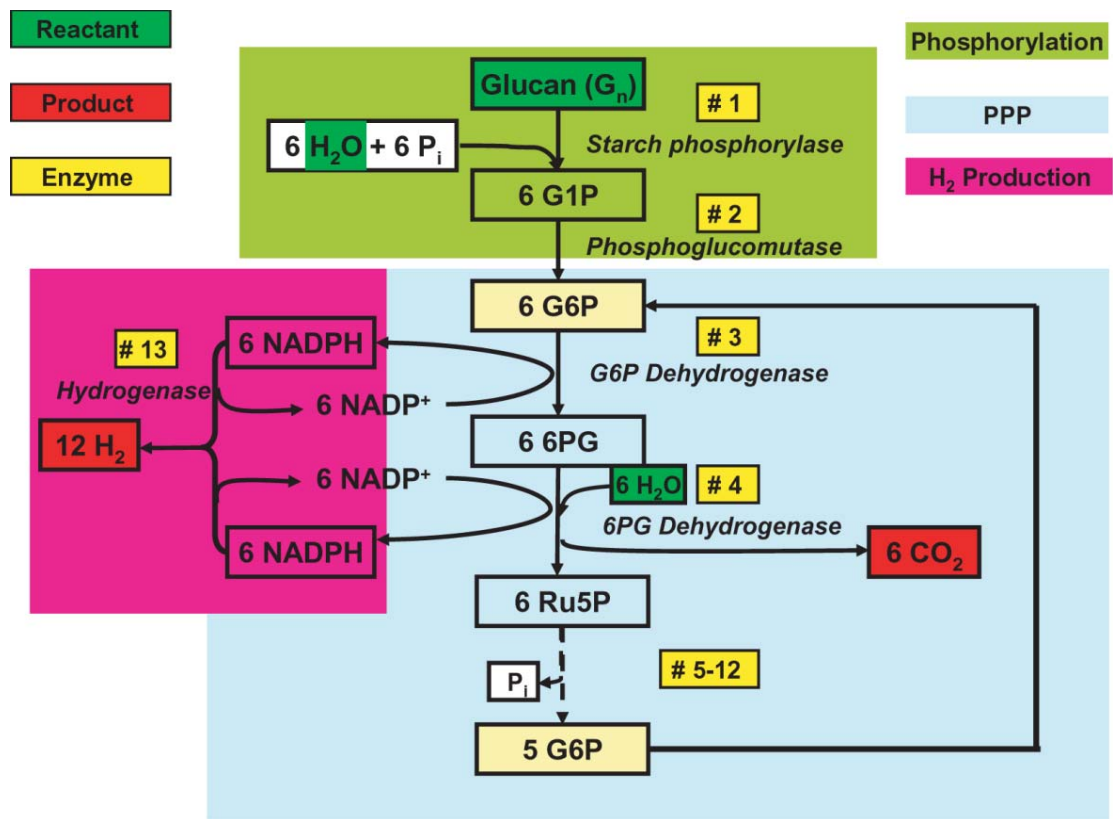
Hydrogenases fill diverse metabolic roles. Just as nature has adapted these enzymes to activate hydrogen for a plethora of cellular functions, the industrial and non-physiological applications of these unique proteins are equally as vast. Applications range from biohydrogen production to denitrification, bioremediation, and molecular biosensors [196]. As detailed in chapters two and three, SHI from

Pyrococcus furiosus lends itself as a model for hyperthermophilic hydrogenase research. Hydrogenase, however, is not a commodity enzyme. It cannot be purchased from any scientific vendor and obtaining large amounts of enzyme from the native organism is impractical. Although the heterologous expression of SHI in *E. coli* (Chapter 2) was reported, the yield with respect to total cell protein was very poor. Western blot analysis of the SHI catalytic subunit revealed a large amount of expressed, soluble protein but only a small fraction of active enzyme (unpublished results). Presumably the bottleneck in enzyme production is at the post-translational processing steps required for a catalytically active enzyme. The ten-fold homologous overexpression of His₉-tagged SHI in *Pf* was reported by Chandrayan *et al.* and demonstrates a great stride towards producing large amounts of hydrogenase enzyme [89].

The practical applications of hydrogenase were noted well before the ability to overexpress the enzyme came about. Obvious applications exist in renewable biofuel production as the biological catalyst for hydrogen production. It was demonstrated that *in vitro* reactions of α -linked polysaccharides, *Pf* SHI, and twelve enzymes involved in starch hydrolysis and the pentose phosphate pathway (PPP), were able to efficiently evolve hydrogen without any additional energy addition other than the carbon source (Figure 4.1)[181]. Surprisingly, the system worked extremely well with an overall yield of 5.19 mol H₂/mol glucose (43% conversion). These reactions were carried out at 30°C with a hyperthermophilic hydrogenase, mesophilic starch hydrolysis and PPP enzymes. This un-optimized system, operating at a significantly

Figure 4.1

The synthetic metabolic pathway for conversion of polysaccharides and water to hydrogen and carbon dioxide [181].



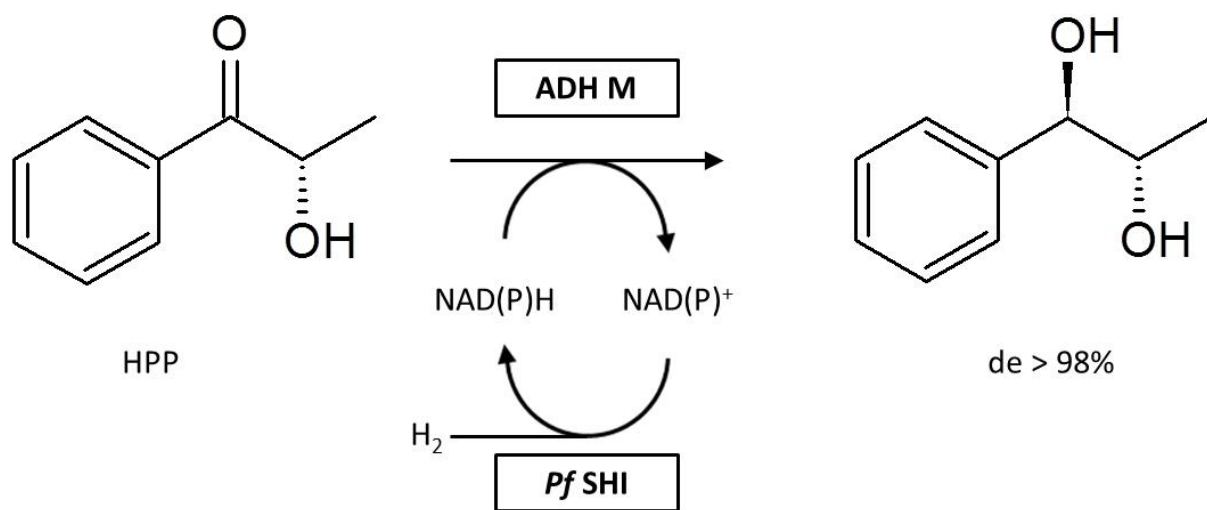
lower temperature than that for maximal hydrogenase activity, was able to evolve hydrogen more efficiently than the theoretical limit of microbial fermentation of glucose to H₂ (4 mol H₂/mol glucose)[197]. The stability of *Pf* SHI is as remarkable as the range of catalytic activity. Aside from tolerating extreme temperatures, Woodward *et al.* and Davison *et al.* reported the activity of polyethylene glycol-modified *Pf* SHI in various organic solvents, including high percentage acetonitrile and toluene [198,199]. The ability of this enzyme to function in organic solvent opens a broad range of applications in organic synthesis.

Perhaps the most significant characteristic of many thermophilic hydrogenases is the ability to accept and donate electrons from the coenzyme NAD(P)(H) and this is of great importance as many pharmaceuticals, flavors, and agrochemicals require NADPH [200]. A large majority of oxidoreductases utilized in these processes catalyze the enantioselective reduction of prochiral ketones and require reducing equivalents of NADPH [201,202]. At a current market price of ~\$780,000 mol⁻¹ (Sigma-Aldrich, St. Louis, MO) stoichiometric equivalents of NADPH in synthesis reactions are cost prohibitive. More feasible is the *in situ* regeneration of NADPH from NADP during a reaction. Chemical and electrical reduction of NADP would be difficult to apply in these instances; the most attractive method is the enzymatic substrate-coupled system [203]. Enzymes currently used in this method require input of substrates that can be costly and may interfere with the current or downstream processing reactions (e.g. formate and formate dehydrogenase) [204,205]. The simplest and most cost-effective scheme would use the cheapest reductant available, gaseous hydrogen, and an NADP-dependent hydrogenase. *Pf* SHI, an NADP

dependent enzyme, is an excellent catalyst for the enzymatic production of NADPH. *Pf* SHI was used to efficiently catalyze hydrogen-dependent NADP reduction in an *in vitro* enzyme mixture and a proof-of-principle synthesis of (1S)-phenyl ethanol in a by-product free reaction mixture was demonstrated (Figure 4.2)[203]. Moreover SHI reactions were catalyzed at 40°C, 60° below the optimal growth temperature of *Pf*, again demonstrating the broad temperature range of activity. These poof-of-principle reactions demonstrate the robust nature of the soluble hydrogenase from *P. furiosus*. The enzyme is readily reversible, catalyzing hydrogen oxidation or proton reduction, depending on the electron carrier of the reaction. Removing gaseous hydrogen from a hydrogen production system pushes the reaction towards hydrogen synthesis and saturating a process with hydrogen favors the reduction of NADP, according to Le Chatelier's principle. While the prospects of utilizing SHI in a hydrogen producing context are still at infancy, employing the enzyme for *in vitro* NADPH production is not. With the price difference of NADPH and NADP (\$780k v \$380k respectively) at \$400k mol⁻¹, one could straightforwardly use hydrogen and SHI to reduce NADP to NADPH on a large scale for commercial purposes. Virtually all reactions that require NADPH could satisfy this cheaply and efficiently by introducing hydrogen and SHI. As NADPH is the standard cell currency for many anabolic processes, SHI could provide the reducing equivalents for synthesis of a plethora of industrially relevant biomolecules. Until recently the tools for genetic manipulation of *Pyrococcus furiosus* have been unavailable. Mirroring the efforts of the Imanaka lab with *Thermococcus kodakarensis*, great strides were made in the ability to create

Figure 4.2

Proof-of-principle synthesis of (1S)-phenyl ethanol in a by-product free reaction mixture from hydrogen and soluble hydrogenase I from *Pyrococcus furiosus* [203].



knockouts, utilize multiple markers, and perform promoter swaps [88,89,206]. Researchers are now investigating the possibility of *Pf* serving as a host to homologously and heterologously (over)express enzymes and genetically engineer the organism for *in vivo* processes. *Pf* SHI is well established in its hydrogen-dependent NADP reduction ability *in vitro*. It is generally accepted that the *in vivo* role of SHI is also hydrogen oxidation to produce reducing equivalents of NADPH [87]. Processes that require reductant in the form of NADPH could easily be supplied *in vivo* by adding hydrogen to a growing culture. Before describing the projects in progress, some consideration must be made of the economics of using hydrogen. For commodity chemicals of high value (such as 1,3-Propanediol which is discussed further below) it is obvious that hydrogen is relatively cheap when considering production costs. For other processes, especially those relating to biofuels, it may seem counterintuitive using hydrogen to produce another energetic compound as a fuel. Hypothetically, if hydrogen were available in plentiful amounts, much work on infrastructure would still be needed to convert existing systems to use such a different fuel. A fungible fuel created from hydrogen, on the other hand, would be economically preferred as pertaining to infrastructure and conversion expense. For the purpose of in progress and future projects described we will assume that a plentiful and renewable source of hydrogen will be available.

Before describing specific genes to be introduced into *Pf* one must consider how to promote transcription for a range of purposes. The first promoter swap for overexpression of an operon in *Pf* used the upstream region of PF1399 (annotated as S-layer protein) [89]. Based on microarray analysis (Schut and Adams, unpublished

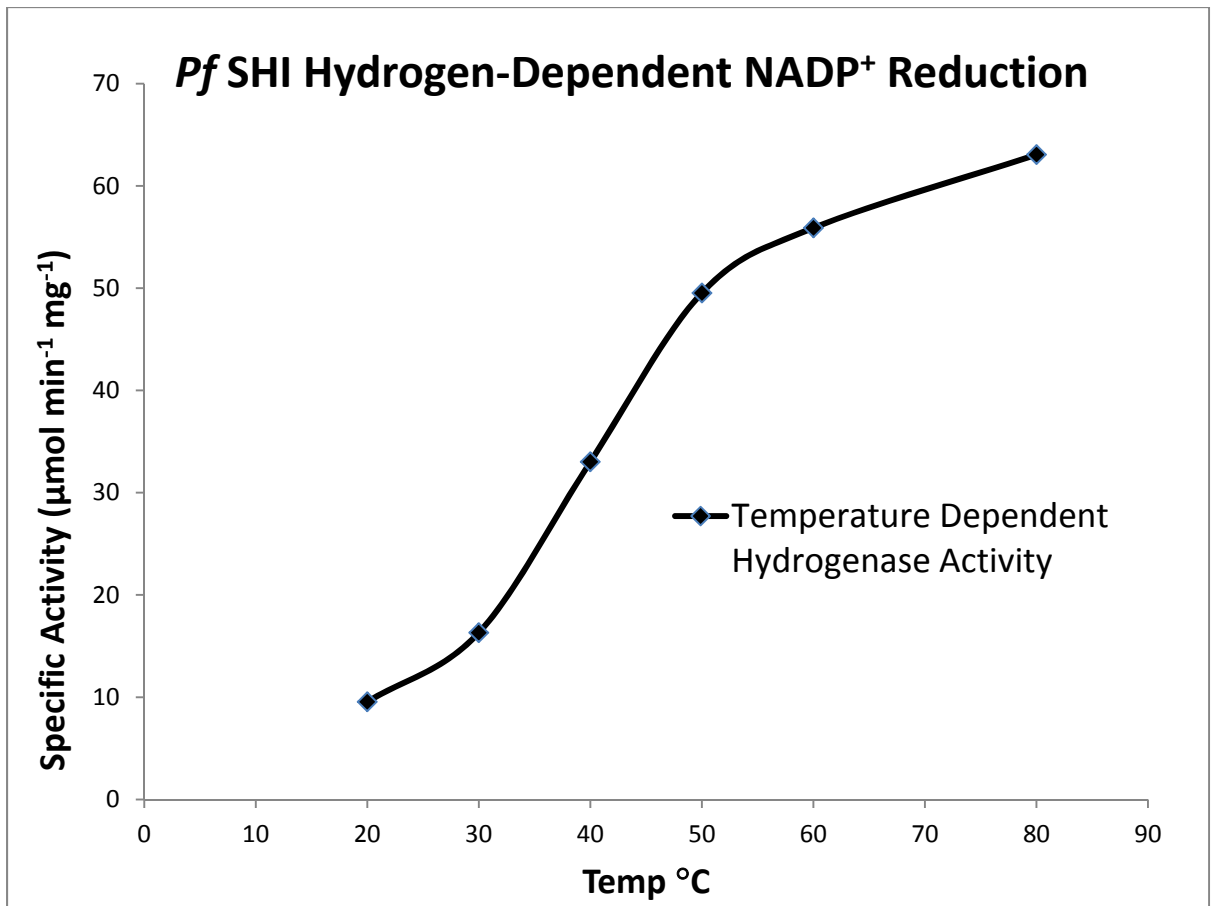
results) the transcript for PF1399 is the most highly constitutively expressed mRNA over nearly all growth conditions analyzed. When defining the promoter region of a gene based on microarray data, usually 150-200bp of upstream DNA are excised and used in designing expression constructs. Other promoters have seen utility as the transcription driving force for resistance markers (e.g. PF1602 glutamate dehydrogenase P_{gdh} -HMG-CoA reductase (Simvastatin resistance)) [88,207]. An inducible promoter (PF0613 fructose-1,6 biphosphatase) was employed for the expression of subunit D of the native *Pf* RNAP [207]. This system, however, required harvesting cells and resuspending in different growth medium for induction (glycolytic to gluconeogenic medium) and can hardly be considered for large scale expression utility. The cold shock transcriptional response of *Pf* has been characterized (shift from 95 to 72°C) and revealed the substantial upregulation of two genes, PF0190 and PF1408, termed cold induced proteins (Cip) A and B [208]. The promoter region for CipA was recently used to drive expression of an exogenous lactate dehydrogenase under cold growth conditions [209]. This promoter is active in both cold-adapted and cold-shocked cells and allows for simple cooling of a culture to induce gene expression. For the proposed research projects discussed herein we consider two of these promoter systems, P_{slp} (S-layer promoter) and P_{cip} (cold induced promoter).

When attempting to use *Pf* as an expression host for *in vivo* bioprocessing it becomes immediately apparent that there are not hyperthermophilic homologs for many genes of interest. *Pf*'s utility as an expression host may not be limited to its hyperthermophilic physiology, but more interestingly in its behavior during relative

cold fermentation. The doubling time in an optimal culture of *Pf* at 95°C is 45 minutes but drops to nearly five hours at 72°C [208]. Though gene expression is still observed at 72°C, the lack of microbial growth suggests the cells are in a state of metabolic stasis. Some enzymes native to *Pf*, though, have extraordinarily large catalytically active temperature ranges, notably SHI. *In vitro* assays demonstrate that hydrogen-dependent reduction of NADP can be observed from 80° down to 20°C (Figure 4.3). Operating under the assumption that SHI *in vivo* exhibits the same activity, it should be possible to generate a large NADPH:NADP ratio in *Pf* at 72°C by adding hydrogen to a static culture. Heterologously expressing NADPH-dependent enzymes in *Pf* that have a $T_{\text{opt}} \sim 72^{\circ}\text{C}$ would allow optimal activity of exogenous enzymes while effectively eliminating maintenance energy of the host organism and directing all reducing equivalents to a desired process. This hypothesis will be tested by introducing genes of potential industrial significance into *Pf* that produce commodity chemicals.

Figure 4.3

Temperature dependence of *Pf* SHI hydrogen-catalyzed NADP⁺ reduction



1,3-Propanediol Synthesis

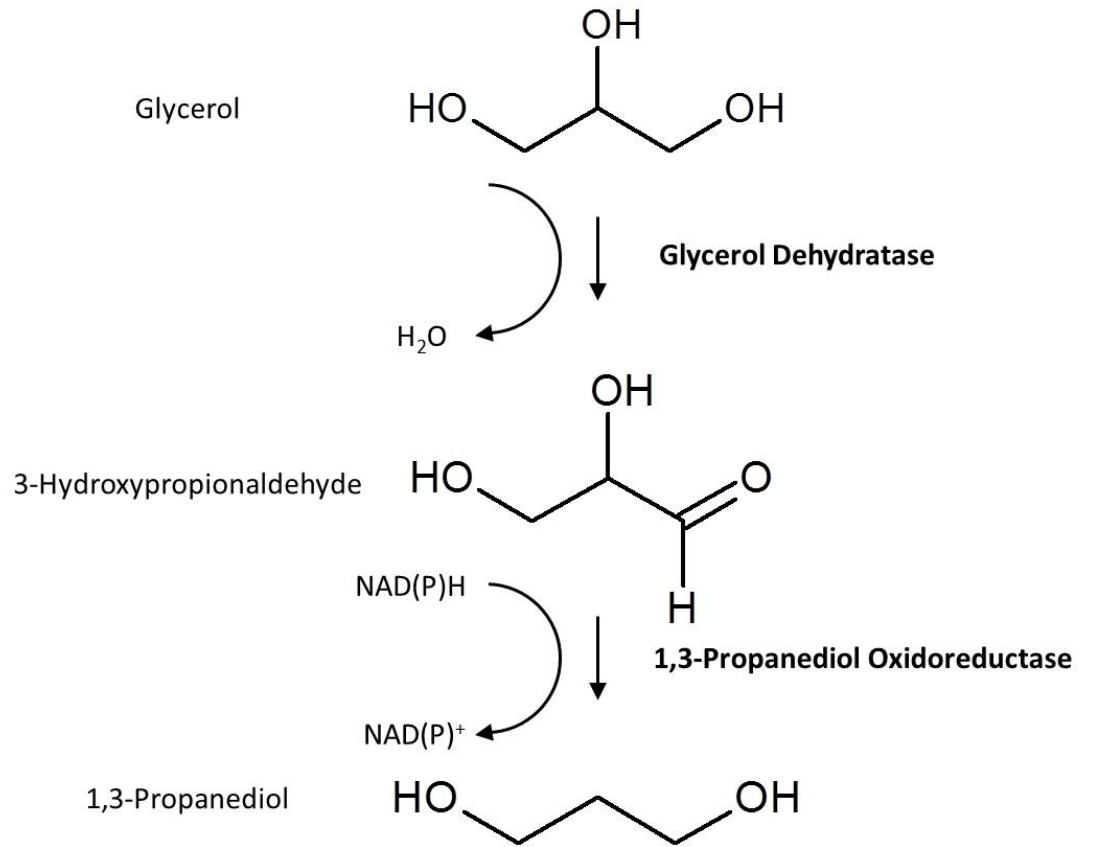
1,3-Propanediol (PD) is a promising bulk chemical that has attracted much attention due to its vast potential in applications such as polymers, cosmetics, foods, adhesives, lubricants, laminates, solvents, antifreeze, and medicines [210,211,212,213]. PD is a versatile intermediate compound used in the synthesis of heterocycles and, due to the presence of hydroxyl groups at the one and three position, it finds applications in the production of polymers such as polyesters and polyurethanes [214]. Polymers based on PD are more resistant to stains and exhibit superior color fastness. A new polyester based on PD, polytrimethylene terephthalate (PTT), has caused a strong increase in demand due to the superior stretching and stretch recovery characteristics [215]. Earlier in the century PD could not compete with other bulk chemicals as sufficient quantity and quality product was not available. Recently the development of biological processes and novel strains have pushed PD synthesis back to the forefront and can now compete with chemical synthesis from non-renewable petrochemicals [210,214,216,217].

PD is produced naturally in several genera of microorganisms: *Klebsiella* [218,219,220], *Clostridia* [221,222], *Citrobacter* [213,223], *Enterobacter* [224], and *Lactobacilli* [225]. Some of these organisms are classified as opportunistic pathogens and require special precautions for fermentation. Some non-pathogenic *Clostridia* strains are used in PD synthesis but obligate anaerobes suffer from sub-optimal fermentation characteristics. Of the natural producers, *C. butyricum* and *K. pneumonia* are considered the most efficient and have attracted attention due to their substrate tolerance, yield, and productivity [226]. The biochemical mechanism of

reductive glycerol dissimilation has been characterized and involves two enzymes: B₁₂-dependent glycerol dehydratase (GDHt) and 1,3-propanediol oxidoreductase (PDOR) (Figure 4.4). The first enzyme, GDHt, requires adenosylcobalamin as a cofactor to dehydrate glycerol to 3-hydroxypropionaldehyde (3HPA) by a radical mechanism [227]. Although adenosylcobalamin is required for dehydration, it is not catalytic and GDHt experiences a mechanism-based inactivation by glycerol during the reaction [216]. Coenzyme B₁₂ undergoes an irreversible cleavage of the Co-C bond forming 5' deoxyadenosine and a cobalamin like species that binds tightly to inactive GDHt [228,229]. It was demonstrated in permeabilized cells of *K. pneumonia* that rapid reactivation of the GDHt is observed by exchange of the modified coenzyme for intact adenosylcobalamin in the presence of adenosine triphosphate (ATP) and Mg²⁺, suggesting that a reactivating component participates in the reaction [230]. Encoded in the same operon as GDHt (*dhaBCE*) in many organisms are two open reading frames (*dhaFG*) that have homology to ATPase domains, GroEL, and Hsp70 group of molecular chaperones. The gene products of *dhaFG* were shown *in situ* to be responsible for the ATP-dependent reactivation of B₁₂-dependent dehydratase [231]. The second step of PD synthesis is catalyzed by NADH-dependent 1,3-propanediol oxidoreductase (PDOR) and functions to reduce the aldehyde of 3HPA and produce PD (Figure 4.4) [232]. In efforts to improve the efficiency of PD synthesis, another oxidoreductase has been employed, NADPH-dependent YqhD, and coexpression with B₁₂-independent GDHt generated superior titers of PD *in vivo* [233].

Figure 4.3

Biological mechanism of dissimilative reduction of glycerol to 1,3-propanediol.



The thermophilic conversion of glycerol to PD has received little research attention and nearly all commercially investigated PD producers are mesophilic [234]. Of the characterized thermophilic organisms capable of producing PD, none have a sequenced genome [235]. BLAST (Basic Local Alignment Search Tool) searches of the non-redundant sequence database with representative members of the GDHt family returned no significant homologs in organisms with a $T_{opt} > 50^{\circ}\text{C}$. Recently, however, the efforts of a sequencing project involving 20 species relevant to biofuel production deposited the genome of *Thermoanaerobacter* sp. X514 [236]. *Thermoanaerobacter* sp. X514 (*Tx514*) is a thermophilic anaerobe isolated 2,000 meters below the surface of the Piceance Basin in Colorado [162]. *Tx514* has an optimal growth temperature of 60°C , ferments simple sugars, and can utilize non-fermentative small acids and hydrogen in reducing Fe(III) [162]. Most interestingly the genome of *Tx514* contains the typical genes and operon structure for B₁₂-dependent glycerol dehydratases and presumably possesses the ability to convert glycerol to PD (Figure 4.5). Having a T_{opt} of 60°C , the gene products expressed by *Tx514* (assuming their stability directly reflects optimal growth temperature) fall within the threshold as candidates for relative cold heterologous expression in *Pf*. To investigate the ability of *Pf* in converting glycerol to PD, the genes encoding the GDHt, reactivase, and NADPH-dependent dehydrogenase from *Tx514* will be integrated into the *Pf* genome under the control of the P_{slp} and P_{cip} promoters.

Figure 4.5

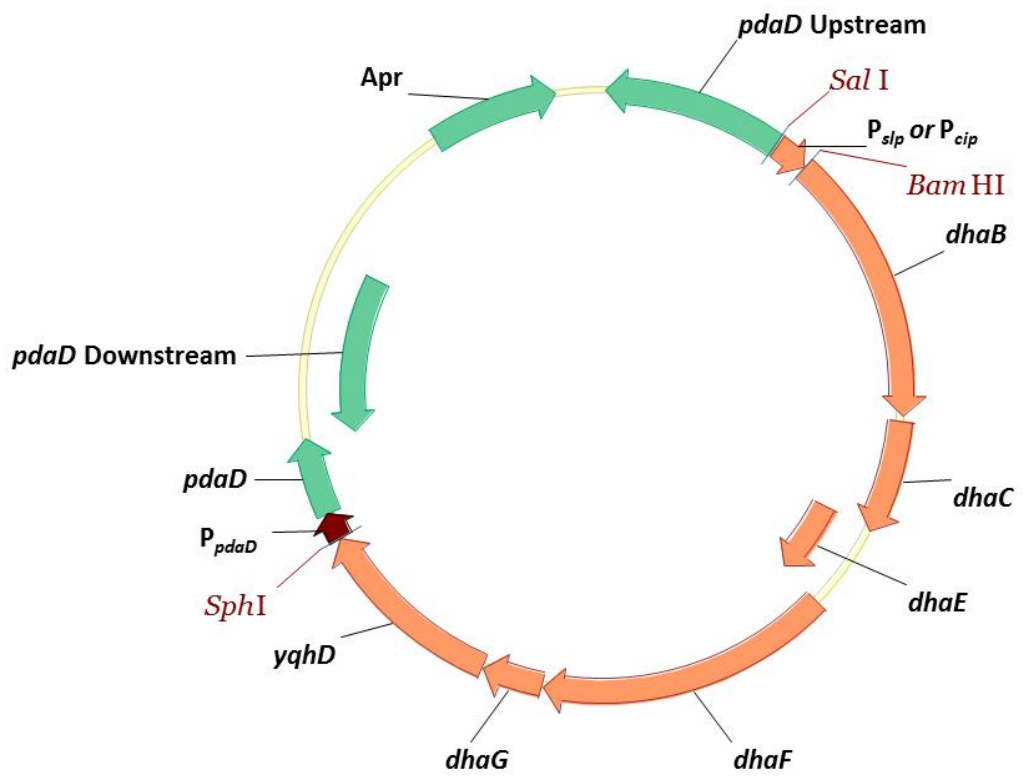
**Operon structure of 1,3-propanediol related genes in *Thermoanaerobacter* X514.
dhaBCE, B12-dependent glycerol dehydratase, *dhaFG*, dehydratase reactivase,
dhaT, propanediol oxidoreductase**



Thermoanaerobacter X514 GDHt Operon

Figure 4.6

pdaD suicide vector for *Tx* 514 PD gene integration on the chromosome of *Pf*.



Design of constructs for cloning of the GDHt region from *Tx514* in *Pf* was done essentially as described for the dimeric hydrogenase in Chapter 3. Figure 4.6 outlines plasmids constructed for integrating genes at the *pdaD* locus under either a constitutive promoter (P_{slp}) or inducible promoter (P_{cip}). Plasmids were transformed into *Pf* as previously described in Chapter 3. Current efforts with the PD research project involve sequencing of the *pdaD* locus to confirm integration of *Tx 514* PD genes on the *Pf* chromosome. After successful gene integration recombinant *Pf* strains will be probed for the *Tx 514* PD gene transcripts and recombinant activity to convert glycerol to PD *in vitro* and *in vivo*. In parallel with recombinant *Pf* growths and *in vitro* assays, *Tx 514* growth studies mirroring conditions known to produce PD from other well characterized organisms will be carried out to confirm ability of the native organism to convert glycerol to PD.

Heterologous Thermophilic Rhodopsin

The ability to create high NADPH:NADP ratios in *Pf* simply by adding hydrogen presents a unique opportunity to exploit this organism as a reaction vessel for industrially relevant biomolecule synthesis. While many anabolic reactions utilize NADPH as the electron donor, many others additionally require ATP during synthesis reactions. If in fact *Pf* is in metabolic stasis due to the temperature, *vide supra*, a proton motive force (PMF) will not actively be generated. For example, the synthesis of 1,3-propanediol at 70°C would inevitably be prematurely terminated without the necessary ATP for reactivating the B₁₂-dependent glycerol dehydratase. Assuming the membrane bound ATP synthase of *Pf* still functions at a significant rate similar to

SHI, one would only need to create a $\Delta\Psi$ to readily catalyze the hydration of adenosine diphosphate (ADP) to ATP. The simplest and most direct method for creating an ion gradient can be accomplished with the light-driven proton-pumping integral membrane protein rhodopsin.

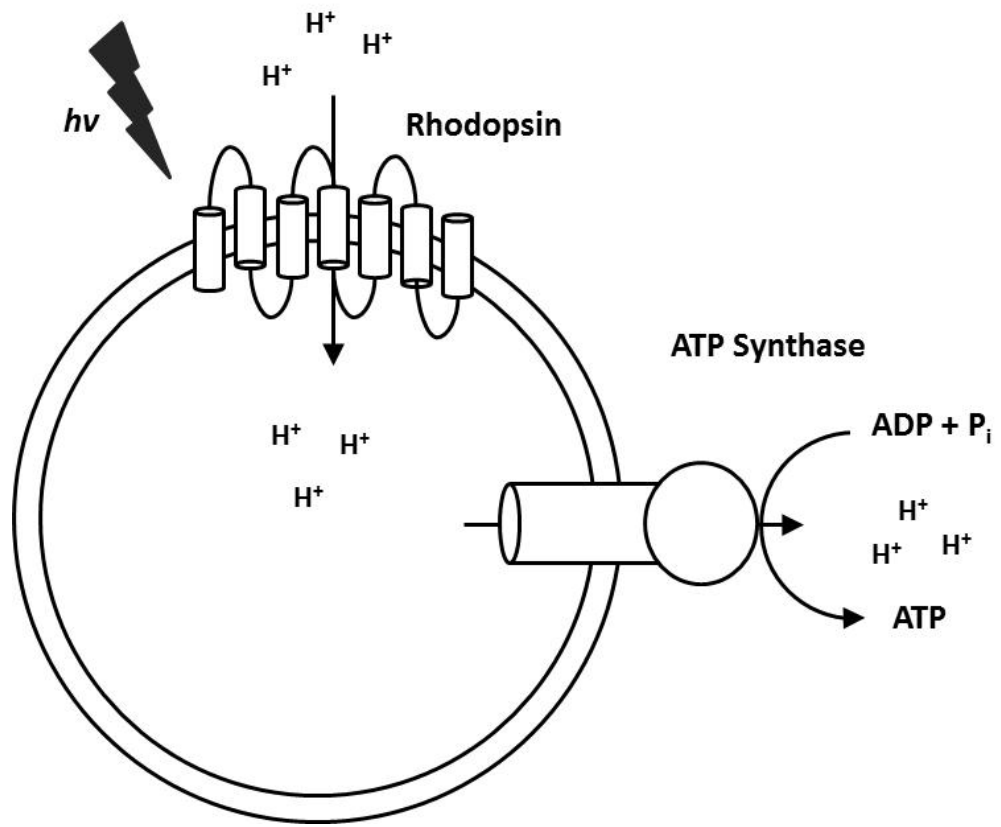
Rhodopsin was first characterized from the membrane fraction of *Halobacterium halobium* as a pigment that responds to illumination with an absorption maxima shift from 560 to 415 nm and a marked decrease in the rate of oxygen consumption by the native organism [237]. Oesterheldt, *et al.* correctly hypothesized that the purple pigment generated a light-dependent PMF arising from a vectorial uptake and release of protons across the membrane. Rhodopsin contains seven transmembrane domains and utilize as a cofactor either *all-trans* or *1,3-cis* retinal as their chromophore [238]. When activated by the absorption of a photon the chromophore of rhodopsin isomerizes on a femtosecond timescale to generate photovoltage by releasing a proton from the cytoplasm. [239]. Genomic and metagenomic sequencing have revealed that rhodopsins are not limited to the haloarchaea. Homologs involved in sensory functions and ion transport are distributed across many disparate eukaryotes and bacteria [240]. Recently metagenomic sequencing of oceanic samples revealed that type 1 rhodopsin-based phototrophy in marine bacteria are phylogenetically and biogeographically widespread [241,242]. Although the distribution of rhodopsin appears extensive yet sporadic indicating a common evolutionary ancestor several recent robust phylogenetic trees suggest lateral gene transfer to be a more plausible explanation [240].

Rhodopsin has many practical applications and the ultrafast photodetection aspects of its activity have been exploited for use in two-dimensional photoelectric arrays, artificial retinas, and electro-optically controlled spatial light modulators [243,244,245]. Utilization of rhodopsin for the *in vitro* production of ATP was first reported by Racker *et al.* in 1974. Reconstitution of membranes from *Halobacterium halobium* in the presence of bovine heart mitochondrial ATP synthase yielded vesicles capable of catalyzing light-dependent phosphorylation of ADP [246]. Several recent reports of advancements on this process include the heterologous co-expression of *Haloterrigena turkmenica* Δ -rhodopsin and thermostable *Bacillus* PS3 F₀F₁ ATP synthase [247] and *Gleobacter violaceus* bacteriorhodopsin in *E.coli* [239]. Figure 4.7 demonstrates the general model of inside-out membranes catalyzing the light dependent phosphorylation of ADP. Hara *et al.* reported the expression of *H. turkmenica* rhodopsin with the *Bacillus* PS3 ATP synthase as an improvement on *in vitro* ATP production due to the increased stability of the thermophile-derived enzyme. For industrial applications this system still suffers from a few undesirable characteristics. The ATP synthase is thermostable but *E. coli* membranes and *H. turkmenica* rhodopsin are not. For commercial applications utilizing harsh reaction conditions it would be preferential to employ a system in which all components of the reaction mixture are thermostable.

With the utility of rhodopsin well established the prospect of light-catalyzed ATP generation in *Pf* is an obvious next step. In order to heterologously express an active rhodopsin in *Pf* the gene must originate from a thermophilic organism but to date no thermophilic homologs have been characterized in the literature. However,

Figure 4.7

**Model of inverted membrane vesicles catalyzing light dependent ATP synthesis
via rhodopsin and ATP synthase.**



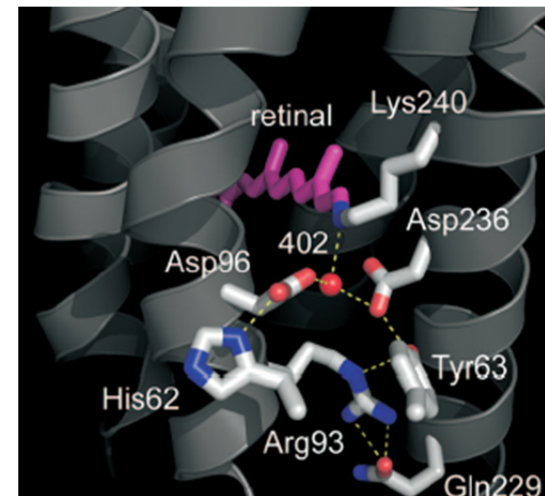
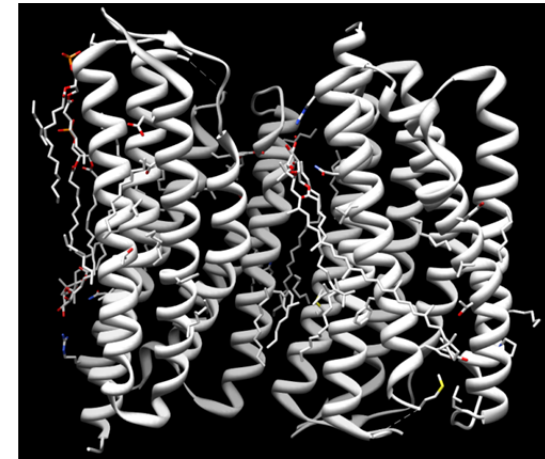
BLAST searches of the non-redundant sequence database with representative members of the rhodopsin families returns one homolog from the thermophilic bacterium *Thermus aquaticus* Y51MC23 (*Taq* Y51) most similar to the xanthorhodopsin from *Salinibacter ruber* (Figure 4.8). Xanthorhodopsin is unique in that it contains two light harvesting antennas, *all-trans* retinal and the carotenoid salinixanthin [248]. Although the presence of an additional light harvesting compound is predicted to increase overall efficiency, it has been shown that the selective removal of salinixanthin retards activity only 1.5 fold [249].

Taq Y51 was the subject of a now defunct US DOE Joint Genome Institute (JGI-PGF) initiative to compare thermophilic bacteria and the genome sequence is in permanent draft status. Although *Taq* Y51 is not deposited in either the American Type Culture Collection (ATCC) or Deutsche Sammlung von Mikroorganismen (DSMZ) utilization of native DNA sequence for *Taq* rhodopsin in *Pf* would be extremely unfavorable due to a large codon bias. For expression in *Pf* codon optimized gene sequence must be synthesized to preclude any translational stalling potentially caused by use of rare codons in *Taq* Y51 as compared to *Pf*. Other potential problems may arise from the disparity between biological membrane compositions when performing a trans-domain expression of a transmembrane protein: bacteria typically contain ester-linked lipid bilayers and archaea ether-linked monolayers. The successful heterologous expression of an archaeal rhodopsin from *Haloterrigena turkmenica* in *E. coli* suggests membrane bias may not be a problem [247]. One particular issue to overcome is the source of *all-trans* retinal *in vivo*, a compound synthesized from the oxygen dependent cleavage of β -carotene by β -

Figure 4.8

Sequence alignment of *Thermus aquaticus* Y51MC23 and *Salinibacter ruber* rhodopsin. Residues involved in retinal coordination are highlighted in red and depicted in the inset x-ray structure. From PDB 3DDL.

		1		40
Taq Rhodopsin	(1)	-MRMLPELSFGQYWL	VFNMLS	LTIIAGMFAAFVFFLLARSY
Xanthorhodopsin	(1)	MLQELPTLT	PGQYSLVFNMF	FTVATMTASFVFFVLARNN
		41		80
Taq Rhodopsin	(40)	VAPRYHIALYLSALIV	FIAGYHLRIFESW	VGAYQLQGGV
Xanthorhodopsin	(41)	VAPKYRISMMVSALV	VFIAGYHYFRITSS	WEAAYALQNGM
		81		120
Taq Rhodopsin	(80)	YVPTGKPFNDFYRYA	WLLTVPLLELIL	VVLGGLPAARTW
Xanthorhodopsin	(81)	YQPTGELFNDAIRYV	WLLTVPLLTVEL	VLMGLEPKNERG
		121		160
Taq Rhodopsin	(120)	NLGIKLVVASVLM	LGLGYVGEVNT	EP---GPRTLWGALSS
Xanthorhodopsin	(121)	PLAAKLGFLAALM	IVLGYPGEVSENA	ALFTRGLWGFLLST
		161		200
Taq Rhodopsin	(157)	VPFYILYVLWVEL	QQAIREAKFGPR	VLELLGATRLVLLM
Xanthorhodopsin	(161)	IPFVWILYILFTQ	LGDITQRQSS--	RVSTLLGNARLLLLA
		201		240
Taq Rhodopsin	(197)	SWGFPYIAYALGT	WLPGGAAQ----	EVAIILGYSLAHLI
Xanthorhodopsin	(199)	TWGFYPIAYMIPMA	FPEAFPSNTPGT	IVALVGYTIALVLI
		241		275
Taq Rhodopsin	(232)	AKPIYGLLVFAI	ARAKSLEEGFG	GEGVKAA-----
Xanthorhodopsin	(239)	AKAGYGVLIYNI	AKAKSEEEGF	NVSEMVEPATASA

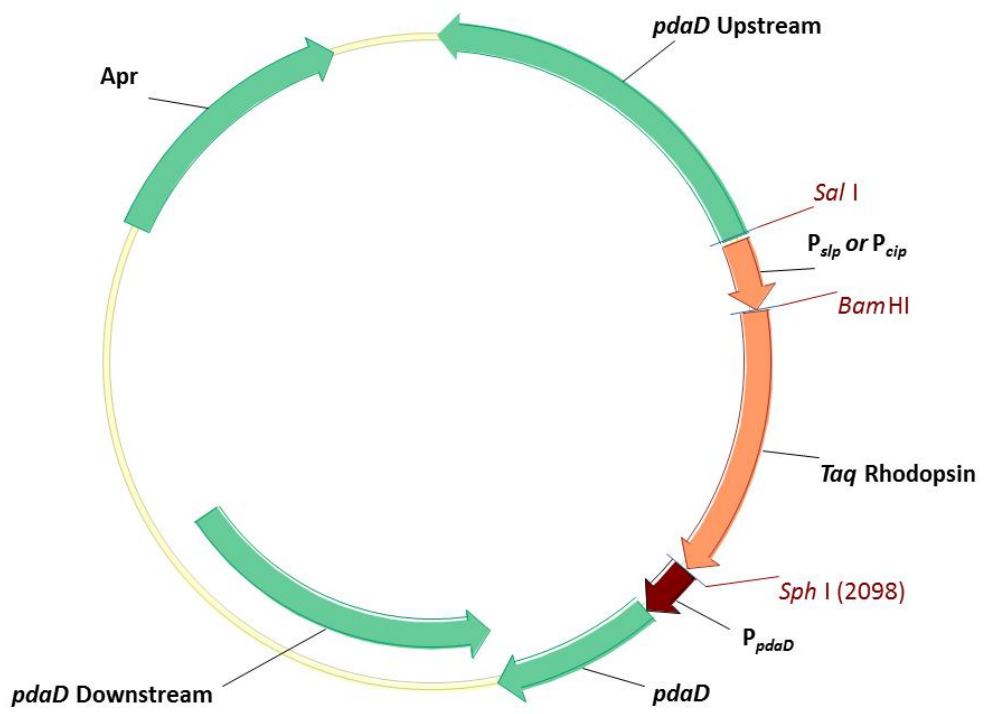


carotene 15,15'-monooxygenase [250]. *E. coli* also does not synthesize *all-trans* retinal and heterologously-expressed rhodopsin is efficiently supplied with this cofactor by addition to growth medium, a strategy that will presumably succeed when expressing rhodopsin in the strict anaerobe *Pf* [247]. The carotenoid salinixanthin may or may not be synthesized by *Pf* and incorporated into the recombinantly-expressed rhodopsin but this could be a nonissue as it was previously reported to have minimal effects on *in vitro* activity [249]. Potentially a problem may exist in translating the $\Delta\Psi$ created by rhodopsin to a usable ion gradient in *Pf*. The current model of metabolism in *Pf* implicates the membrane bound hydrogenase responsible for creating a H^+ gradient, but the native ATP synthase utilizes a Na^+ ion for ATP synthesis [251]. The H^+ gradient in *Pf* is proposed to be exchanged for Na^+ by the integral membrane complex monovalent cation/proton antiporter (MRP). For *in vivo* and *in vitro* ATP regeneration at relative cold fermentation temperatures in *Pf* we would rely on the assumption that the native ATP synthase and MRP would both retain substantial catalytic activity, which may not be true. This system may require the heterologous co-expression of an ATP synthase from another organism that grows near 70°C.

A codon optimized sequence of rhodopsin from *Taq* Y51 was generated by Genscript (Piscataway, NJ) and the next step would be to clone this gene into *Pf pdaD* recombination vectors under the control of both a constitutive promoter (P_{slp}) and inducible promoter (P_{cip}) (Figure 4.9). Subsequent work would include verifying the incorporation of *Taq* Y51 rhodopsin at the *pdaD* locus and probing for the presence of rhodopsin mRNA. Successful expression of *Taq* Y51 rhodopsin in *Pf*

Figure 4.9

***pdaD* suicide vector for *Taq* Y51 rhodopsin gene integration on the chromosome
of *Pf*.**



should be obvious as the membranes will exhibit a dark red coloring indicative of retinal incorporation and coordination. After heterologous expression of rhodopsin in *Pf* is demonstrated it will be interesting to establish that a proton gradient generated from illumination is able to catalyze ATP synthesis in inverted membrane vesicles. Successful demonstration of this will lend credence to the hypothesis that high ATP:ADP ratios may be generated *in vivo* by simple illumination of rhodopsin-expressing recombinant *Pf*.

CHAPTER 5

DISCUSSION AND CONCLUSIONS

The mechanism of biological hydrogen activation has been the subject of study for more than 80 years, highlighting the interest it inspires in the scientific community and the incredible difficulty it poses as a research model. Decades of investigation by many prodigious scientists have elucidated the biological enzyme responsible for hydrogen metabolism, hydrogenase, and deciphered the complex pathway by which nature assembles this unique blend of biological and inorganic chemistries. While much has been learned about the basic biochemistry surrounding these complex metalloenzymes, only recently has the ability to apply hydrogenase for useful purposes become feasible. The classical models of hydrogenase, namely those of *E. coli*, *Ralstonia eutropha*, and *Synechocystis* spp, have been excellent research models but fall short of expectations when attempting to utilize these enzymes for practical purposes. Soluble hydrogenase I (SHI) from *Pyrococcus furiosus* (*Pf*), the subject of this dissertation, has excellent prospects for industrial applications but the development of heterologous expression, genetic manipulation, and homologous overexpression techniques have only been reported in the past two years. Perhaps only limited numbers of researchers employ SHI experimentally due to the recent nature of successes and the specialized skills required to obtain native biomass of the host organism *Pf*. Chapters two and three demonstrate the newfound status SHI enjoys as a model hydrogenase. These and other publications centered on SHI have aroused interest in the scientific community and led to multiple collaborations.

Notably an investigation of SHI using protein film electron chemistry in the lab of Anne Jones (Arizona State University) and its response (and resistance) to oxygen inhibition may challenge the current dogma of oxygen tolerance in [NiFe] hydrogenases [252]. Personal communication with Dr. Jones reveals that SHI, as compared to other mesophilic hydrogenases, exhibits superior characteristics in experimental settings with regards to overall ease of use and stability, further cementing the place of *Pf* SHI as a model enzyme.

The possibilities surrounding this research are not solely limited to hydrogenase investigations but perhaps more exciting are the applications of SHI and the newly developed genetic system in *Pf*. Chapter four highlights two ongoing projects, 1,3-propanediol synthesis from glycerol and heterologous thermophilic rhodopsin, but these studies are the beginning of a much larger field of research. With facile genetics in a hyperthermophile the possibility exists to turn *Pf* into the “hot *E. coli*” of biochemistry. This prospect brings about more questions than answers, however, as with all exciting research. How does one truly overexpress an enzyme in *Pf*? *E. coli* recombinant protein expression can easily yield 10-30% total cell protein for a gene product of interest [253]. The first report of the homologous overexpression of an enzyme in *Pf*, P_{slp} -promoted SHI, yielded a 10-fold increase but total cell protein was only increased from 0.01 to 0.1% [89]. The S-layer promoter used in that study is the highest transcribed region of the *Pf* genome as determined by microarray analysis and it would seem higher levels of transcription are not possible using native elements [254]. The dogma of *E. coli* and mammalian systems for overexpression is to utilize elements of phage or virus transcription machinery, but

hyperthermophilic virus research is extremely limited. If we consider the mechanism by which phage polymerase (e.g. T7 RNA polymerase (RNAP)) is able to specifically and efficiently generate massive amounts of transcript in bacteria a simplistic view is that an exogenous polymerase and promoter sequence themselves are responsible for this effect. Unlike native RNAP, which is titrated between many promoter sequences by a complex system of activators and repressors, a heterologous system would be directed to only the promoter(s) of choice. One may be able to test this hypothesis by exploiting differences in transdomain transcriptional machinery and differential growth temperatures of other characterized thermophiles for making an over-transcribing strain of *Pf*. For instance, the RNAP of the aerobic thermophilic bacterium *Thermus aquaticus* (*Taq*) which grows optimally near 75°C, is well characterized and utilizes the classical bacterial $\alpha_2\beta\beta'\omega\sigma$ RNAP complex [255]. The hyperthermophilic archaeon *Pf* utilizes TATA box-binding proteins (TBP) and transcription factors (TF)IIB more similar to Eucarya [256]. Engineering an inducible *Taq* RNAP, σ^{70} , and σ^{70} promoter sequence behind a gene of interest in *Pf* may generate an expression system similar to the T7 RNAP / T7 promoter sequence used in standard *E. coli* systems.

Merging the known mechanism of SHI *in vivo* with the proposed rhodopsin expression and the *Taq* RNAP transcription system, *Pf* could potentially be poised to efficiently host any process that necessitates the overexpression of enzymes and proteins in systems that require NADPH and/or ATP. Many anabolic processes, such as the dicarboxylate/4-hydroxybutyrate cycle discovered in *Ignicoccus hospitalis* for carbon assimilation, are NADPH-dependent (thermophilic homologous pathway 3-

hydroxypropionate/4-hydroxybutyrate found in *Metallosphaera sedula*) [257]. This presents the unique opportunity to assimilate and possibly direct reduced carbon to potential biofuel molecules. Recently it was demonstrated in *Synechococcus elongatus* PCC7942 the two gene operon responsible for the NADPH-dependent biological conversion of fatty acyl-ACP units to long chain alkanes, the main constituents of diesel fuel [258]. Homologs of these two enzymes, acyl-ACP reductase and aldehyde decarbonylase, exist in the related *Thermosynechococcus elongatus*, an organism with an optimal growth temperature of 55°C. The respective enzymes from *T. elongatus* would presumably function if heterologously expressed in *Pf* near 60°C in a hydrogen-dependent reaction scheme converting CO₂ into diesel fuel.

From commodity chemicals to biofuels the opportunity for *Pyrococcus furiosus* to contribute scientifically is both exciting and feasible. The fundamental studies now possible with the advent of genetics open new realms to the research possibilities on a hyperthermophilic model organism. From these initial proof-of-principle projects to the systems biology and genetic engineering projects of tomorrow, it is evident that *Pyrococcus furiosus* could potentially play a major role in the biochemical developments of the future.

REFERENCES

1. Tian F, Toon OB, Pavlov AA, De Sterck H (2005) A hydrogen-rich early Earth atmosphere. *Science* 308: 1014-1017.
2. Takai K, Gamo T, Tsunogai U, Nakayama N, Hirayama H, et al. (2004) Geochemical and microbiological evidence for a hydrogen-based, hyperthermophilic subsurface lithoautotrophic microbial ecosystem (HyperSLiME) beneath an active deep-sea hydrothermal field. *Extremophiles* 8: 269-282.
3. Weiss BP, Yung YL, Nealson KH (2000) Atmospheric energy for subsurface life on Mars? *Proc Natl Acad Sci U S A* 97: 1395-1399.
4. Stephenson M, Stickland LH (1931) Hydrogenase: a bacterial enzyme activating molecular hydrogen: The properties of the enzyme. *Biochemical Journal* 25: 205-214.
5. Adams MW, Mortenson LE, Chen JS (1980) Hydrogenase. *Biochim Biophys Acta* 594: 105-176.
6. Cammack R, Frey M, Robson R, editors (2001) *Hydrogen as a fuel, learning from Nature*. London: Taylor and Francis.
7. Friedrich B, Schwartz E (1993) Molecular biology of hydrogen utilization in aerobic chemolithotrophs. *Annual Review of Microbiology* 47: 351-383.
8. Przybyla AE, Robbins J, Menon N, Peck HD (1992) Structure-function-relationships among the nickel-containing hydrogenases. *Fems Microbiology Reviews* 88: 109-135.
9. Vignais PM, Colbeau A (2004) Molecular biology of microbial hydrogenases. *Curr Issues Mol Biol* 6: 159-188.
10. Armstrong FA, Belsey NA, Cracknell JA, Goldet G, Parkin A, et al. (2009) Dynamic electrochemical investigations of hydrogen oxidation and production by enzymes and implications for future technology. *Chem Soc Rev* 38: 36-51.
11. Vignais PM, Billoud B (2007) Occurrence, classification, and biological function of hydrogenases: an overview. *Chem Rev* 107: 4206-4272.
12. Shima S, Pilak O, Vogt S, Schick M, Stagni MS, et al. (2008) The crystal structure of [Fe]-hydrogenase reveals the geometry of the active site. *Science* 321: 572-575.
13. Adams MWW (1990) The Structure and Mechanism of Iron-Hydrogenases. *Biochimica Et Biophysica Acta* 1020: 115-145.
14. Albracht SPJ (1994) Nickel Hydrogenases - in Search of the Active-Site. *Biochimica Et Biophysica Acta-Bioenergetics* 1188: 167-204.
15. Vignais PM, Billoud B, Meyer J (2001) Classification and phylogeny of hydrogenases. *Fems Microbiology Reviews* 25: 455-501.
16. Shima S, Thauer RK (2007) A third type of hydrogenase catalyzing H₂ activation. *Chem Rec* 7: 37-46.
17. Zirngibl C, Van Dongen W, Schworer B, Von Bunau R, Richter M, et al. (1992) H₂-forming methylenetetrahydromethanopterin dehydrogenase, a novel type

- of hydrogenase without iron-sulfur clusters in methanogenic archaea. *Eur J Biochem* 208: 511-520.
18. Tard C, Pickett CJ (2009) Structural and functional analogues of the active sites of the [Fe]-, [NiFe]-, and [FeFe]-hydrogenases. *Chem Rev* 109: 2245-2274.
 19. Kubas GJ (2007) Fundamentals of H₂ binding and reactivity on transition metals underlying hydrogenase function and H₂ production and storage. *Chem Rev* 107: 4152-4205.
 20. Peters JW (1999) Structure and mechanism of iron-only hydrogenases. *Curr Opin Struct Biol* 9: 670-676.
 21. Nicolet Y, Cavazza C, Fontecilla-Camps JC (2002) Fe-only hydrogenases: structure, function and evolution. *J Inorg Biochem* 91: 1-8.
 22. Schut GJ, Adams MWW (2009) The iron-hydrogenase of *Thermotoga maritima* utilizes ferredoxin and NADH synergistically: A new perspective on anaerobic hydrogen production. *Journal of Bacteriology* 191: 4451-4457.
 23. Chen ZJ, Lemon BJ, Huang S, Swartz DJ, Peters JW, et al. (2002) Infrared studies of the CO-inhibited form of the Fe-only hydrogenase from *Clostridium pasteurianum* I: Examination of its light sensitivity at cryogenic temperatures. *Biochemistry* 41: 2036-2043.
 24. Nicolet Y, de Lacey AL, Vernede X, Fernandez VM, Hatchikian EC, et al. (2001) Crystallographic and FTIR spectroscopic evidence of changes in Fe coordination upon reduction of the active site of the Fe-only hydrogenase from *Desulfovibrio desulfuricans*. *Journal of the American Chemical Society* 123: 1596-1601.
 25. Nicolet Y, Lemon BJ, Fontecilla-Camps JC, Peters JW (2000) A novel FeS cluster in Fe-only hydrogenases. *Trends in Biochemical Sciences* 25: 138-143.
 26. Peters JW, Lanzilotta WN, Lemon BJ, Seefeldt LC (1998) X-ray crystal structure of the Fe-only hydrogenase (Cpl) from *Clostridium pasteurianum* to 1.8 angstrom resolution. *Science* 282: 1853-1858.
 27. Ryde U, Greco C, De Gioia L (2010) Quantum refinement of [FeFe] hydrogenase indicates a dithiomethylamine ligand. *Journal of the American Chemical Society* 132: 4512-4513.
 28. Posewitz MC, King PW, Smolinski SL, Zhang LP, Seibert M, et al. (2004) Discovery of two novel radical S-adenosylmethionine proteins required for the assembly of an active [Fe] hydrogenase. *Journal of Biological Chemistry* 279: 25711-25720.
 29. Posewitz MC, King PW, Smolinski SL, Smith RD, Ginley AR, et al. (2005) Identification of genes required for hydrogenase activity in *Chlamydomonas reinhardtii*. *Biochem Soc Trans* 33: 102-104.
 30. King PW, Posewitz MC, Ghirardi ML, Seibert M (2006) Functional studies of [FeFe] hydrogenase maturation in an *Escherichia coli* biosynthetic system. *Journal of Bacteriology* 188: 2163-2172.
 31. Kuchenreuther JM, George SJ, Grady-Smith CS, Cramer SP, Swartz JR (2011) Cell-free H-cluster synthesis and [FeFe] hydrogenase activation: all five CO and CN ligands derive from tyrosine. *PLoS ONE* 6: e20346.

32. Rubach JK, Brazzolotto X, Gaillard J, Fontecave M (2005) Biochemical characterization of the HydE and HydG iron-only hydrogenase maturation enzymes from *Thermatoga maritima*. FEBS Lett 579: 5055-5060.
33. Brazzolotto X, Rubach JK, Gaillard J, Gambarelli S, Atta M, et al. (2006) The [Fe-Fe]-hydrogenase maturation protein HydF from *Thermotoga maritima* is a GTPase with an iron-sulfur cluster. Journal of Biological Chemistry 281: 769-774.
34. McGlynn SE, Ruebush SS, Naumov A, Nagy LE, Dubini A, et al. (2007) In vitro activation of [FeFe] hydrogenase: new insights into hydrogenase maturation. J Biol Inorg Chem 12: 443-447.
35. Driesener RC, Challand MR, McGlynn SE, Shepard EM, Boyd ES, et al. (2010) [FeFe]-hydrogenase cyanide ligands derived from S-adenosylmethionine-dependent cleavage of tyrosine. Angew Chem Int Ed Engl 49: 1687-1690.
36. Krasna AI (1979) Hydrogenase: Properties and applications. Enzyme and Microbial Technology 1: 165-172.
37. Cammack R, Fernandez VM, Hatchikian EC (1994) Nickel-Iron Hydrogenase. Inorganic Microbial Sulfur Metabolism 243: 43-68.
38. Roseboom W, De Lacey AL, Fernandez VM, Hatchikian EC, Albracht SP (2006) The active site of the [FeFe]-hydrogenase from *Desulfovibrio desulfuricans*. II. Redox properties, light sensitivity and CO-ligand exchange as observed by infrared spectroscopy. J Biol Inorg Chem 11: 102-118.
39. Pandelia ME, Ogata H, Lubitz W (2010) Intermediates in the catalytic cycle of [NiFe] hydrogenase: Functional spectroscopy of the active site. Chemphyschem 11: 1127-1140.
40. Lemon BJ, Peters JW (1999) Binding of exogenously added carbon monoxide at the active site of the iron-only hydrogenase (CpI) from *Clostridium pasteurianum*. Biochemistry 38: 12969-12973.
41. Lemon BJ, Peters JW (2000) Photochemistry at the active site of the carbon monoxide inhibited form of the iron-only hydrogenase (CpI). Journal of the American Chemical Society 122: 3793-3794.
42. Silakov A, Kamp C, Reijerse E, Happe T, Lubitz W (2009) Spectroelectrochemical Characterization of the Active Site of the [FeFe] Hydrogenase HydA1 from *Chlamydomonas reinhardtii*. Biochemistry 48: 7780-7786.
43. Thauer RK, Klein AR, Hartmann GC (1996) Reactions with molecular hydrogen in microorganisms: Evidence for a purely organic hydrogenation catalyst. Chem Rev 96: 3031-3042.
44. Cao Z, Hall MB (2001) Modeling the active sites in metalloenzymes. 3. Density functional calculations on models for [Fe]-hydrogenase: structures and vibrational frequencies of the observed redox forms and the reaction mechanism at the Diiron Active Center. Journal of the American Chemical Society 123: 3734-3742.
45. Zampella G, Greco C, Fantucci P, De Gioia L (2006) Proton reduction and dihydrogen oxidation on models of the [2Fe]H cluster of [Fe] hydrogenases. A density functional theory investigation. Inorg Chem 45: 4109-4118.

46. Liu XM, Ibrahim SK, Tard C, Pickett CJ (2005) Iron-only hydrogenase: Synthetic, structural and reactivity studies of model compounds. *Coordination Chemistry Reviews* 249: 1641-1652.
47. Fan HJ, Hall MB (2001) A capable bridging ligand for Fe-only hydrogenase: Density functional calculations of a low-energy route for heterolytic cleavage and formation of dihydrogen. *Journal of the American Chemical Society* 123: 3828-3829.
48. Tsuda M, Dino WA, Kasai H (2005) Hydrogenase-based nanomaterials as anode electrode catalyst in polymer electrolyte fuel cells. *Solid State Communications* 133: 589-591.
49. Liu ZP, Hu P (2002) A density functional theory study on the active center of Fe-only hydrogenase: Characterization and electronic structure of the redox states. *Journal of the American Chemical Society* 124: 5175-5182.
50. Bruschi M, Fantucci P, De Gioia L (2003) Density functional theory investigation of the active site of [Fe]-hydrogenases: Effects of redox state and ligand characteristics on structural, electronic, and reactivity properties of complexes related to the [2Fe](H) subcluster. *Inorganic Chemistry* 42: 4773-4781.
51. Zhou TJ, Mo YR, Liu AM, Zhou ZH, Tsai KR (2004) Enzymatic mechanism of Fe-only hydrogenase: Density functional study on H-H making/breaking at the diiron cluster with concerted proton and electron transfers. *Inorganic Chemistry* 43: 923-930.
52. Nicolet Y, Piras C, Legrand P, Hatchikian CE, Fontecilla-Camps JC (1999) *Desulfovibrio desulfuricans* iron hydrogenase: the structure shows unusual coordination to an active site Fe binuclear center. *Structure with Folding & Design* 7: 13-23.
53. Dermoun Z, De Luca G, Asso M, Bertrand P, Guerlesquin F, et al. (2002) The NADP-reducing hydrogenase from *Desulfovibrio fructosovorans*: functional interaction between the C-terminal region of HndA and the N-terminal region of HndD subunits. *Biochimica Et Biophysica Acta-Bioenergetics* 1556: 217-225.
54. Garcin E, Vernede X, Hatchikian EC, Volbeda A, Frey M, et al. (1999) The crystal structure of a reduced [NiFeSe] hydrogenase provides an image of the activated catalytic center. *Structure* 7: 557-566.
55. Higuchi Y, Ogata H, Miki K, Yasuoka N, Yagi T (1999) Removal of the bridging ligand atom at the Ni-Fe active site of [NiFe] hydrogenase upon reduction with H₂, as revealed by X-ray structure analysis at 1.4 Å resolution. *Structure* 7: 549-556.
56. Higuchi Y, Toujou F, Tsukamoto K, Yagi T (2000) The presence of a SO molecule in [NiFe] hydrogenase from *Desulfovibrio vulgaris* Miyazaki as detected by mass spectrometry. *J Inorg Biochem* 80: 205-211.
57. Volbeda A, Charon MH, Piras C, Hatchikian EC, Frey M, et al. (1995) Crystal structure of the nickel iron hydrogenase from *Desulfovibrio gigas*. *Nature* 373: 580-587.
58. Volbeda A, Garcia E, Piras C, deLacey AL, Fernandez VM, et al. (1996) Structure of the [NiFe] hydrogenase active site: Evidence for biologically

- uncommon Fe ligands. Journal of the American Chemical Society 118: 12989-12996.
59. Ogata H, Kellers P, Lubitz W (2010) The crystal structure of the [NiFe] hydrogenase from the photosynthetic bacterium *Allochromatium vinosum*: characterization of the oxidized enzyme (Ni-A state). J Mol Biol 402: 428-444.
 60. Bagley KA, Duin EC, Roseboom W, Albracht SPJ, Woodruff WH (1995) Infrared-detectable groups sense changes in charge density on the nickel center in hydrogenase from *Chromatium vinosum*. Biochemistry 34: 5527-5535.
 61. Happe RP, Roseboom W, Pierik AJ, Albracht SPJ, Bagley KA (1997) Biological activation of hydrogen. Nature 385: 126-126.
 62. Pierik AJ, Roseboom W, Happe RP, Bagley KA, Albracht SPJ (1999) Carbon monoxide and cyanide as intrinsic ligands to iron in the active site of [NiFe]-hydrogenases - NiFe(CN)₂CO, biology's way to activate H₂. Journal of Biological Chemistry 274: 3331-3337.
 63. Adams MW, Stiefel EI (2000) Organometallic iron: the key to biological hydrogen metabolism. Curr Opin Chem Biol 4: 214-220.
 64. Van der Linden E, Burgdorf T, Bernhard M, Bleijlevens B, Friedrich B, et al. (2004) The soluble [NiFe]-hydrogenase from *Ralstonia eutropha* contains four cyanides in its active site, one of which is responsible for the insensitivity towards oxygen. Journal of Biological Inorganic Chemistry 9: 616-626.
 65. Bleijlevens B, Buhrke T, van der Linden E, Friedrich B, Albracht SP (2004) The auxiliary protein HypX provides oxygen tolerance to the soluble [NiFe]-hydrogenase of *Ralstonia eutropha* H16 by way of a cyanide ligand to nickel. Journal of Biological Chemistry 279: 46686-46691.
 66. Higuchi Y, Yagi T, Yasuoka N (1997) Unusual ligand structure in Ni-Fe active center and an additional Mg site in hydrogenase revealed by high resolution X-ray structure analysis. Structure 5: 1671-1680.
 67. Higuchi Y, Yagi T (1999) Liberation of hydrogen sulfide during the catalytic action of *Desulfovibrio hydrogenase* under the atmosphere of hydrogen. Biochemical and Biophysical Research Communications 255: 295-299.
 68. Ogata H, Mizoguchi Y, Mizuno N, Miki K, Adachi S, et al. (2002) Structural studies of the carbon monoxide complex of [NiFe]hydrogenase from *Desulfovibrio vulgaris* Miyazaki F: Suggestion for the initial activation site for dihydrogen. Journal of the American Chemical Society 124: 11628-11635.
 69. Lamle SE, Albracht SP, Armstrong FA (2004) Electrochemical potential-step investigations of the aerobic interconversions of [NiFe]-hydrogenase from *Allochromatium vinosum*: insights into the puzzling difference between unready and ready oxidized inactive states. Journal of the American Chemical Society 126: 14899-14909.
 70. Volbeda A, Fontecilla-Camps JC (2003) The active site and catalytic mechanism of NiFe hydrogenases. Dalton Transactions: 4030-4038.
 71. De Lacey AL, Fernández VM, Marc Rousset M (2005) Native and mutant nickel-iron hydrogenases: Unravelling structure and function Coordination Chemistry Reviews 249: 1596-1608.

72. Saggi M, Zebger I, Ludwig M, Lenz O, Friedrich B, et al. (2009) Spectroscopic insights into the oxygen-tolerant membrane-associated [NiFe] hydrogenase of *Ralstonia eutropha* H16. *Journal of Biological Chemistry* 284: 16264-16276.
73. Saggi M, Teutloff C, Ludwig M, Brecht M, Pandelia ME, et al. (2010) Comparison of the membrane-bound [NiFe] hydrogenases from *R. eutropha* H16 and *D. vulgaris* Miyazaki F in the oxidized ready state by pulsed EPR. *Physical Chemistry Chemical Physics* 12: 2139-2148.
74. Shomura Y, Yoon KS, Nishihara H, Higuchi Y (2011) Structural basis for a [4Fe-3S] cluster in the oxygen-tolerant membrane-bound [NiFe]-hydrogenase. *Nature* 479: 253-256.
75. Fritsch J, Scheerer P, Frielingsdorf S, Kroschinsky S, Friedrich B, et al. (2011) The crystal structure of an oxygen-tolerant hydrogenase uncovers a novel iron-sulphur centre. *Nature* 479: 249-252.
76. Cammack R, Bagyinka C, Kovacs KL (1989) Spectroscopic characterization of the nickel and iron-sulphur clusters of hydrogenase from the purple photosynthetic bacterium *Thiocapsa roseopersicina*: Electron spin resonance spectroscopy. *Eur J Biochem* 182: 357-362.
77. Foerster S, Gastel MV, Brecht M, Lubitz W (2004) An orientation-selected ENDOR and HYSCORE study of the Ni-C active state of *Desulfovibrio vulgaris* Miyazaki F hydrogenase. *J Biol Inorg Chem*.
78. Jones AK, Lamle SE, Pershad HR, Vincent KA, Albracht SP, et al. (2003) Enzyme electrokinetics: electrochemical studies of the anaerobic interconversions between active and inactive states of *Allochromatium vinosum* [NiFe]-hydrogenase. *Journal of the American Chemical Society* 125: 8505-8514.
79. Trofanchuk O, Stein M, Gessner C, Lendzian F, Higuchi Y, et al. (2000) Single crystal EPR studies of the oxidized active site of [NiFe] hydrogenase from *Desulfovibrio vulgaris* Miyazaki F. *J Biol Inorg Chem* 5: 36-44.
80. Stein M, van Lenthe E, Baerends EJ, Lubitz W (2001) Relativistic DFT calculations of the paramagnetic intermediates of [NiFe] hydrogenase. Implications for the enzymatic mechanism. *Journal of the American Chemical Society* 123: 5839-5840.
81. Weiner JH, Bilous PT, Shaw GM, Lubitz SP, Frost L, et al. (1998) A novel and ubiquitous system for membrane targeting and secretion of cofactor-containing proteins. *Cell* 93: 93-101.
82. Sargent F, Bogsch EG, Stanley NR, Wexler M, Robinson C, et al. (1998) Overlapping functions of components of a bacterial Sec-independent protein export pathway. *Embo Journal* 17: 3640-3650.
83. Buhrke T, Lenz O, Porthun A, Friedrich B (2004) The H₂-sensing complex of *Ralstonia eutropha*: interaction between a regulatory [NiFe] hydrogenase and a histidine protein kinase. *Molecular Microbiology* 51: 1677-1689.
84. Duche O, Elsen S, Cournac L, Colbeau A (2005) Enlarging the gas access channel to the active site renders the regulatory hydrogenase HupUV of *Rhodobacter capsulatus* O₂ sensitive without affecting its transducing activity. *FEBS J* 272: 3899-3908.

85. Buhrke T, Lenz O, Krauss N, Friedrich B (2005) Oxygen tolerance of the H₂-sensing [NiFe] hydrogenase from *Ralstonia eutropha* H16 is based on limited access of oxygen to the active site. *Journal of Biological Chemistry* 280: 23791-23796.
86. Cournac L, Guedeney G, Peltier G, Vignais PM (2004) Sustained photoevolution of molecular hydrogen in a mutant of *Synechocystis* sp strain PCC 6803 deficient in the type I NADPH-dehydrogenase complex. *Journal of Bacteriology* 186: 1737-1746.
87. van Haaster DJ, Silva PJ, Hagedoorn PL, Jongejan JA, Hagen WR (2008) Reinvestigation of the steady-state kinetics and physiological function of the soluble NiFe-hydrogenase I of *Pyrococcus furiosus*. *Journal of Bacteriology* 190: 1584-1587.
88. Lipscomb GL, Stirrett K, Schut GJ, Yang F, Jenney FE, et al. (2011) Natural competence in the hyperthermophilic archaeon *Pyrococcus furiosus* facilitates genetic manipulation: Construction of markerless deletions of genes encoding the two cytoplasmic hydrogenases. *Applied and Environmental Microbiology* 77: 2232-2238.
89. Chandrayan SK, McTernan PM, Hopkins RC, Sun J, Jenney FE, Jr., et al. (2011) Engineering the hyperthermophilic archaeon *Pyrococcus furiosus* to overproduce its cytoplasmic [NiFe]-hydrogenase. *Journal of Biological Chemistry*.
90. Sawers RG (2005) Formate and its role in hydrogen production in *Escherichia coli*. *Biochemical Society Transactions* 33: 42-46.
91. Hedderich R, Forzi L (2005) Energy-converting [NiFe] hydrogenases: More than just H₂ activation. *J Mol Microbiol Biotechnol* 10: 92-104.
92. Albracht SPJ, Hedderich R (2000) Learning from hydrogenases: location of a proton pump and of a second FMN in bovine NADH-ubiquinone oxidoreductase (Complex I). *Febs Letters* 485: 1-6.
93. Brandt U, Kerscher S, Drose S, Zwicker K, Zickermann V (2003) Proton pumping by NADH : ubiquinone oxidoreductase. A redox driven conformational change mechanism? *Febs Letters* 545: 9-17.
94. Friedrich T, Scheide D (2000) The respiratory complex I of bacteria, archaea and eukarya and its module common with membrane-bound multisubunit hydrogenases. *Febs Letters* 479: 1-5.
95. Blokesch M, Albracht SP, Matzanke BF, Drapal NM, Jacobi A, et al. (2004) The complex between hydrogenase-maturation proteins HypC and HypD is an intermediate in the supply of cyanide to the active site iron of [NiFe]-hydrogenases. *J Mol Biol* 344: 155-167.
96. Blokesch M, Bock A (2002) Maturation of [NiFe]-hydrogenases in *Escherichia coli*: The HypC cycle. *Journal of Molecular Biology* 324: 287-296.
97. Lutz S, Jacobi A, Schlenzog V, Bohm R, Sawers G, et al. (1991) Molecular characterization of an operon (hyp) necessary for the activity of the three hydrogenase isoenzymes in *Escherichia coli*. *Mol Microbiol* 5: 123-135.
98. Paschos A, Glass RS, Bock A (2001) Carbamoylphosphate requirement for synthesis of the active center of [NiFe]-hydrogenases. *FEBS Lett* 488: 9-12.

99. Reissmann S, Hochleitner E, Wang HF, Paschos A, Lottspeich F, et al. (2003) Taming of a poison: Biosynthesis of the NiFe-hydrogenase cyanide ligands. *Science* 299: 1067-1070.
100. Paschos A, Bauer A, Zimmermann A, Zehelein E, Bock A (2002) HypF, a carbamoyl phosphate-converting enzyme involved in [NiFe] hydrogenase maturation. *Journal of Biological Chemistry* 277: 49945-49951.
101. Blokesch M, Paschos A, Bauer A, Reissmann S, Drapal N, et al. (2004) Analysis of the transcarbamoylation-dehydration reaction catalyzed by the hydrogenase maturation proteins HypF and HypE. *European Journal of Biochemistry* 271: 3428-3436.
102. Watanabe S, Matsumi R, Arai T, Atomi H, Imanaka T, et al. (2007) Crystal structures of [NiFe] hydrogenase maturation proteins HypC, HypD, and HypE: insights into cyanation reaction by thiol redox signaling. *Mol Cell* 27: 29-40.
103. Blokesch M, Paschos A, Theodoratou E, Bauer A, Hube M, et al. (2002) Metal insertion into NiFe-hydrogenases. *Biochemical Society Transactions* 30: 674-680.
104. Roseboom W, Blokesch M, Bock A, Albracht SP (2005) The biosynthetic routes for carbon monoxide and cyanide in the Ni-Fe active site of hydrogenases are different. *FEBS Lett* 579: 469-472.
105. Forzi L, Hellwig P, Thauer RK, Sawers RG (2007) The CO and CN(-) ligands to the active site Fe in [NiFe]-hydrogenase of *Escherichia coli* have different metabolic origins. *FEBS Lett* 581: 3317-3321.
106. Lenz O, Zebger I, Hamann J, Hildebrandt P, Friedrich B (2007) Carbamoylphosphate serves as the source of CN(-), but not of the intrinsic CO in the active site of the regulatory [NiFe]-hydrogenase from *Ralstonia eutropha*. *FEBS Lett* 581: 3322-3326.
107. Menon S, Ragsdale SW (1996) Evidence that carbon monoxide is an obligatory intermediate in anaerobic acetyl-CoA synthesis. *Biochemistry* 35: 12119-12125.
108. Tenhunen R, Marver HS, Schmid R (1969) Microsomal heme oxygenase. Characterization of the enzyme. *Journal of Biological Chemistry* 244: 6388-6394.
109. Wray JW, Abeles RH (1993) A bacterial enzyme that catalyzes formation of carbon monoxide. *Journal of Biological Chemistry* 268: 21466-21469.
110. Cheesbrough TM, Kolattukudy PE (1984) Alkane biosynthesis by decarbonylation of aldehydes catalyzed by a particulate preparation from *Pisum sativum*. *Proc Natl Acad Sci U S A* 81: 6613-6617.
111. Hino S, Tauchi H (1987) Production of carbon monoxide from aromatic amino acids by *Morganella morganii*. *Archives of Microbiology* 148: 167-171.
112. Ingo Bürstel PH, Elisabeth Siebert, Nattawadee Wisitruangsakul,, Ingo Zebger BF, and Oliver Lenz (2011) Probing the origin of the metabolic precursor of the CO ligand in the catalytic center of [NiFe]-hydrogenase. *Journal of Biological Chemistry*.

113. Magalon A, Bock A (2000) Analysis of the HypC-hycE complex, a key intermediate in the assembly of the metal center of the *Escherichia coli* hydrogenase 3. *Journal of Biological Chemistry* 275: 21114-21120.
114. Jacobi A, Rossmann R, Bock A (1992) The hyp operon gene products are required for the maturation of catalytically active hydrogenase isoenzymes in *Escherichia coli*. *Arch Microbiol* 158: 444-451.
115. Atanassova A, Zamble DB (2005) *Escherichia coli* HypA is a zinc metalloprotein with a weak affinity for nickel. *Journal of Bacteriology* 187: 4689-4697.
116. Maier T, Jacobi A, Sauter M, Bock A (1993) The product of the hypB gene, which is required for nickel incorporation into hydrogenases, is a novel guanine nucleotide-binding protein. *Journal of Bacteriology* 175: 630-635.
117. Waugh R, Boxer DH (1986) Pleiotropic hydrogenase mutants of *Escherichia coli* K12: growth in the presence of nickel can restore hydrogenase activity. *Biochimie* 68: 157-166.
118. Hube M, Blokesch M, Bock A (2002) Network of hydrogenase maturation in *Escherichia coli*: Role of accessory proteins HypA and HybF. *Journal of Bacteriology* 184: 3879-3885.
119. Gasper R, Scrima A, Wittinghofer A (2006) Structural insights into HypB, a GTP-binding protein that regulates metal binding. *Journal of Biological Chemistry* 281: 27492-27502.
120. Zhang JW, Butland G, Greenblatt JF, Emili A, Zamble DB (2005) A role for SlyD in the *Escherichia coli* hydrogenase biosynthetic pathway. *Journal of Biological Chemistry* 280: 4360-4366.
121. Theodoratou E, Paschos A, Magalon A, Fritsche E, Huber R, et al. (2000) Nickel serves as a substrate recognition motif for the endopeptidase involved in hydrogenase maturation. *Eur J Biochem* 267: 1995-1999.
122. Theodoratou E, Paschos A, Mintz W, Bock A (2000) Analysis of the cleavage site specificity of the endopeptidase involved in the maturation of the large subunit of hydrogenase 3 from *Escherichia coli*. *Arch Microbiol* 173: 110-116.
123. Rossmann R, Maier T, Lottspeich F, Bock A (1995) Characterization of a protease from *Escherichia coli* involved in hydrogenase maturation. *European Journal of Biochemistry* 227: 545-550.
124. Magalon A, Bock A (2000) Dissection of the maturation reactions of the [NiFe] hydrogenase 3 from *Escherichia coli* taking place after nickel incorporation. *FEBS Lett* 473: 254-258.
125. Stetter KO (1996) Hyperthermophilic procaryotes. *Fems Microbiology Reviews* 18: 149-158.
126. Stetter KO (1999) Extremophiles and their adaptation to hot environments. *Febs Letters* 452: 22-25.
127. Madigan MT (2012) Brock biology of microorganisms. San Francisco: Benjamin Cummings. xxviii, 1043, 1077 p. p.
128. Littlechild JA (2011) Thermophilic archaeal enzymes and applications in biocatalysis. *Biochemical Society Transactions* 39: 155-158.

129. Sellek GA, Chaudhuri JB (1999) Biocatalysis in organic media using enzymes from extremophiles. *Enzyme and Microbial Technology* 25: 471-482.
130. Di Giulio M (2001) The universal ancestor was a thermophile or a hyperthermophile. *Gene* 281: 11-17.
131. Kasting JF (1993) Earth's early atmosphere. *Science* 259: 920-926.
132. Miller SL, Lazcano A (1995) The origin of life - Did it occur at high temperatures? *Journal of Molecular Evolution* 41: 689-692.
133. Wachtershauser G (1988) Before Enzymes and Templates - Theory of Surface Metabolism. *Microbiological Reviews* 52: 452-484.
134. Wächtershäuser G (2000) Origin of life. Life as we don't know it. *Science* 289: 1307-1308.
135. Wagner ID, Wiegel J (2008) Diversity of thermophilic anaerobes. *Incredible Anaerobes: From Physiology to Genomics to Fuels* 1125: 1-43.
136. Cypionka H, Widdel F, Pfenning N (1985) Survival of Sulfate-Reducing Bacteria after Oxygen Stress, and Growth in Sulfate-Free Oxygen-Sulfide Gradients. *Fems Microbiology Ecology* 31: 39-45.
137. Jenney FE, Verhagen MFJM, Cui XY, Adams MWW (1999) Anaerobic microbes: Oxygen detoxification without superoxide dismutase. *Science* 286: 306-309.
138. Amend JP, Shock EL (2001) Energetics of overall metabolic reactions of thermophilic and hyperthermophilic Archaea and Bacteria. *Fems Microbiology Reviews* 25: 175-243.
139. Slobodkin AI (2005) Thermophilic microbial metal reduction. *Microbiology* 74: 501-514.
140. Imanaka T, Atomi H (2002) Catalyzing "hot" reactions: enzymes from hyperthermophilic Archaea. *Chem Rec* 2: 149-163.
141. Wiegel J (1990) Temperature spans for growth - hypothesis and discussion. *Fems Microbiology Reviews* 75: 155-169.
142. Yamada T, Sekiguchi Y, Hanada S, Imachi H, Ohashi A, et al. (2006) *Anaerolinea thermolimosa* sp nov., *Levilinea saccharolytica* gen. nov., sp nov and *Leptolinea tardivitalis* gen. nov., so. nov., novel filamentous anaerobes, and description of the new classes Anaerolineae classis nov and Caldilineae classis nov in the bacterial phylum *Chloroflexi*. *International Journal of Systematic and Evolutionary Microbiology* 56: 1331-1340.
143. Sekiguchi Y, Yamada T, Hanada S, Ohashi A, Harada H, et al. (2003) *Anaerolinea thermophila* gen. nov., sp nov and *Caldilinea aerophila* gen. nov., sp nov., novel filamentous thermophiles that represent a previously uncultured lineage of the domain Bacteria at the subphylum level. *International Journal of Systematic and Evolutionary Microbiology* 53: 1843-1851.
144. Stetter KO (2006) Hyperthermophiles in the history of life. *Philosophical Transactions of the Royal Society B-Biological Sciences* 361: 1837-1842.
145. Adams MWW (1994) Biochemical Diversity among Sulfur-Dependent, Hyperthermophilic Microorganisms. *Fems Microbiology Reviews* 15: 261-277.

146. Takai K, Nakamura K, Toki T, Tsunogai U, Miyazaki M, et al. (2008) Cell proliferation at 122 degrees C and isotopically heavy CH₄ production by a hyperthermophilic methanogen under high-pressure cultivation. *Proceedings of the National Academy of Sciences of the United States of America* 105: 10949-10954.
147. Siebers B, Schonheit P (2005) Unusual pathways and enzymes of central carbohydrate metabolism in Archaea. *Curr Opin Microbiol* 8: 695-705.
148. Siebers B, Schonheit P (2005) Unusual pathways and enzymes of central carbohydrate metabolism in Archaea. *Current Opinion in Microbiology* 8: 695-705.
149. Reher M, Gebhard S, Schonheit P (2007) Glyceraldehyde-3-phosphate ferredoxin oxidoreductase (GAPOR) and nonphosphorylating glyceraldehyde-3-phosphate dehydrogenase (GAPN), key enzymes of the respective modified Embden-Meyerhof pathways in the hyperthermophilic crenarchaeota *Pyrobaculum aerophilum* and *Aeropyrum pernix*. *FEMS Microbiol Lett* 273: 196-205.
150. Reher M, Fuhrer T, Bott M, Schonheit P (2010) The nonphosphorylative Entner-Doudoroff pathway in the thermoacidophilic euryarchaeon *Picrophilus torridus* involves a novel 2-keto-3-deoxygluconate-specific aldolase. *Journal of Bacteriology* 192: 964-974.
151. Perevalova AA, Svetlichny VA, Kublanov IV, Chernyh NA, Kostrikina NA, et al. (2005) *Desulfurococcus fermentans* sp. nov., a novel hyperthermophilic archaeon from a Kamchatka hot spring, and emended description of the genus *Desulfurococcus*. *Int J Syst Evol Microbiol* 55: 995-999.
152. Biely P (1985) Microbial Xylanolytic Systems. *Trends in Biotechnology* 3: 286-290.
153. Ragsdale SW (2008) Enzymology of the Wood-Ljungdahl pathway of acetogenesis. *Incredible Anaerobes: From Physiology to Genomics to Fuels* 1125: 129-136.
154. Bryant DA, Frigaard NU (2006) Prokaryotic photosynthesis and phototrophy illuminated. *Trends in Microbiology* 14: 488-496.
155. Xiong J, Bauer CE (2002) Complex evolution of photosynthesis. *Annual Review of Plant Biology* 53: 503-521.
156. Zavarzina DG, Sokolova TG, Tourova TP, Chernyh NA, Kostrikina NA, et al. (2007) *Thermincola ferriacetica* sp. nov., a new anaerobic, thermophilic, facultatively chemolithoautotrophic bacterium capable of dissimilatory Fe(III) reduction. *Extremophiles* 11: 1-7.
157. Slobodkin AI (2005) [Thermophilic microbial metal reduction]. *Mikrobiologiya* 74: 581-595.
158. Segerer A, Neuner A, Kristjansson JK, Stetter KO (1986) *Acidianus infernus* gen. nov., sp. nov., and *Acidianus brierleyi* comb. nov.: facultatively aerobic, extremely acidophilic thermophilic sulfur-metabolizing archaeobacteria. *International Journal of Systematic Bacteriology* 36: 559-564.
159. Slobodkin AI, Tourova TP, Kuznetsov BB, Kostrikina NA, Chernyh NA, et al. (1999) *Thermoanaerobacter siderophilus* sp nov., a novel dissimilatory

- Fe(III)-reducing, anaerobic, thermophilic bacterium. *International Journal of Systematic Bacteriology* 49: 1471-1478.
160. Zavarzina DG, Tourova TP, Kuznetsov BB, Bonch-Osmolovskaya EA, Slobodkin AI (2002) *Thermovenabulum ferriorganovorum* gen. nov., sp nov., a novel thermophilic, anaerobic, endospore-forming bacterium. *International Journal of Systematic and Evolutionary Microbiology* 52: 1737-1743.
 161. Brierley CL, Brierley JA (1982) Anaerobic Reduction of Molybdenum by *Sulfolobus* Species. *Zentralblatt Fur Bakteriologie Mikrobiologie Und Hygiene I Abteilung Originale C-Allgemeine Angewandte Und Okologische Mikrobiologie* 3: 289-294.
 162. Roh Y, Liu SV, Li GS, Huang HS, Phelps TJ, et al. (2002) Isolation and characterization of metal-reducing *Thermoanaerobacter* strains from deep subsurface environments of the Piceance Basin, Colorado. *Applied and Environmental Microbiology* 68: 6013-6020.
 163. Fiala G, Stetter KO (1986) *Pyrococcus furiosus* sp represents a novel genus of marine heterotrophic archaeobacteria growing optimally at 100 degrees C. *Archives of Microbiology* 145: 56-61.
 164. van der Oost J, Schut G, Kengen SWM, Hagen WR, Thomm M, et al. (1998) The ferredoxin-dependent conversion of glyceraldehyde-3-phosphate in the hyperthermophilic archaeon *Pyrococcus furiosus* represents a novel site of glycolytic regulation. *Journal of Biological Chemistry* 273: 28149-28154.
 165. van de Werken HJG, Verhees CH, Akerboom J, de Vos WM, van der Oost J (2006) Identification of a glycolytic regulon in the archaea *Pyrococcus* and *Thermococcus*. *Fems Microbiology Letters* 260: 69-76.
 166. Mukund S, Adams MWW (1995) Glyceraldehyde-3-phosphate ferredoxin oxidoreductase, a novel tungsten-containing enzyme with a potential glycolytic role in the Hyperthermophilic archaeon *Pyrococcus furiosus*. *Journal of Biological Chemistry* 270: 8389-8392.
 167. Kengen SWM, Debok FAM, Vanloo ND, Dijkema C, Stams AJM, et al. (1994) Evidence for the Operation of a Novel Embden-Meyerhof Pathway That Involves ADP-Dependent Kinases during Sugar Fermentation by *Pyrococcus furiosus*. *Journal of Biological Chemistry* 269: 17537-17541.
 168. Verhees CH, Kengen SWM, Tuininga JE, Schut GJ, Adams MWW, et al. (2003) The unique features of glycolytic pathways in Archaea. *Biochemical Journal* 375: 231-246.
 169. Blamey JM, Adams MWW (1993) Purification and Characterization of Pyruvate Ferredoxin Oxidoreductase from the Hyperthermophilic Archaeon *Pyrococcus furiosus*. *Biochimica Et Biophysica Acta* 1161: 19-27.
 170. Sapro R, Bagramyan K, Adams MW (2003) A simple energy-conserving system: proton reduction coupled to proton translocation. *Proc Natl Acad Sci U S A* 100: 7545-7550.
 171. Adams MWW, Holden JF, Menon AL, Schut GJ, Grunden AM, et al. (2001) Key role for sulfur in peptide metabolism and in regulation of three hydrogenases in the hyperthermophilic archaeon *Pyrococcus furiosus*. *Journal of Bacteriology* 183: 716-724.

172. Bryant FO, Adams MW (1989) Characterization of hydrogenase from the hyperthermophilic archaeobacterium, *Pyrococcus furiosus*. *Journal of Biological Chemistry* 264: 5070-5079.
173. Ma K, Adams MW (1994) Sulfide dehydrogenase from the hyperthermophilic archaeon *Pyrococcus furiosus*: a new multifunctional enzyme involved in the reduction of elemental sulfur. *Journal of Bacteriology* 176: 6509-6517.
174. Ma K, Adams MW (2001) Hydrogenases I and II from *Pyrococcus furiosus*. *Methods Enzymol* 331: 208-216.
175. Ma K, Weiss R, Adams MW (2000) Characterization of hydrogenase II from the hyperthermophilic archaeon *Pyrococcus furiosus* and assessment of its role in sulfur reduction. *Journal of Bacteriology* 182: 1864-1871.
176. Sapra R, Verhagen MF, Adams MW (2000) Purification and characterization of a membrane-bound hydrogenase from the hyperthermophilic archaeon *Pyrococcus furiosus*. *Journal of Bacteriology* 182: 3423-3428.
177. Adams MW, Holden JF, Menon AL, Schut GJ, Grunden AM, et al. (2001) Key role for sulfur in peptide metabolism and in regulation of three hydrogenases in the hyperthermophilic archaeon *Pyrococcus furiosus*. *Journal of Bacteriology* 183: 716-724.
178. Schut GJ, Zhou J, Adams MW (2001) DNA microarray analysis of the hyperthermophilic archaeon *Pyrococcus furiosus*: evidence for an new type of sulfur-reducing enzyme complex. *Journal of Bacteriology* 183: 7027-7036.
179. Robb FT, Maeder DL, Brown JR, DiRuggiero J, Stump MD, et al. (2001) Genomic sequence of hyperthermophile, *Pyrococcus furiosus*: Implications for physiology and enzymology. *Hyperthermophilic Enzymes, Pt A* 330: 134-157.
180. Peck HD, Jr., Gest H (1956) A new procedure for assay of bacterial hydrogenases. *Journal of Bacteriology* 71: 70-80.
181. Zhang YH, Evans BR, Mielenz JR, Hopkins RC, Adams MW (2007) High-yield hydrogen production from starch and water by a synthetic enzymatic pathway. *PLoS ONE* 2: e456.
182. Asada Y, Miyake J (1999) Photobiological hydrogen production. *J Biosci Bioeng* 88: 1-6.
183. Esper B, Badura A, Rogner M (2006) Photosynthesis as a power supply for (bio-)hydrogen production. *Trends Plant Sci* 11: 543-549.
184. Prince RC, Kheshgi HS (2005) The photobiological production of hydrogen: potential efficiency and effectiveness as a renewable fuel. *Crit Rev Microbiol* 31: 19-31.
185. Haki GD, Rakshit SK (2003) Developments in industrially important thermostable enzymes: A review. *Bioresource Technology* 89: 17-34.
186. Demirjian DC, Moris-Varas F, Cassidy CS (2001) Enzymes from extremophiles. *Current Opinion in Chemical Biology* 5: 144-151.
187. Nigam P, Singh D (1995) Enzyme and microbial systems involved in starch processing. *Enzyme and Microbial Technology* 17: 770-778.
188. Saiki RK, Scharf S, Faloona F, Mullis KB, Horn GT, et al. (1992) Enzymatic amplification of beta-globin genomic sequences and restriction site analysis for diagnosis of sickle cell anemia. 1985. *Biotechnology* 24: 476-480.

189. Saiki RK, Gelfand DH, Stoffel S, Scharf SJ, Higuchi R, et al. (1988) Primer directed enzymatic amplification of DNA with a thermostable DNA polymerase. *Science* 239: 487-491.
190. Vieille C, Zeikus GJ (2001) Hyperthermophilic enzymes: sources, uses, and molecular mechanisms for thermostability. *Microbiol Mol Biol Rev* 65: 1-43.
191. de Miguel Bouzas T, Barros-Velazquez J, Villa TG (2006) Industrial applications of hyperthermophilic enzymes: a review. *Protein Pept Lett* 13: 645-651.
192. Haney PJ, Stees M, Konisky J (1999) Analysis of thermal stabilizing interactions in mesophilic and thermophilic adenylate kinases from the genus *Methanococcus*. *Journal of Biological Chemistry* 274: 28453-28458.
193. Kirino H, Aoki M, Aoshima M, Hayashi Y, Ohba M, et al. (1994) Hydrophobic interaction at the subunit interface contributes to the thermostability of 3-isopropylmalate dehydrogenase from an extreme thermophile, *Thermus thermophilus*. *European Journal of Biochemistry* 220: 275-281.
194. Hough DW, Danson MJ (1999) Extremozymes. *Current Opinion in Chemical Biology* 3: 39-46.
195. Sato T, Fukui T, Atomi H, Imanaka T (2003) Targeted gene disruption by homologous recombination in the hyperthermophilic archaeon *Thermococcus kodakaraensis* KOD1. *Journal of Bacteriology* 185: 210-220.
196. Eberly JO, Ely RL (2008) Thermotolerant Hydrogenases: Biological Diversity, Properties, and Biotechnological Applications. *Critical Reviews in Microbiology* 34: 117-130.
197. Woodward J, Orr M, Cordray K, Greenbaum E (2000) Biotechnology - enzymatic production of biohydrogen. *Nature* 405: 1014-1015.
198. Davison BH (2000) Characterization of Chemically Modified Enzymes for Bioremediation Reactions. EMSP-55033; R&D Project: EMSP 55033; TRN: US200425%%620 United States10.2172/827362R&D Project: EMSP 55033; TRN: US200425%%620Tue Feb 05 04:57:53 EST 2008DOEEM; RN04089584English EMSP-55033; R&D Project: EMSP 55033; TRN: US200425%%620 United States10.2172/827362R&D Project: EMSP 55033; TRN: US200425%%620Tue Feb 05 04:57:53 EST 2008DOEEM; RN04089584English. Medium: ED; Size: vp. p.
199. Woodward J, Mattingly SM, Danson M, Hough D, Ward N, et al. (1996) *In vitro* hydrogen production by glucose dehydrogenase and hydrogenase. *Nature Biotechnology* 14: 872-874.
200. Chartrain M, Greasham R, Moore J, Reider P, Robinson D, et al. (2001) Asymmetric bioreductions: application to the synthesis of pharmaceuticals. *Journal of Molecular Catalysis B-Enzymatic* 11: 503-512.
201. Hummel W, Kula M-R (1989) Dehydrogenases for the synthesis of chiral compounds. *European Journal of Biochemistry* 184: 1-13.
202. Hummel W (1999) Large-scale applications of NAD(P)-dependent oxidoreductases: recent developments. *Trends in Biotechnology* 17: 487-492.
203. Mertens R, Greiner L, van den Ban ECD, Haaker HBCM, Liese A (2003) Practical applications of hydrogenase I from *Pyrococcus furiosus* for NADPH

- generation and regeneration. *Journal of Molecular Catalysis B-Enzymatic* 24-5: 39-52.
204. Tishkov VI, Galkin AG, Fedorchuk VV, Savitsky PA, Rojkova AM, et al. (1999) Pilot scale production and isolation of recombinant NAD(+)- and NADP(+)-specific formate dehydrogenases. *Biotechnology and Bioengineering* 64: 187-193.
 205. Seelbach K, Riebel B, Hummel W, Kula MR, VI T, et al. (1996) A novel, efficient regenerating method of NADPH using a new formate dehydrogenase. *Tetrahedron Letters* 37: 1377-1380.
 206. Hopkins RC, Sun JS, Jenney FE, Chandrayan SK, McTernan PM, et al. (2011) Homologous expression of a subcomplex of *Pyrococcus furiosus* hydrogenase that interacts with pyruvate ferredoxin oxidoreductase. *PLoS ONE* 6.
 207. Waage I, Schmid G, Thumann S, Thomm M, Hausner W (2010) Shuttle vector-based transformation system for *Pyrococcus furiosus*. *Applied and Environmental Microbiology* 76: 3308-3313.
 208. Weinberg MV, Schut GJ, Brehm S, Datta S, Adams MWW (2005) Cold shock of a hyperthermophilic archaeon: *Pyrococcus furiosus* exhibits multiple responses to a suboptimal growth temperature with a key role for membrane-bound glycoproteins. *Journal of Bacteriology* 187: 336-348.
 209. Basen M, Sun J, Adams MWW (2012) Engineering a hyperthermophilic archaeon for temperature-dependent product formation. *mBio*.
 210. Zhu MM, Lawman PD, Cameron DC (2002) Improving 1,3-propanediol production from glycerol in a metabolically engineered *Escherichia coli* by reducing accumulation of sn-glycerol-3-phosphate. *Biotechnology Progress* 18: 694-699.
 211. Cheng KK, Zhang JA, Liu DH, Sun Y, Liu HJ, et al. (2007) Pilot-scale production of 1,3-propanediol using *Klebsiella pneumoniae*. *Process Biochemistry* 42: 740-744.
 212. Colin T, Bories A, Moulin G (2000) Inhibition of *Clostridium butyricum* by 1,3-propanediol and diols during glycerol fermentation. *Applied Microbiology and Biotechnology* 54: 201-205.
 213. Homann T, Tag C, Biebl H, Deckwer WD, Schink B (1990) Fermentation of glycerol to 1,3-propanediol by *Klebsiella* and *Citrobacter* strains. *Applied Microbiology and Biotechnology* 33: 121-126.
 214. Saxena RK, Anand P, Saran S, Isar J (2009) Microbial production of 1,3-propanediol: Recent developments and emerging opportunities. *Biotechnology Advances* 27: 895-913.
 215. Kurian JV (2005) A new polymer platform for the future - Sorona (R) from corn derived 1,3-propanediol. *Journal of Polymers and the Environment* 13: 159-167.
 216. Deckwer WD (1995) Microbial Conversion of Glycerol to 1,3-Propanediol. *Fems Microbiology Reviews* 16: 143-149.
 217. Gunzel B, Yonsel S, Deckwer WD (1991) Fermentative production of 1,3-propanediol from glycerol by *Clostridium butyricum* up to a scale of 2 M3. *Applied Microbiology and Biotechnology* 36: 289-294.

218. Forage RG, Foster MA (1982) Glycerol fermentation in *Klebsiella pneumoniae* - Functions of the coenzyme-B12-dependent glycerol and diol dehydratases. *Journal of Bacteriology* 149: 413-419.
219. Menzel K, Zeng AP, Deckwer WD (1997) High concentration and productivity of 1,3-propanediol from continuous fermentation of glycerol by *Klebsiella pneumoniae*. *Enzyme and Microbial Technology* 20: 82-86.
220. Barbirato F, Himmi EH, Conte T, Bories A (1998) 1,3-propanediol production by fermentation: An interesting way to valorize glycerin from the ester and ethanol industries. *Industrial Crops and Products* 7: 281-289.
221. Biebl H, Marten S, Hippe H, Deckwer WD (1992) Glycerol Conversion to 1,3-Propanediol by Newly Isolated *Clostridia*. *Applied Microbiology and Biotechnology* 36: 592-597.
222. Forsberg CW (1987) Production of 1,3-propanediol from glycerol by *Clostridium acetobutylicum* and other *Clostridium* species. *Applied and Environmental Microbiology* 53: 639-643.
223. Seifert C, Bowien S, Gottschalk G, Daniel R (2001) Identification and expression of the genes and purification and characterization of the gene products involved in reactivation of coenzyme B-12-dependent glycerol dehydratase of *Citrobacter freundii*. *European Journal of Biochemistry* 268: 2369-2378.
224. Barbirato F, Soucaille P, Bories A (1996) Physiologic mechanisms involved in accumulation of 3-hydroxypropionaldehyde during fermentation of glycerol by *Enterobacter agglomerans*. *Applied and Environmental Microbiology* 62: 4405-4409.
225. Schutz H, Radler F (1984) Anaerobic reduction of glycerol to 1,3-propanediol by *Lactobacillus brevis* and *Lactobacillus buchneri*. *Systematic and Applied Microbiology* 5: 169-178.
226. Gonzalez-Pajuelo M, Meynial-Salles I, Mendes F, Soucaille P, Vasconcelos I (2006) Microbial conversion of glycerol to 1,3-propanediol: Physiological comparison of a natural producer, *Clostridium butyricum* VPI 3266, and an engineered strain, *Clostridium acetobutylicum* DG1(pSPD5). *Applied and Environmental Microbiology* 72: 96-101.
227. Sun JB, van den Heuvel J, Soucaille P, Qu YB, Zeng AP (2003) Comparative genomic analysis of dha regulon and related genes for anaerobic glycerol metabolism in bacteria. *Biotechnology Progress* 19: 263-272.
228. Tobimatsu T, Kajiura H, Toraya T (2000) Specificities of reactivating factors for adenosylcobalamin-dependent diol dehydratase and glycerol dehydratase. *Archives of Microbiology* 174: 81-88.
229. Bachovchin WW, Eagar RG, Moore KW, Richards JH (1977) Mechanism of Action of Adenosylcobalamin - Glycerol and Other Substrate Analogs as Substrates and Inactivators for Propanediol Dehydratase-Kinetics, Stereospecificity, and Mechanism. *Biochemistry* 16: 1082-1092.
230. Honda S, Toraya T, Fukui S (1980) In situ reactivation of glycerol-inactivated coenzyme B12-dependent enzymes, glycerol dehydratase and diol dehydratase. *Journal of Bacteriology* 143: 1458-1465.

231. Mori K, Tobimatsu T, Hara T, Toraya T (1997) Characterization, sequencing, and expression of the genes encoding a reactivating factor for glycerol-inactivated adenosylcobalamin-dependent diol dehydratase. *Journal of Biological Chemistry* 272: 32034-32041.
232. Skrally FA, Lytle BL, Cameron DC (1998) Construction and characterization of a 1,3-propanediol operon. *Appl Environ Microbiol* 64: 98-105.
233. Tang X, Tan Y, Zhu H, Zhao K, Shen W (2009) Microbial conversion of glycerol to 1,3-propanediol by an engineered strain of *Escherichia coli*. *Appl Environ Microbiol* 75: 1628-1634.
234. Khanna S, Goyal A, Moholkar VS (2011) Microbial conversion of glycerol: present status and future prospects. *Crit Rev Biotechnol*.
235. Wittlich P, Themann A, Vorlop K-D (2001) Conversion of glycerol to 1,3-propanediol by a newly isolated thermophilic strain. *Biotechnology Letters* 23: 463-466.
236. Hemme CL, Mouttaki H, Lee YJ, Zhang GX, Goodwin L, et al. (2010) Sequencing of multiple *Clostridial* genomes related to biomass conversion and biofuel production. *Journal of Bacteriology* 192: 6494-6496.
237. Oesterhe D, Stoecken W (1973) Functions of a new photoreceptor membrane. *PNAS* 70: 2853-2857.
238. Jung KH (2007) The distinct signaling mechanisms of microbial sensory rhodopsins in Archaea, Eubacteria and Eukarya. *Photochem Photobiol* 83: 63-69.
239. Lee KA, Jung KH (2011) ATP regeneration system using *E. coli* ATP synthase and *Gloeobacter* rhodopsin and its stability. *J Nanosci Nanotechnol* 11: 4261-4264.
240. Sharma AK, Spudich JL, Doolittle WF (2006) Microbial rhodopsins: functional versatility and genetic mobility. *Trends in Microbiology* 14: 463-469.
241. Beja O, Aravind L, Koonin EV, Suzuki MT, Hadd A, et al. (2000) Bacterial rhodopsin: evidence for a new type of phototrophy in the sea. *Science* 289: 1902-1906.
242. Venter JC, Remington K, Heidelberg JF, Halpern AL, Rusch D, et al. (2004) Environmental genome shotgun sequencing of the Sargasso Sea. *Science* 304: 66-74.
243. Miyasaka T, Koyama K, Itoh I (1992) Quantum conversion and image detection by a bacteriorhodopsin-based artificial photoreceptor. *Science* 255: 342-344.
244. Chen Z, Birge RR (1993) Protein-based artificial retinas. *Trends in Biotechnology* 11: 292-300.
245. Hampp N, Oesterhelt D (2008) Bacteriorhodopsin and its potential in technical applications. *Protein Science Encyclopedia: Wiley-VCH Verlag GmbH & Co. KGaA*.
246. Racker E, Stoeckenius W (1974) Reconstitution of purple membrane vesicles catalyzing light-driven proton uptake and adenosine triphosphate formation. *Journal of Biological Chemistry* 249: 662-663.
247. Hara KY, Suzuki R, Suzuki T, Yoshida M, Kino K (2011) ATP photosynthetic vesicles for light-driven bioprocesses. *Biotechnology Letters* 33: 1133-1138.

248. Balashov SP, Imasheva ES, Boichenko VA, Anton J, Wang JM, et al. (2005) Xanthorhodopsin: a proton pump with a light-harvesting carotenoid antenna. *Science* 309: 2061-2064.
249. Imasheva ES, Balashov SP, Wang JM, Lanyi JK (2011) Removal and reconstitution of the carotenoid antenna of xanthorhodopsin. *J Membr Biol* 239: 95-104.
250. Lakshman MR, Mychkovsky I, Attlesey M (1989) Enzymatic conversion of all-trans-beta-carotene to retinal by a cytosolic enzyme from rabbit and rat intestinal mucosa. *Proc Natl Acad Sci U S A* 86: 9124-9128.
251. Pisa KY, Huber H, Thomm M, Muller V (2007) A sodium ion-dependent A(1)A(o) ATP synthase from the hyperthermophilic archaeon *Pyrococcus furiosus*. *Febs Journal* 274: 3928-3938.
252. McIntosh CL, Hopkins RC, Adams MWW, Jones AK (2012) A new type of oxygen-tolerant [NiFe]-hydrogenase. *Nature Chem Biol* In review.
253. Hannig G, Makrides SC (1998) Strategies for optimizing heterologous protein expression in *Escherichia coli*. *Trends in Biotechnology* 16: 54-60.
254. Schut GJ, Brehm SD, Datta S, Adams MW (2003) Whole-genome DNA microarray analysis of a hyperthermophile and an archaeon: *Pyrococcus furiosus* grown on carbohydrates or peptides. *Journal of Bacteriology* 185: 3935-3947.
255. Minakhin L, Nechaev S, Campbell EA, Severinov K (2001) Recombinant *Thermus aquaticus* RNA polymerase, a new tool for structure-based analysis of transcription. *Journal of Bacteriology* 183: 71-76.
256. Kyrpides NC, Ouzounis CA (1999) Transcription in archaea. *Proc Natl Acad Sci U S A* 96: 8545-8550.
257. Hawkins AS, Han YJ, Lian H, Loder AJ, Menon AL, et al. (2011) Extremely thermophilic routes to microbial electrofuels. *Acs Catalysis* 1: 1043-1050.
258. Schirmer A, Rude MA, Li XZ, Popova E, del Cardayre SB (2010) Microbial biosynthesis of alkanes. *Science* 329: 559-562.